A QUANTITATIVE SCALE FOR DIRECTING GROUP POWER IN RUTHENIUM(II)-CATALYSED *ORTHO*-DIRECTED C-H ARYLATION REACTIONS

JAMIE MCINTYRE

A thesis submitted to the Department of Pure and Applied Chemistry, University of Strathclyde, in part fulfillment of the regulations for the degree of MPhil in Pure and Applied Chemistry.

I certify that the thesis has been written by me. Any help I have received in my research work and the preparation of the thesis itself has been acknowledged. In addition, I certify that all information sources and literature used are indicated in the thesis.

31st July 2017

1. Abstract

Directed ruthenium-catalysed C-H functionalisation of heteroarenes, such as 2-phenylpyridine or 1-phenylpyrazole, has emerged as an efficient and environmentally benign alternative to traditional cross-coupling chemistry. Using readily available and inexpensive aryl halides, the mechanisms of these transformations are beginning to be understood. However, there has been no work completed towards understanding the different directing group power of these substrates. Many of the literature examples consider only the behaviour of substrates with one functional group, and the behaviour of more densely functionalised substrates remains unpredictable.

In this work we have presented a quantitative reactivity scale of directing group power for a series of ruthenium(II)-catalysed *ortho*-directed intermolecular C-H arylation reactions across a range of substrates. The scale of directing group power has been determined using sets of competition reactions that were analysed by calibrated GC-FID. Using least squares minimisation, relative reaction rates were obtained for each substrate delivering the first quantifiable assessment of directing group power.

These results have found that, in our series, 2-phenylpyridine $\gg$ 2-phenylpyrazole $>$ *N*-methyl-2-phenyl-imidazole $>$ 2-phenyloxazoline $\gg$ *N*-(1-phenylethylidene)aniline. These results cover a synthetically useful reactivity range of 10^2 and allow a quantitative prediction of site selectivity under the conditions examined.

Additionally, we have presented initial experimental findings that support the intermolecular quantitative predictions within an intramolecular substrate. This sets the scene for prediction of regioselectivity in more densely functionalised molecules, on an inter- and intramolecular setting.

2. Acknowledgments

3. Table of Contents

4. Abbreviations

|	
Acac	Acetylacetone
DCE	1,2-Dichloroethane
DCM	Dichloromethane
DMF	Dimethylformamide
GC-FID	Gas chromatography - Flame ionisation detector
GC-MS	Gas chromatography - Mass spectrometry
HFIP	Hexafluoroisopropanol
MesCOOH	2,4,6-trimethyl benzoic acid
MesCOOK	Potassium 2,4,6-trimethyl benzoate
NHC	*N*-heterocyclic carbene
NMP	*N*-Methyl-2-pyrrolidone
PhMe	Toluene
TBATB	Tetrabutylammonium tribromide
THF	Tetrahydrofuran
TMEDA	Tetramethylethylenediamine

1. Introduction

The introductory section shall first discuss traditional cross-coupling with a view of selectivity and reactivity in the field using examples from the Suzuki-Miyaura, Negishi, and Heck reactions that highlight the need for alternative synthetic protocols. Following this, the C-H functionalisation protocol shall be discussed from distinct viewpoints of steric, electronic and directing group control of reactivity and selectivity.

1.1. Cross-Coupling

Transition metal-catalysed cross-coupling is a cornerstone reaction in organic synthesis to efficiently make carbon-carbon or carbon-heteroatom bonds.[1,2] The growth of organic frameworks is efficiently and predictably achieved through the transition metal-catalysed unison of organic halides or sulfonates with organometallic partners such as organo-boron, -zinc, or –tin species, among others. The Nobel Prize in Chemistry in 2010 was awarded to Richard F. Heck (alkene), Ei-Ichi Negishi (organozinc), and Akira Suzuki (organoboron) for their contributions to the field of palladium-catalysed cross-coupling.[3,4]

The Suzuki-Miyaura is the most popular of the cross-coupling methodologies.[2] The Suzuki-Miyaura reagents are commercially available, with *ca*. 800 phenylboronic acids and *ca*. 300 heteroarylboronic acids available through Sigma Aldrich, for example.[5] This wide availability of reagents together with the mild reaction conditions and high functional group tolerance make the Suzuki-Miyaura reaction a highly versatile and popular methodology.[6] Additionally, there are many examples of highly efficient regio- and stereo-selective Suzuki-Miyaura reactions.[6]

Heterocyclic substrates present a general barrier for the cross-coupling methodology because the heterocycles can act as ligands for the transition metal catalyst through lone-pair donation. The Suzuki-Miyaura protocol has found application in this area. For example, consider Scheme 1.1 in which 2-phenylpyridine (**3**) is rapidly obtained in high yield under ligand-free, aerobic conditions from 2-bromopyridine (**1**) and phenylboronic acid (**2**) in a Suzuki-Miyaura palladium-catalysed cross-coupling.[7]
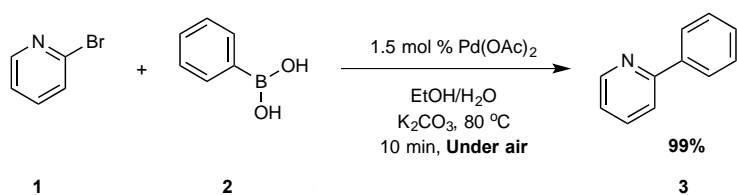
Scheme 1.1 – Synthesis of 2-phenylpyridine under palladium-catalysed Suzuki conditions.

Palladium is the most effective catalyst for this reaction. To the best of our knowledge, there is no alternative method to synthesise pyridine **3** that is as rapid and simple in that it contains no complicated and expensive ligands or inert conditions. The major advantage in the Suzuki-Miyaura methodology is demonstrated in this example also: the reaction proceeds smoothly under aqueous aerobic conditions. Consider that alternative methodologies, such as Grignard reagents, require the complete exclusion of air and moisture to avoid rapid decomposition or explosion in some cases.[8]

While this reaction proceeds without added ligand, some cross-couplings indeed require a ligand such as a phosphine or a carbene. These can be quite expensive and, in some cases, very specific to a particular transformation. Buchwald, has developed a very broad and mild set of Suzuki-Miyaura conditions employing a new biaryl phosphine ligand.[9] The author shows the efficient cross-coupling of highly sterically-encumbered, electron poor, electron rich, and heterocyclic species at room temperature to 100 ℃.[9] Consider the example in Scheme 1.2.
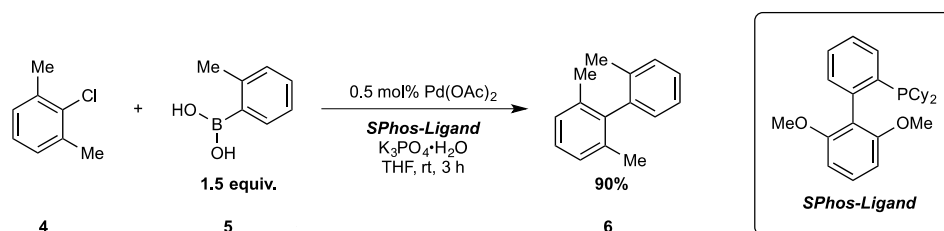
Scheme 1.2 – Cross-coupling of highly sterically-encumbered aryl chloride species (4) under mild conditions.[9]

The coupling of sterically-hindered substrates is traditionally problematic, so too is the coupling of aryl-chloride species. The coupling of aryl chlorides is desirable because they are more readily available and cheaper than -iodo and -bromo species but their coupling is harder because of a stronger C-Cl bond. Here, the authors have taken the Suzuki-Miyaura reaction to the next level in terms of scope and general methodology for challenging reactions.

Using electron-donating ligands such as *N*-heterocyclic carbenes (NHCs) or trialkylphosphines helps facilitate the coupling of aryl-chlorides. For example, NHCs have been used to couple unactivated aryl chlorides with palladium loadings of 0.05 mol%; ten times lower than in Scheme 1.2.[10]
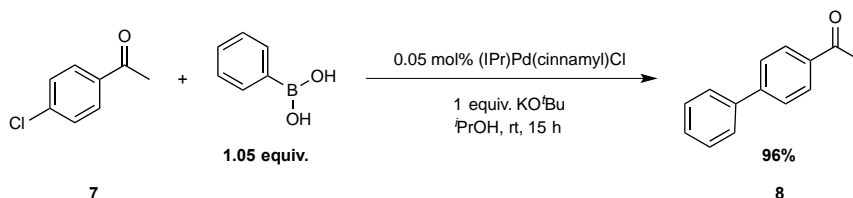
Scheme 1.3 – NHC palladium-catalysed coupling of unactivated aryl chloride (7) at low catalyst loading.[10]

The installation of the boron functionality in, for example, a bespoke pharmaceutical compound is a huge drawback for the Suzuki-Miyaura coupling protocol. The boron must either be maintained from the beginning or installed at a later stage assuming a suitable halogen remains. The introduction of boron, or indeed another cross-coupling partner, may be simplified using C-H functionalisation and this is discussed in Section 1.2 C-H Activation.

A further drawback for the Suzuki-Miyaura coupling may be certain stability issues in the boronic acid coupling partner, namely the propensity of electron rich boronic acids (example, **9**) to undergo protodeborylation either in storage or during reaction; however the use of trifluoroborate salts (example **10**) has been shown to be a general solution to this issue.[11,12]
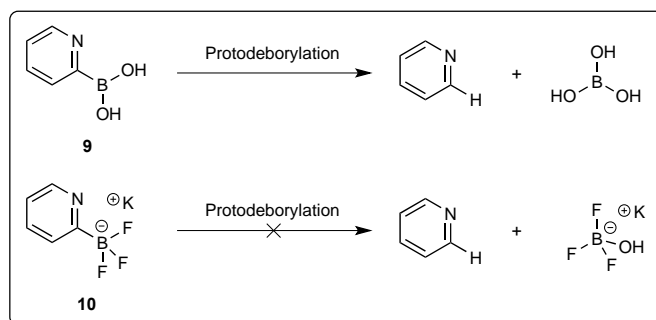
Figure 1.1 – Protodeborylation pathway for boronic acid 9 and trifluoroborate potassium salt 10.

Less reactive than organolithium or organomagnesium cousins, organozinc reagents show a wide functional group tolerance, although less so than for Suzuki-Miyaura cross-coupling reactions.[13,14] Additionally, organozinc nucleophiles are regarded as excellent partners in palladium-catalysed cross-coupling reactions due to their rapid transmetalation with palladium and that they generally provide high product yields and high catalyst turnover numbers.[13,14]

Similar to Suzuki-Miyaura coupling, problematic heterocyclic species such as **3** have also been successfully cross-coupled as demonstrated in Scheme 1.4.[15]
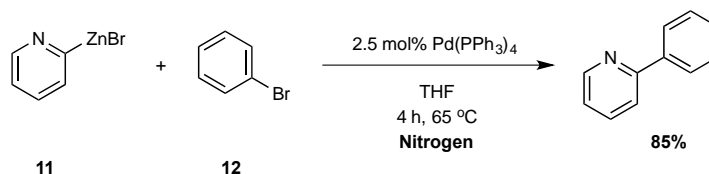
Scheme 1.4 – Negishi-type synthesis of 3.[15]

In comparison with Scheme 1.1, the Negishi protocol employed in Scheme 1.4 is lower yielding, conducted at higher temperature and under nitrogen, uses a high catalyst loading (2.5 mol % compared with 1.5 mol %), and requires preparation of 2-pyridylzinc bromide (**11**) shortly before use.

The general organozinc methodology developed by Negishi remains underutilised in comparison to organoboron cross-coupling, particularly in an industrial setting.[14] This is most likely due to the need to synthesise the zinc reagents prior to use at very low temperatures. Despite this, advances in the Negishi reaction methodology include the coupling of activated and unactivated, aryl and vinyl chlorides,[16,17] and a general and widely applicable methodology using an air-stable palladium-NHC pre-catalyst.[18]

Similar to work on the Suzuki-Miyaura reaction, Buchwald has developed a general approach for the Negishi reaction employing a similar phosphine ligand for the construction of biaryls.[19] Consider Scheme 1.5.
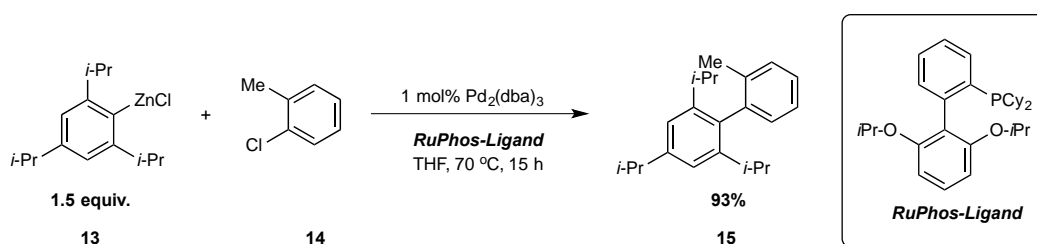
Scheme 1.5 – Cross-coupling of highly sterically-encumbered aryl chloride 13.[19]

The arylzinc chlorides such as **13** are prepared *in-situ* from the corresponding bromide via bromide/lithium exchange at -78 °C, which is then followed by a transmetalation with $ZnCl_2$. This is a huge drawback, however the highly sterically-encumbered biaryl product **15** is obtained in an excellent yield of 93%. The RuPhos-ligand allows for the Negishi cross-coupling of electron rich and poor species, with a wide functional group tolerance including

cyano, nitro, amino, ester and alkoxy. Furthermore, the authors show suitability in the cross-coupling of heteroaryl halides to generate heteroaryl biaryl species.

The Buchwald ligands achieve two main objectives for Suzuki-Miyaura and Negishi reactions: they allow the smooth and facile generation of highly sterically-encumbered biaryl species and they overcome the traditional challenge of cross coupling aryl chloride species that are more readily available than –bromo or –iodo congeners. Additionally, the ligands are commercially available but they can be expensive; consider that SPhos costs £3883 per mol and RuPhos costs £5949 per mol.[20] Consider that these ligands are similar in price to the precious metal palladium which costs £7925 per mol.[20]

The Mizoroki-Heck reaction is generally the coupling of alkenyl or aryl halides with alkenes.[21] It occurs through a slightly different catalytic cycle compared to the Suzuki-Miyaura and Negishi reactions since there is no transmetalation step from an organoboron or –zinc partner. Instead, ligand dissociation at the metal centre allows the alkene partner to enter the coordination sphere of the catalyst after which the product is obtained from a β-hydride elimination in high regio- and stereoisomeric ratios.[22] The nature of the Mizoroki-Heck reaction depends on the alkene, the catalyst, and the conditions used in the cross-coupling but it is generally regarded as a highly powerful and general protocol.[2,23]

The Mizoroki-Heck reaction is particularly useful for generating tertiary and quaternary stereocentres and has found wide application in the synthesis of natural products.[14,24,25] For example, the indanone motif is found widely in pharmacophores and the Mizoroki-Heck reaction provides a protocol to general chiral indanone motifs.

5 mol% Pd(OAc)$_2$
10 mol% (*R*)-3,5-XylMeOBIPHEN

Proton sponge (2 equiv.)
DMF, 100 °C, 12 h

90%
78% ee

16   **17**
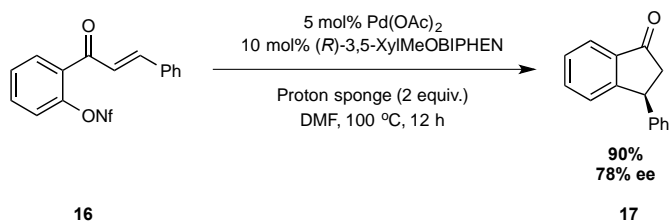
Scheme 1.6 – Palladium-catalysed asymmetric reductive-Heck cyclisation for the synthesis of chiral 3-substituted indanones.[26]

For completeness, it is also important to mention that cross-coupling methodology is not exclusively carbon-carbon bond forming. C-N bond formation is highly desirable, particularly in the pharmaceutical industry where it is one of the most widely used protocols.[27] The Buchwald-Hartwig reaction is a versatile, reliable and generally applicable methodology in both academic and industrial settings.[28,29] For example, Pfizer have used a Buchwald-Hartwig amination of 1-chloro-4-(trifluoromethyl)-benzene (**18**) as part of a synthetic route towards CP 529 414 for the treatment of coronary heart disease.[28,30]

0.5 mol% Pd(OAc)$_2$
Phos-Ligand
Cs$_2$CO$_3$
PhMe, 79 °C, 16 h

75%

18   **19**   **20**

CP 529 414
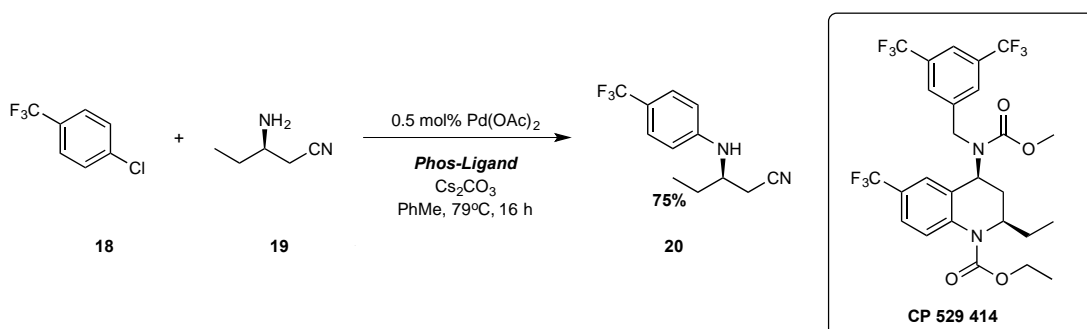
Scheme 1.7 – Synthesis of CP 519 414 showing Buchwald-Hartwig amination step.[30]

Mechanistically, this cross-coupling is very similar to the Suzuki-Miyraura and Negishi methodologies but further discussion is beyond the scope of this report.

In brief, from the contributions of Suzuki, Negishi, and Heck, metal-catalysed cross-coupling has allowed the facile construction of molecular complexity and revolutionised the synthetic chemist's handbook. The Suzuki-Miyaura is one of the most used protocols in industry.[27] Many synthetic challenges have been overcome; the coupling of aryl-aryl, and heteroaryl, sp^2 bonds; the coupling of aryl chlorides, which is valuable due to their increased availability; and the coupling of sterically-encumbered species by using specific ligands such as the Buchwald ligands or NHCs. The cross-coupling of sp^3 bonds, such as alkyl-alkyl coupling, remains a current challenge, and β–hydride elimination remains a general problem in cross-coupling but not for a C-H activation protocol (*vide infra*). Control of selectivity comes from having the

complementary functional groups in the desired locations, and control of reactivity comes from the choice of reagents, catalyst and ligand.

1.2. C-H Activation

From a sustainability and cost interest, the need to develop alternative synthetic methods that do not involve precious metals such as palladium is of current interest. Given the ubiquity of C-H bonds in molecules, there is a huge interest to treat these generally unactivated bonds as functional groups thus eliminating the need to have, maintain, or install, sensitive functional groups, halogens, or sulfonate coupling partners. On the other hand, the ubiquity of C-H bonds presents issues in reaction selectivity.

The challenge of C-H functionalisation is to cleave a specific C-H bond in the starting molecule and generate functionalisation catalytically.[31] Because C-H bonds are harder to activate, due to a large C-H bond energy, there are issues of reactivity in C-H activations. There are several approaches that are used to control the reactivity and selectivity of C-H transformations: using steric control to guide the functionalisation to a less encumbered C-H bond in the molecule (Figure 1.2 (**A**)); using electronic control to functionalise a more reactive C-H site (Figure 1.2 (**B**)); using directing groups as ligands to guide the catalyst to functionalise proximal C-H bonds (Figure 1.2 (**C**)).

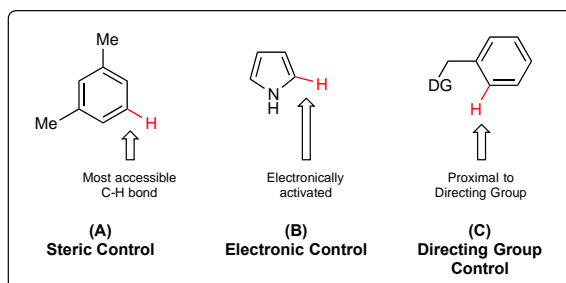**Figure 1.2 – Three general approaches to controlling regiochemistry of C-H functionalisation reactions.**

The three control approaches in Figure 1.2 are useful when one method dominates and these will be fully explored below. Sometimes, however, there is a mixture of factors to consider. For example, White *et. al.,* have shown a highly selective intramolecular iron-catalysed allylic C-H amination as shown in Scheme 1.8.[32]
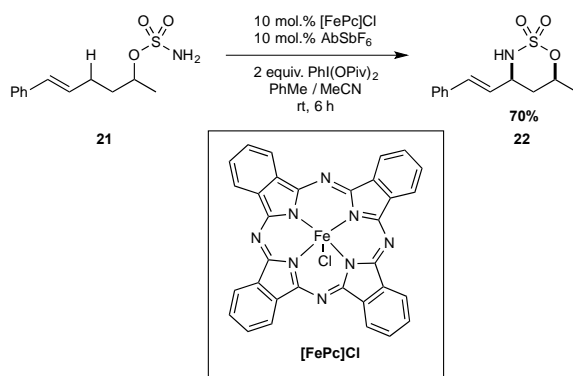
Scheme 1.8 – Iron-catalysed allylic C-H amination.

Here, a combination of factors is exploited in this C-H amination. The iron catalyst is non-toxic, bulky and electron deficient. It is guided to the nucleophilic allylic position through a sulfamate ester directing group on **21**. The authors show the subtle electronic differences between the allylic and alkyl preference in controlling site selectivity as shown in Scheme 1.9.
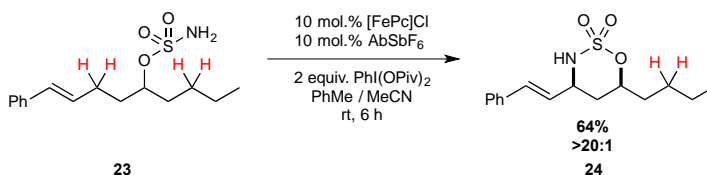
Scheme 1.9 – Iron-catalyst C-H amination of allylic position compared to non-allylic position in 23.

This is a very mild and highly regioselective reaction however it is very specific and relies entirely on having a sulfamate ester directing group in the molecule.

Over the remaining sections of the introduction, discussions will focus on the manifolds in which steric, electronic, and directing group control dominate the reaction reactivity and selectivity.

1.2.1. Steric Control

The growth of organic frameworks through C-H activation chemistry is a growing area of current academic research. The driving force behind research is a move away from the need to pre-functionalise organic molecules with sometimes expensive and disposable functional groups. For example, consider the borylation of substrates in the generation of cross-coupling partners for the Suzuki-Miyaura reaction. Traditionally, boron is installed by lithium-halogen exchange, Grignard chemistry, or via palladium-catalysed cross-coupling with alkoxydiboron species **26** as shown in Scheme 1.10.[33-36]
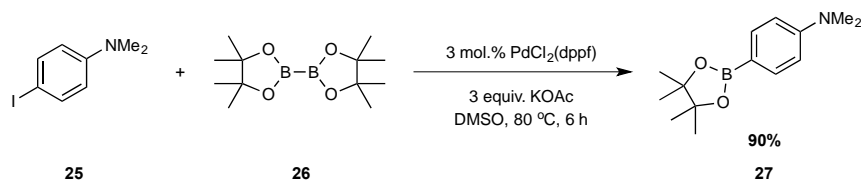
Scheme 1.10 – Palladium-catalysed boron halogen cross-coupling for installation of boron functionality.[34]

This obviates the need to either install iodine at a desired location prior to performing a palladium-catalysed cross-coupling or ensuring it is maintained there from a starting material and does not compete in other transformations.

C-H activation avoids this issue, and using steric control Ishiyama and Miyaura have shown the iridium-catalysed borylation of a series of electron rich, neutral, and poor arene rings.[37]
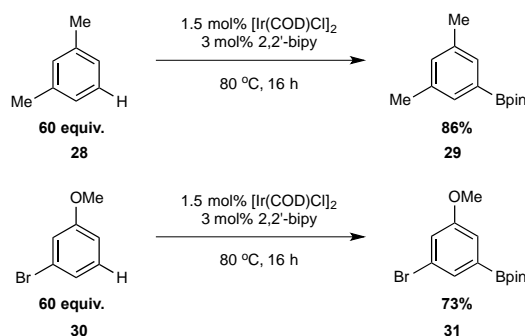
Scheme 1.11 – Iridium-catalysed C-H borylation of arene rings under steric control.[37]

The most accessible 5-positions of the arene rings in Scheme 1.11 are arylated. With 3-bromo-anisole **30**, the natural electronics of the ring are overruled. If this were a S_EAr reaction, one would expect the -bromo and -methoxy groups, both ortho directing, to electronically favour arylation of the 2-position, between both substituents. This product is not observed therefore the reaction must be proceeding under steric control.

The iridium catalyst is air stable and the reaction components are commercially available. However, the starting materials are used as the solvent, and so in 60 equivalents the utility of this reaction for application on expensive or indeed precious starting materials is unsuitable. This could find reasonable applications in the borylation of cheap building blocks.

Since such a large excess of starting material is used there is potentially some reactivity issue that is not discussed in the paper.[37] Generally, reactivity in C-H activations can be problematic and sterics can influence the site of reactivity.[31] Consider Scheme 1.12 in which increasing steric bulk influences the location of borylation.[35,38]
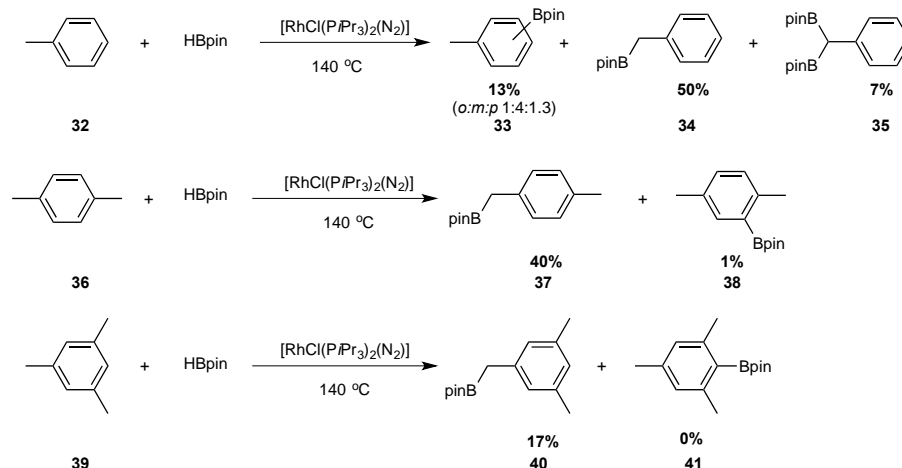
Scheme 1.12 – Increasing substitution influences the site of borylation.

In Scheme 1.12, increasing substitution disfavours arene borylation with sp^2 versus sp^3 selectivity. The borylation of toluene (**32**) yields a mixture of arene and benzylic products (**33-35**). Adding a methyl substituent, *p*-xylene (**36**) shows only 1% of borylation on the arene ring **38** compared to 40% at the benzylic position **37**. With mesityl **39**, the most sterically-hindered arene examined, borylation at the benzylic position gives exclusively **40**.

An interesting approach to steric control of C-H activations is shown in the recently published palladium-catalysed functionalisation of primary amino alcohols such as **42** using temporary steric control as shown in Scheme 1.13.[39]
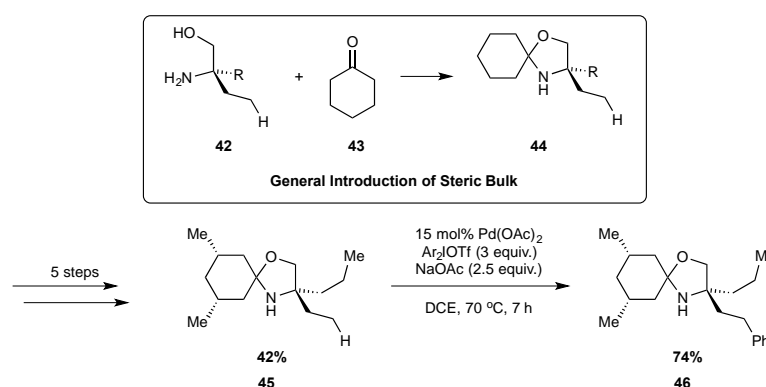
Scheme 1.13 – Transient steric control in the palladium-catalysed C-H arylation of amino alcohols.[39]

The author shows access to the functionalisation of primary amino alcohols, a medicinally important motif and one that is normally difficult to functionalise under traditional conditions. Additionally, an sp^3 carbon is activated here which is a current challenge in cross-coupling chemistry.[40] It is an excellent concept and the author shows arylation, aceotxylation and

carbonylation of primary amino alcohols, however the method employs 15 mol% palladium which is very expensive.

Overcoming the challenge of the ubiquity of C-H bonds can be achieved using steric control but this is not without its disadvantages including using an excess of starting material with high catalyst loading.

## 1.2.2. Electronic Control

Another approach to controlling selectivity in C-H functionalisations is to exploit the natural electronics of the molecule. Substrates with a significant electronic bias such as heterocycles are effective in this approach. Consider the nickel-catalysed borylation of indole derivatives (**47**) that display exclusive C-2 borylation despite increasing steric bulk at the *N*-position.[41]

(1) R = Me
(2) R = *n*-butyl
(3) R = CH$_2$OMe
(4) R = benzyl

(1) 78%
(2) 68%
(3) 68%
(4) 82%
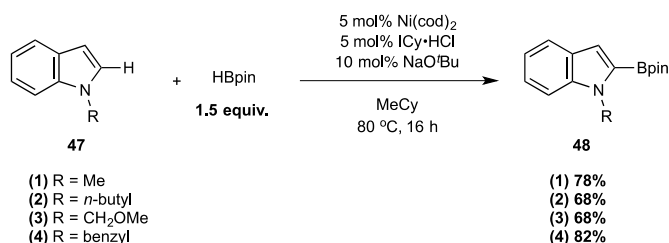
Scheme 1.14 – Regioselective C-2 borylation of indole derivatives under nickel catalysis.[41]

Excellent yields are obtained as steric bulk is increased from a –methyl substituent to a –benzyl substituent. The authors do not observe any borylation product at the C-3 position of the indole derivatives, and they do not attempt any reactions of blocked C-2 indole derivatives that would force C-3, or other, functionalisation. With regards to *N*-benzyl indole **47**-**4**, only borylation on the indole moiety was observed adding further weight to the electronic control in this nickel-catalysed reaction.

Trifluoromethylation is used frequently in drug discovery to alter the distribution and permeability of medicines and so routes to generate trifluoromethylated heteroarene derivatives are highly sought after. A recently published general method provides routes from substrates including *N*-protected pyrrole **49** and thiophene **51** at exclusively the electronically active C-2 position.[42]
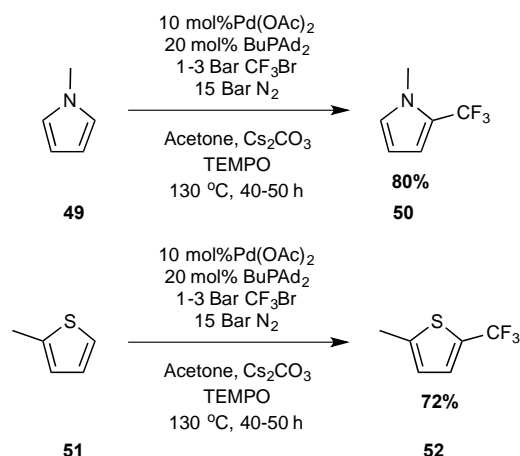
Scheme 1.15 – Trifluoromethylation of 49 and 51 at the electronically active C-2 position.[42]

In excellent yields, the authors provide a general method to these products covering electron-rich and -poor heteroarenes possibly operating via a radical mechanism. The conditions, however, are very harsh. Employing high pressures of reagent and inert atmosphere, long reaction times and 10 mol% palladium loading. Furthermore, the protection of free -NH groups adds additional steps.

Installation and removal of the *N*-protecting groups adds additional steps to the nickel-catalysed C-2 borylation. However other research groups have shown C-2 regioselective C-H functionalisation without protection of the acidic -NH proton in indole derivative **53**.[43]
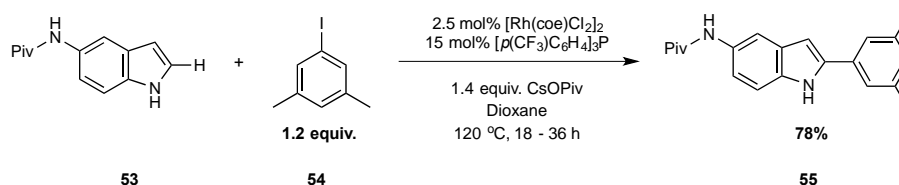
Scheme 1.16 – Arylation of free -NH indole derivative 53.[43]

In Scheme 1.16 arylation occurs exclusively at the C-2 position in excellent yield. Arylation occurs despite the presence of the NH-indole and the C-5 pendant NH-amine in **53**, both acidic protons. The authors show a wide functional group tolerance but, again, they fail to block the C-2 position and fully explore the electronic nature of the regioselectivity observed.

Indeed, significant loss of reactivity is observed when the electronically-preferred position of heteroarenes is blocked.[44] Research covering the functionalisation of these blocked materials is sparse, however some research groups have found methods that overcome the reactivity

issues in non C-2 functionalisation. Consider Scheme 1.17 that shows the palladium-catalysed arylation of 2,5-substituted pyrrole derivatives **56**.[45]
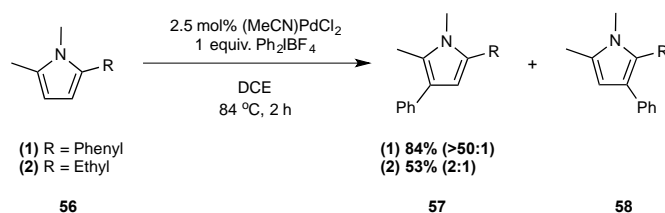
Scheme 1.17 – Arylation of 2,5-substituted pyrrole derivatives.[45]

With the electronically favoured C-2 position blocked, the authors have shown a method to access the C-3 or C-4 sites of **56**. Here, the authors have shown that the reaction proceeds under steric control. When the steric bulk at the C-2 position is reduced from –phenyl to – ethyl substituent, a drop in site selectivity of the arylation is observed from >50:1 with –phenyl to 2:1 with –ethyl.

Another route to control the natural electronics of heteroarenes was published by Gaunt *et al.* wherein free -NH indoles undergo a selective palladium-catalysed C-2 or C-3 Heck reaction that is solvent dependent as shown in Scheme 1.18.[46]
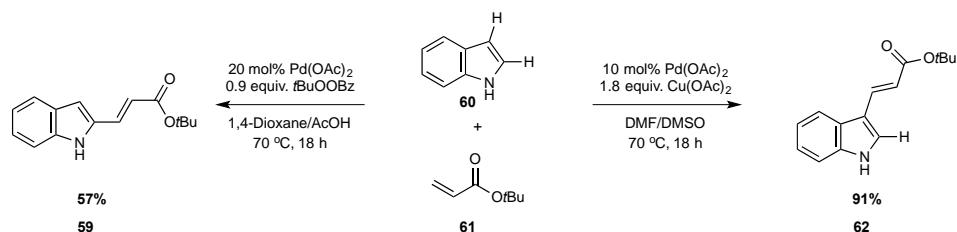

Scheme 1.18 – Selective C-2 or C-3 palladium-catalysed oxidative Heck reaction.[46]

Under electrophilic palladium catalysis, a simple change in solvent and the addition of acetic acid is shown to control either C-2 or C-3 cross coupling. The mechanism proposes that the gradual development of acetic acid from the deprotonation of **60** encourages C-2-functionalisation instead of C-3 as shown on the left hand side of Scheme 1.18.

Steric and electronic control is rarely truly selective nor predictable. In some cases it has been shown very predictable but not practical, for example the sterically-controlled iridium-catalysed borylation of arenes in Scheme 1.11. However, the substrate in these examples are used as the solvent or in huge excess. This method, therefore, is not widely practical because it generates lots of wastage. Selectivity depends on the substrate and the choice of catalyst,

ligand, and solvent, as in Scheme 1.18 but these conditions become very specific for each substrate. A more selective, general and predictable approach is to use directing groups to force C-H activation at sites proximal to the directing group. This is the subject of discussion in the next subchapter.

1.2.3. Directing Groups

Directed C-H functionalisations do not require specific organometallic reagents, such as organoboron or organozinc partners. Instead, a coordinating heteroatom substituent directs the transition metal catalyst towards an adjacent unactivated hydrogen atom that serves two main purposes. First, the coordination allows functionalisation to a metal centre that would not normally add C-H bonds, and secondly, it creates a regiocontrolled environment for C-H functionalisation.[31] This is demonstrated in Figure 1.3 using **3** as an example.
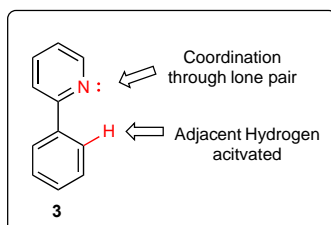
Figure 1.3 – Example showing sites of coordination and activation.

Figure 1.3 demonstrates functionalisation *ortho* to the pyridyl directing group. This represents the majority of directed C-H functionalisations, however there is a growing body of research developing access to *meta* and *para* functionalisations. These will be discussed first, followed by *ortho* functionalisation.

1.2.3.1. Meta or Para Direction

Under mild and inexpensive copper-catalysed conditions, electron-rich benzamides and pivanilides like **63** can be arylated at the *meta* position as shown in Scheme 1.19.[47]

(1) R = Methyl
(2) R = Methoxy
(3) R = Phenyl
(4) R = Fluorine

(1) 79%
(2) 93%
(3) 84%
(4) 55%
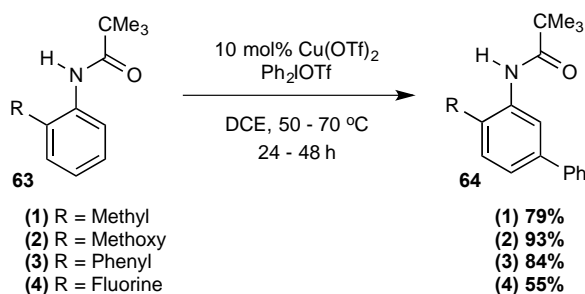
Scheme 1.19 – *Meta* arylation of 2-substituted pivanilides.[47]

Excellent yields are obtained generally except for 2-fluoro pivanilide. In this case, the strong inductive withdrawal of electrons by the fluorine atom could be disruptive of the mechanism of activation that requires an electron rich arene ring. The mechanism of this rare *meta* substitution has not been established. An electrophilic Cu(III) species was suggested although the authors have no evidence.[47]

Using a specifically designed electron-rich quinolone-type ligand, *meta*-selectivity has been achieved across a broad range of alkyl and aryl bromide species in a palladium-catalysed, norbornene-mediated, ligand-enabled reaction.[48]

Scheme 1.20 – Ligand-enabled *meta*-selective C-H functionalisation of *N*-2,3,5,6-tetrafluoro-4-trifluoromethylphenyl amide species.[48]

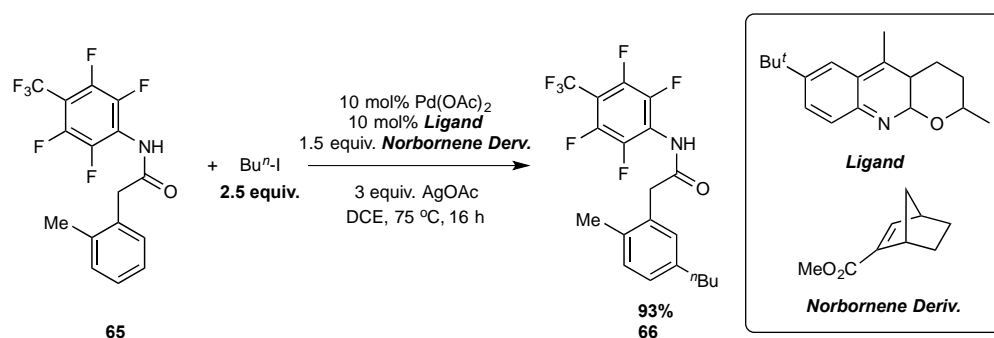In Scheme 1.20 the authors show exclusive *meta* selectivity for 2-substituted fluorophenylamide species **65**.[48] In the absence of 2-substitution the authors note mixtures of mono- and di- *meta* functionalisation. The *meta* selectivity is derived from the norbornene additive which is initially palladium-coupled to the *ortho* position. During the catalytic process it is removed at the end of the catalytic cycle giving a *meta* functionalised product. This is an excellent concept, showing good to excellent yields across a range of iodo-electrophiles however the concept requires 2-substitution to be effective and the fluoroamide functional group is also essential. Published around the same time as this norbornene-mediated *meta* functionalisation from Yu *et. al.*, Dong *et. al.* have shown a similar norbornene-mediated functionalisation using more amenable tertiaryamines as the directing group. This is shown in Scheme 1.21.[49]
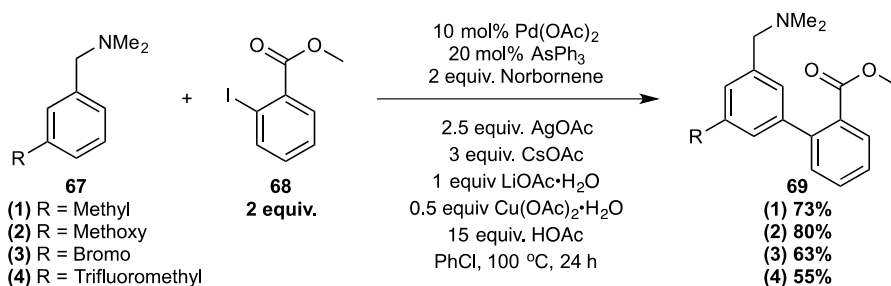
Scheme 1.21 – Tertiaryamine-directed norbornene-mediated *meta* functionalisation.[49]

The downside to this method is the "acetate cocktail" that is essential for the reaction, despite the tertiary amine being a more attractive directing group in terms of synthetic applicability.[49]

Alternative methods designed for remote C-H activation include the use of transient directing templates. This would overcome metallocycle ring strain from sizes smaller or larger than 6-membered rings. Consider Scheme 1.22 which displays a "U-shaped" template that forms weak, transient coordination to a palladium catalyst for *meta* C-H arylation with boronic acids (HFIP = hexafluoroisopropanol).[50]
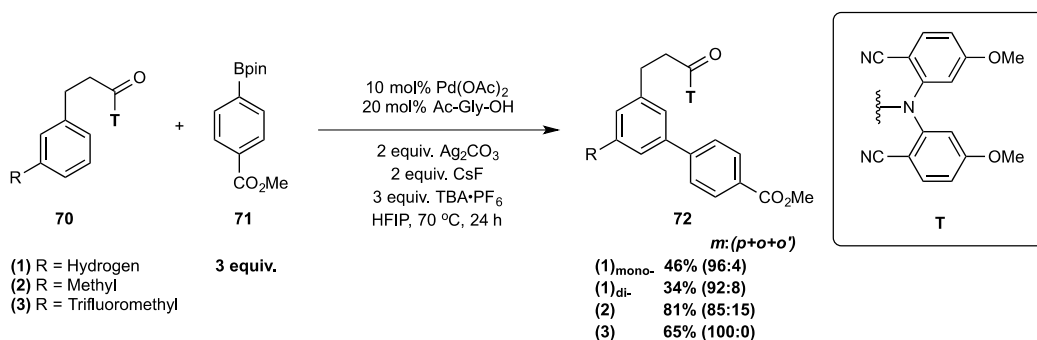
Scheme 1.22 – *Meta* functionalisation of 3-phenylpropanoic acid 70 from a transient "U-shaped" template, T.[50]

The template is added from the 3-phenylpropanoic acid chloride but the author does not comment on the yield of this step; however in one example, its removal is facile and very high yielding with recovery of the template also. *Meta* functionalisation is achieved in very high selectivities across a range of electron-withdrawing and electron-donating substituents. Ortho or meta substitution on the phenyl ring prevents di-functionalisation which occurs when R=H (70(1)) in Scheme 1.22. Indeed, there appears to be no significant preference for selective mono-arylation when R=H with mono-arylation yielding 46% and diarylation yielding 34%.

Using a similar transient template approach, remote *para* selectivity has also been achieved.[51] From phenol derivatives, a silyl-biphenyl template is very easily installed in high-yield, which can then direct functionalisation to the *para* position with high regioselectivities.
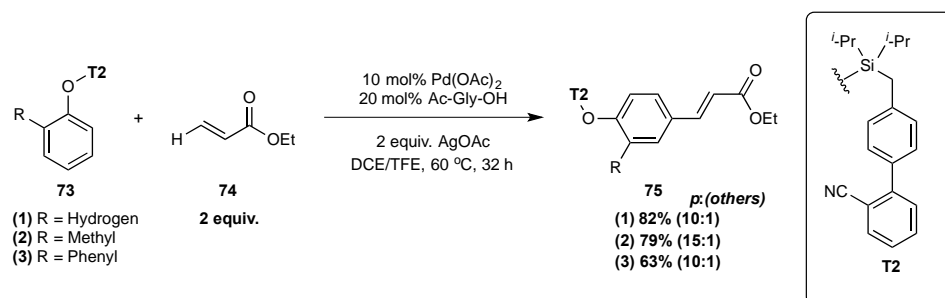
Scheme 1.23 – Remote *para* olefination of phenol derivatives 73 from a transient nitrile director, T2.[51]

Examples of *ortho* substituted phenol derivatives are shown in Scheme 1.23 in **73(1-3)**, however the method is also high yielding for *meta* substituted phenols either electron-rich, electron-poor or sterically-encumbered, with good *para* selectivity. The olefin coupling partner also supports a wide range of functionality including ester, amide, aldehyde, and sulfonyl groups. The main advantage of this methodology is the remote functionalisation of the phenol moiety, which makes it highly desirable from a synthetic point of view given the ubiquity of this group.

In some literature, remote functionalisation is almost accidental or highly unusual given the knowledge base for directed C-H activation. As will be discussed in the subsequent subchapter, and as shown in Figure 1.3, **3** is highly regarded as an *ortho*-directing substrate. Unusual *meta* sulfonation of **3** under ruthenium catalysis is shown in Scheme 1.24.[52]
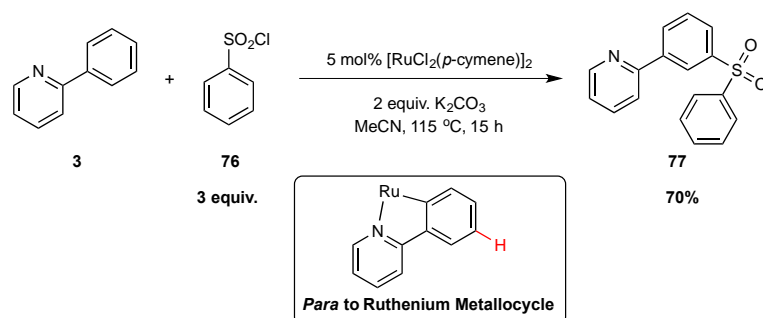
Scheme 1.24 – Unexpected *meta* sulfonation of 3. Box: proposed intermediate in *meta* selectivity.[52]

The unusual *meta* regioselectivity is hypothesised to come from a strong *para*-directing effect that is created from a stable Ru-C$_{aryl}$ metallocle as shown in the box inScheme 1.24. In

support of this, the authors fail to sulfonate a *meta*-substituted **3**. The formation of the metallocycle would hypothetically occur at the least hindered *ortho* position, thus pushing the *meta* substituent furthest away and hence blocking the site of sulfonation.[52] This is advantageous since only the mono-sulfonated product is ever obtained. The authors note that this is technically a catalytic σ-activation process, and it is reported as the first. While the authors do not examine the effects of *ortho* substitution, various electron-donating *para* substituents are tolerated in reasonable yields.

Greaney *et. al.* show a highly *meta* selective bromination using the same catalyst and substrate system and using tetrabutylammonium tribromide (TBATB) as a source of Br_2.[53]
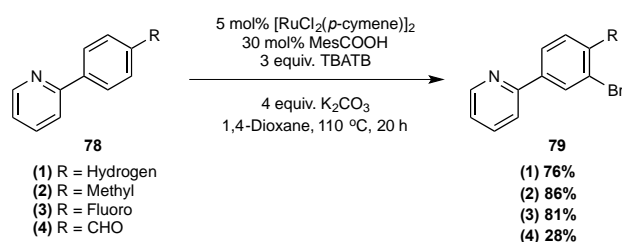
Scheme 1.25 – Unexpected *meta* bromination of 2-phenylpyridine derivatives 78.[53]

Para electron-withdrawing and electron-donating substituents were well tolerated in the reaction, with electron-poor *para* aldehyde **78(4)** the lowest yielding overall. The authors do not observe over-bromination of the substrate, which is probably a feature of the mechanism of functionalisation as for sulfonation.

Meta alkylation has also been shown. Secondary alkyl halides like **80** are sterically-demanding and electron-rich, which makes them more challenging electrophiles however Ackermann *et. al.* have shown the *meta* functionalisation of **3** and derivatives like **82** from unactivated secondary alkyl bromide **80**.[54]
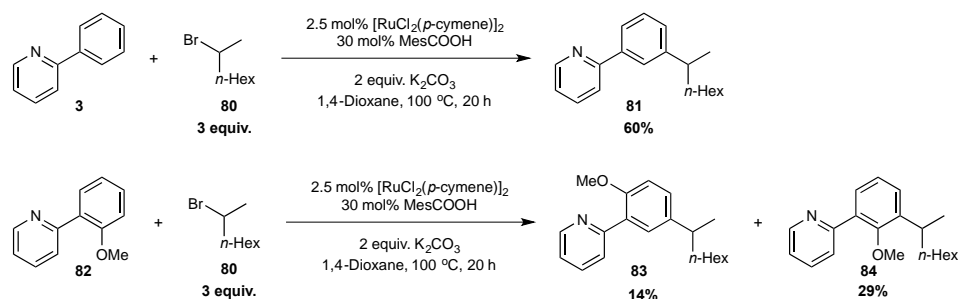
Scheme 1.26 – Ruthenium-catalysed *meta* functionalisation of 2-phenylpyridine derivatives using 3.[54]

Substitution on either the pyridyl moiety or the arene moiety is not well tolerated and yields are significantly reduced below 60%, which is obtained from unsubstituted 2-phenylpyridine **3**. Initial *ortho* metalation followed by *meta* functionalisation is consistent with other *meta* functionalisations that are discussed above. This also explains the unexpected formation of the more sterically encumbered C-3 alkylated product as shown in Scheme 1.26. Generally, the authors note that electron-rich substituents are higher yielding than electron-poor substituents and suggest that this indicates an electrophilic-type alkylation. The authors fail to develop a wider scope of substrate and electrophile.

Tertiary alkyl halides are more sterically demanding than secondary and are regarded as very difficult electrophiles in synthesis however they have recently been used in a directed *meta* functionalisation of **78** to generate quaternary centres.[55]

Scheme 1.27 – *Meta* **functionalisation of 78 using tertiary alkyl chlorides to generate quaternary centres.[55]**

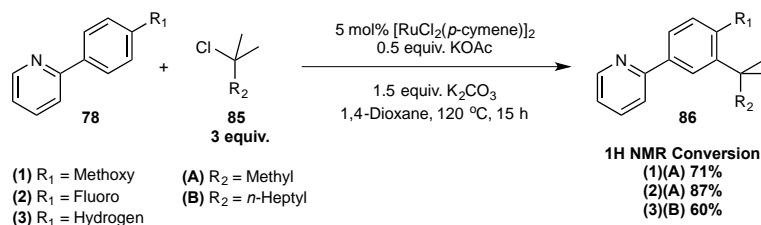The authors find that acetate salts significantly increase the yield compared to other bases. The reaction works better for electron-donating substituents whereas electron-withdrawing substituents inhibited the reaction, which is similar findings to previous reports, as discussed above. Unlike in Scheme 1.26 this reaction uses tertiary alkyl chlorides, which are even less reactive than bromides, and additionally the authors suggest a radical pathway as opposed to an electrophilic-type alkylation. They base this on the isolation of by-products and because TEMPO inhibits the reaction completely.

There is a growing body of literature focussing on *meta* and *para* C-H functionalisation pathways. In directed C-H functionalisation, a major challenge is forming highly strained and distant metallocycle rings at locations further away from the directing group. Several successful approaches include exploiting the directing group's natural preference for *ortho* ligation or *ortho* metallocycle formation to control site selectivity through sterics and electronics respectively. Other methods employ transient, bulky directing groups to force metallocycle formation at sites distant from the primary directing group.

1.2.3.2. Ortho Direction

In this subchapter the main discussion will focus on ruthenium-catalysed *ortho* directing reactions, as this is most relevant to the results that will be presented, particularly focussing on arylation. A mention of alternative functionalisations will be included for completeness and briefly some *ortho* functionalisations from other metal catalysts will be included. The reader can find a more extensive list of ruthenium-catalysed C-H functionalisations in a review by Dixneuf *et. al.*[56]

The typical *ortho* directing groups that are found throughout the literature are heteroarene species, specifically nitrogen-containing heteroarenes such as those of pyridine, pyrazole, pyrazine, and oxazoline to name a few. The first example of a ruthenium catalysed *ortho* arylation with arylhalides was presented by Inoue *et. al.* and this is shown in Scheme 1.28.
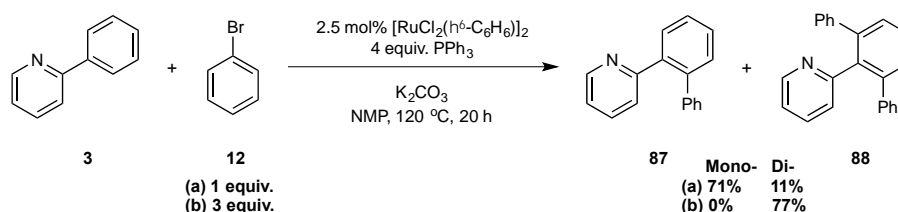
Scheme 1.28 – *Ortho* arylation of 3 under ruthenium catalysis.[57]

The interesting part about this transformation was the observed selectivity in arylation. With only 1 equivalent of **12**, monoarylation of **3** was obtained in 71% yield (**87**). Diarylation (**88**) can be completely achieved with 3 equivalents of **12**, forcing arylation on both sides. The same authors took this methodology and extended it to 2-phenyloxazoline (**89**) and 2-phenylimidazoline (**92**) and observed interesting selectivity and reactivity for these groups.[58]
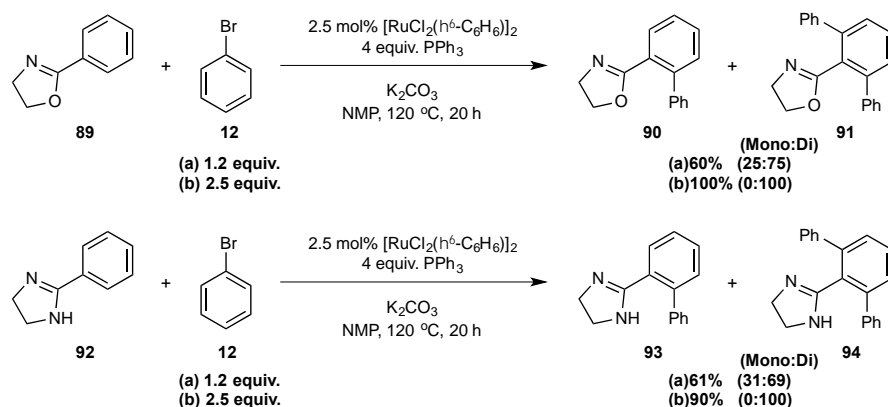
Scheme 1.29 – *Ortho* **arylation of 89 and 92 under ruthenium catalysis.**[58]

The ruthenium-catalysed arylation of **3** shown in Scheme 1.28 shows a distinct preference for monoarylation. In Scheme 1.29, under the same conditions but with a slight excess of **12**, both **89** and **92** show a distinct preference for diarylation and both show lower yields overall, of *ca.* 60%. This could be a reactivity challenge, as both substrates in Scheme 1.29 are lower yielding compared to **3**. Whereas **3** shows the potential to control monoarylation over diarylation, the selective monoarylation of both unsubstituted **89** and **92** is disfavoured. What's missing here is an understanding of the directing group ability of these species and this question will be tackled as part of the Results Chapter (*vide infra*).

These conditions have been widely used across various heterocycles as shown in Scheme 1.30.
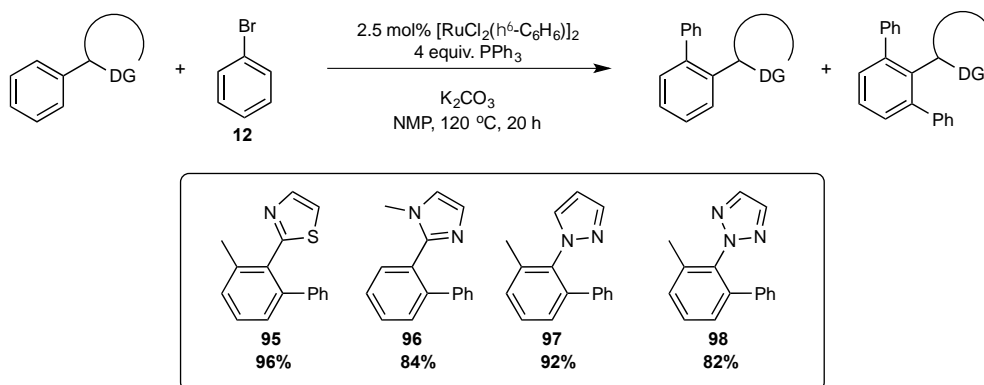
Scheme 1.30 – *Ortho* **arylation of a range of heterocyclic substrates under ruthenium catalysis.**[59]

In Scheme 1.30, selective monoarylation is achieved by steric hindrance and yields are excellent across the range. However, it is difficult to make any reasonable assessment of each directing group's reactivity. Firstly, the methyl substituents inhibit over arylation and secondly because the reactions are conducted over 20 hours. Some of the substrates may have finished reacting after several minutes where others finish after several hours.

Ackermann *et. al.* have expanded upon the ruthenium catalyst system. Using a *para*-cymene ruthenium catalyst, the authors found that 2,4,6-trimethylbenzoic acid (MesCOOH) was a proficient cocatalyst *in lieu* of triphenylphosphine for a small range of electron-rich heterocycles including those of triazole, pyridine, pyrazole and oxazoline.[60]
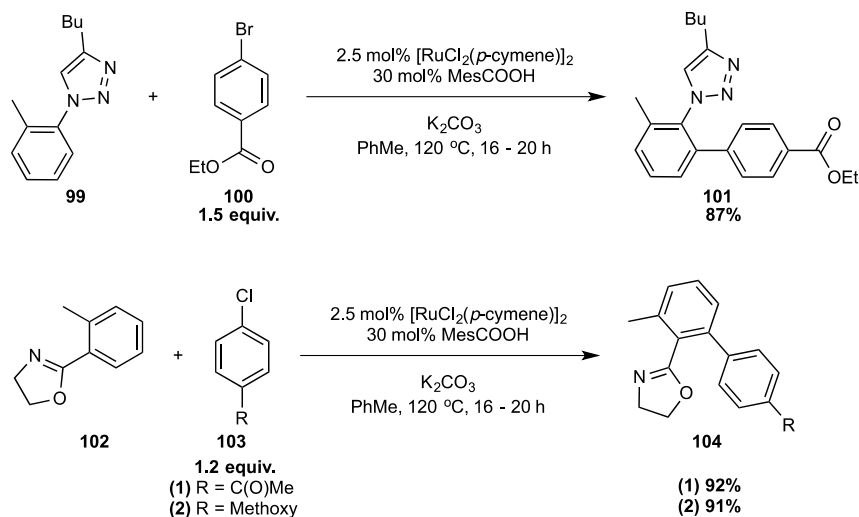
Scheme 1.31 – Ruthenium-catalysed *ortho* arylation of 1-phenyltriazole derivative 99 and 2-phenyloxazoline derivative 102 with 2,4,6-trimethylbenzoic acid cocatalyst.[60]

To the best of our knowledge, Ackermann *et. al.* was the first other to develop the carboxylic acid-cocatalysed ruthenium *ortho* arylation, although the scope is no wider than that presented by Inoue *et. al.*[57,58,61] Scheme 1.31 demonstrates the applicability of this new methodology to electron-rich and electron-poor aryl bromides like **100** and, less reactive but more available, aryl chloride electrophiles **103**. The author, however, fails to confront selectivity in the *ortho* arylation reactions presented since each of the substrates is blocked at one *ortho* position thus preventing diarylation. Interestingly, the conditions for *ortho* arylation from Ackermann *et. al.* are higher yielding than those in Scheme 1.29 (*ca.* 90% compared to 60%).

Diaryliodonium salts can also be used instead of aryl halides as electrophiles in ruthenium-catalysed *ortho* functionalisations. These oxidants act as highly versatile arylating agents because they are highly electron-deficient and have an excellent leaving group ability.[62] Chatani and coworkers showed this for 2-phenylpyridine derivatives **105**.[63]
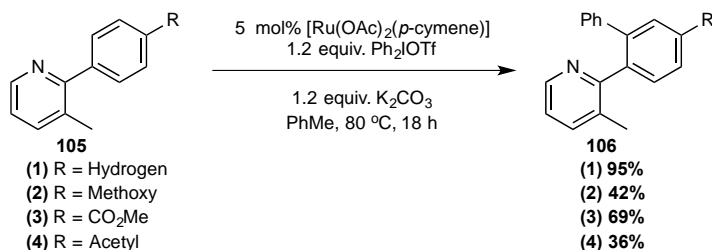
Scheme 1.32 – *Ortho* **arylation of 105 using diaryliodonium salts as oxidants.[63]**

The reaction proceeds at 80 °C, which is a lot lower than similar ruthenium-catalysed arylation of **3** as discussed above. Because these agents are very electron-deficient the energy barrier of oxidative addition should be reduced. The reaction shows a wide range of isolated yields from poor to excellent however the authors fail to identify if this is an issue with reactivity or isolation of products. However, the authors use steric control to prevent diarylation of **105** and it would have been interesting to see an example of the reaction selectivity in unhindered **105**. Furthermore, diaryliodonium salts generate high molecular weight waste leaving behind 'PhIOTf' and so are economically unfriendly.

Other than heterocyclic directing groups, the imine functionality is a very versatile functional group and can readily be converted into amines, ketones or carboxylic acids. Similar to **3**, the arylation of *N*-(4-methoxyphenyl)-1-phenylethylimine (**107**) is high yielding and shows preferential *ortho* monoarylation (**108**).[64]
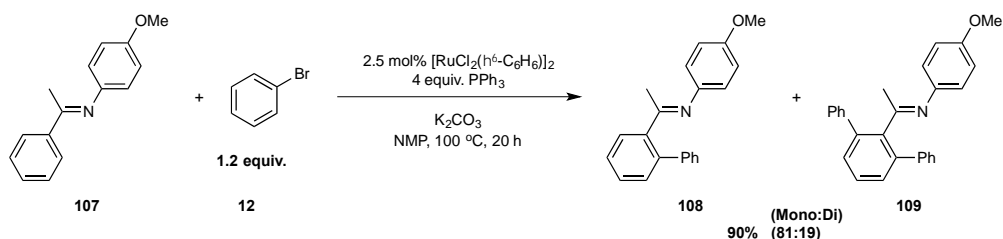
Scheme 1.33 – Arylation of 107 with 12.[64]

Electron-rich and electron-poor bromobenzenes reacted equally well, and the authors note that the electron donating methoxy group possibly encourages metallocycle formation. This is based on a decreased yield when phenyl is used instead of 4-methoxyphenyl. Monoarylation is possibly favoured due to steric interactions between the methyl imino and a second *ortho* arylation.

The amide functionality is widely present in medicinally relevant materials and *ortho* arylation of amides from arylboronic acids has been shown.[65]
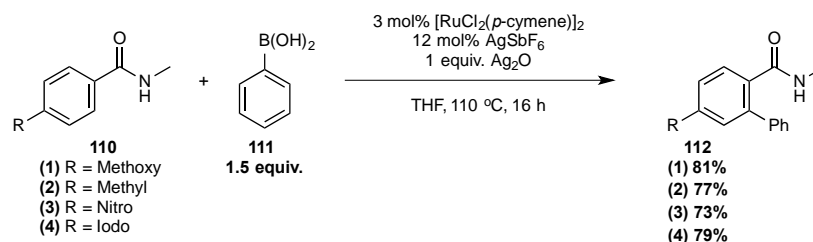
Scheme 1.34 – *Ortho* arylation of benzamides 110 from phenylboronic acid 111.[65]

Excellent yields are obtained for electron-rich and electron-poor benzamides, even displaying tolerance of iodo-substitution **110(4)**, which are very labile bonds in cross-coupling. The main advantage with this methodology is the use of commercially available phenylboronic acids as arylating agents. The authors make no remark about the apparent selective monoarylation in high yields.

The ketone is another desirable functional group in synthesis because it is highly versatile and can readily be transformed through an extensive list of manipulations. With certain ruthenium catalysts the ketone functionality is generally regarded as a weaker directing group compared to nitrogen groups, however *ortho* arylation has been demonstrated with acetophenone (**113**).[66]
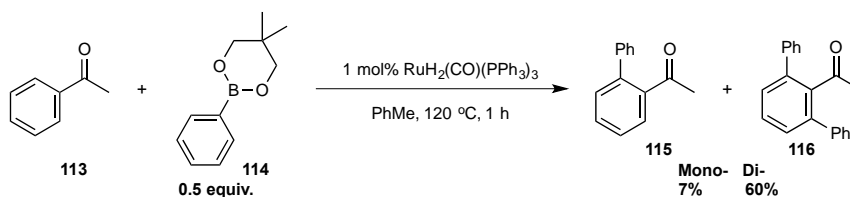
Scheme 1.35 – *Ortho* arylation of 113 under ruthenium catalysis.[66]

Interestingly with 0.5 equiv. of phenylboronate **114**, **113** is preferentially diarylated (9:1, di:mono). The authors make no comment on this unusual diarylation preference nor does their proposed mechanism, which shall not be discussed, offer any insight. They show that electron-rich and electron-poor derivatives of **114** are well tolerated in this transformation and ultimately set a precedent for ruthenium-catalysed *ortho* arylation of ketones.

Directed *ortho* arylation is a valuable transformation and other ruthenium-catalysed *ortho* functionalisations are known. The *ortho* alkylation of ketones under ruthenium-hydride catalysis has become known as the Murai reaction following the seminal publication in 1993.[67] The functionalisation employed a ruthenium-hydride catalyst and proceeded efficiently in a matter of hours or less.
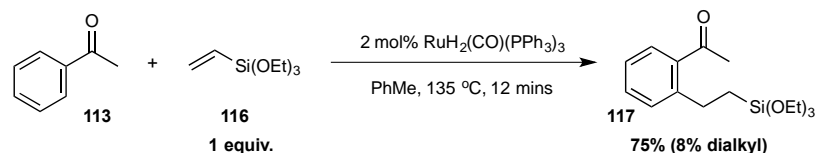
Scheme 1.36 – Murai reaction showing the *ortho* alkylation of 113 with triethoxy(vinyl)silane 116.[67]

The author shows applicability across a small range of acylbenzene derivatives and a small range of mono- and di-substituted olefins. The synthesis of the ruthenium-hydride catalyst is obscure and requires chromatographic purification with benzene eluent, which reduces the desirability of this reaction.[68] This represents a main limitation of this methodology however other groups have developed an *in-situ* protocol for the ortho alkylation based on the Murai reaction.[69]
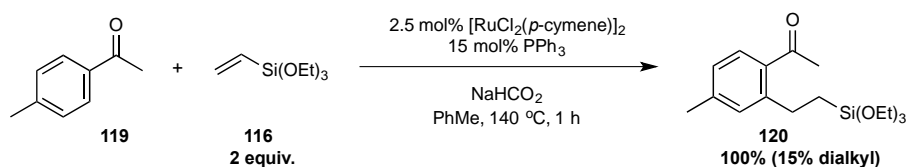
Scheme 1.37 – *Ortho* alkylation of *p*-methylacetophenone 119 with 116 from *in-situ* generated ruthenium catalyst.[69]

By using an *in-situ* generated catalyst there is uncertainty about the true nature of the active catalytic species, however it is able to reproduce the results of Murai: both 75% yielding when considering only mono-functionalisation. The authors show the general applicability across various acylbenzene derivatives similar to those presented by Murai, however they show a wider functional group tolerance that includes imine and α,β-unsaturated amide functionality (**123**) as shown in Scheme 1.38.[69]
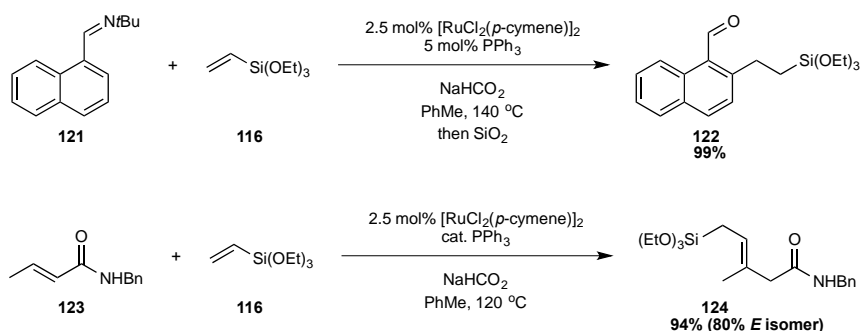
Scheme 1.38 – *Ortho* alkylation of aldimine and α,β-unsaturated amide functionality 123 with *in-situ* generated ruthenium catalyst.[69]

Again, the olefin is a limitation of the reaction as the authors do not evaluate a wider scope beyond **116**, or styrene under more specific conditions (not shown).

Using the ruthenium-hydride catalyst from Murai's work, alkenylation of pivalophenone (**125**) has also been achieved from alkenylboronates like **126**.[70]
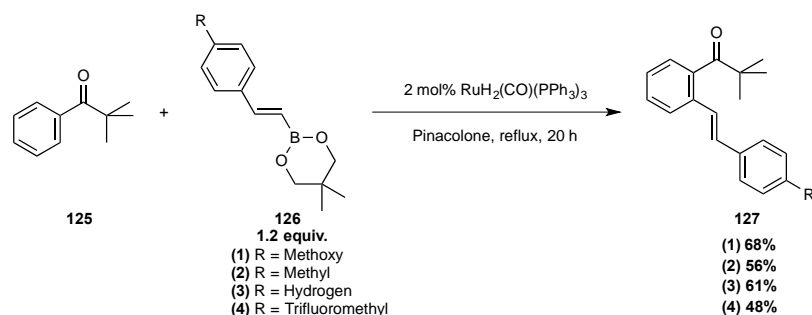
Scheme 1.39 – *Ortho* alkenylation of 125 under ruthenium-hydride catalysis.[70]

Sterically-congested styrylboronate esters were not favoured although the styrylboronate esters could be either electron-rich or electron-poor, with poor to good yields of alkenylated product achieved. The authors note that when a mixture of *E*- and *Z*-alkenylboronate esters is employed ruthenium will isomerise the olefin completely to the *E*-isomer. This was also observed by Inoue *et. al.* in their *ortho* olefination of **102** using a different ruthenium catalyst.[58]
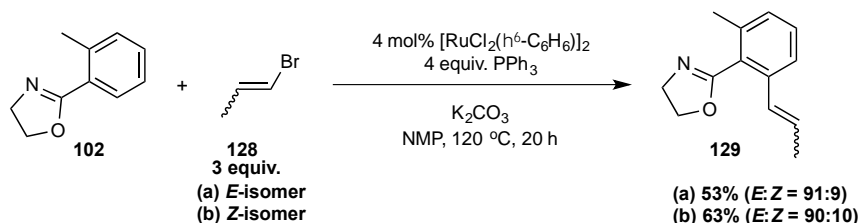
Scheme 1.40 – *Ortho* alkenylation of 102 displaying olefin isomerisation.[58]

As can be seen in Scheme 1.40, no matter which isomer is added into the reaction the isomer ratio is the same. This relates to the mechanism and goes beyond the scope of this discussion. The scope of the alkenes from these authors is also limited to small, unhindered bromostyrenes or bromopropene. In terms of applicability and scope, ruthenium-catalysed alkenylation is limited and is a continuing area of development. Similarly, ruthenium-catalysed directed alkynylation is an area of development but an initial publication proves the competency of ruthenium catalysts.[71]
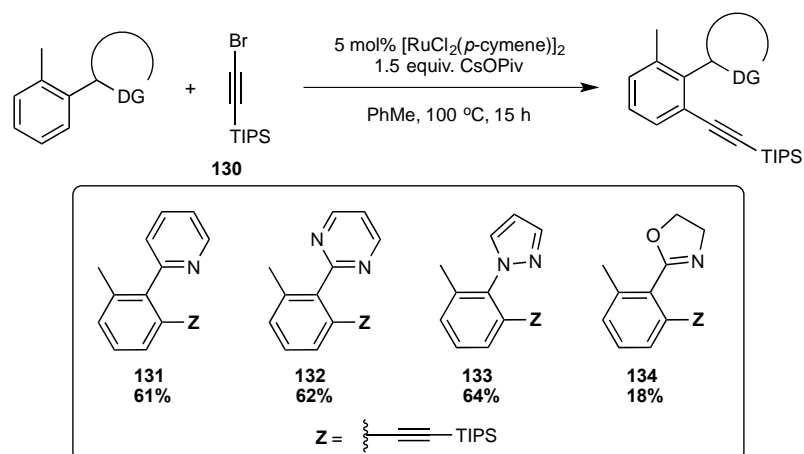
Scheme 1.41 – *Ortho* **alkynylation of various heteroarene substrates under ruthenium catalysis.**[71]

Good yields across various heteroarene substrates were observed but notably poor yields with **134**. The authors did not expand the alkyne scope and only explored the silylbromoalkyne shown in Scheme 1.41. This is reported as the first publication of ruthenium-catalysed *ortho* alkynylation and while competency has been demonstrated there remains a gap in the literature here.

C-N bond forming reactions are medicinally very important as introduced in Section 1.1 through the Buchwald-Hartwig reaction. Complimentary to this C-N bond creation is the ruthenium-catalysed *ortho* amidation of acetophenone derivatives using tosyl azide as shown in Scheme 1.42.[72]
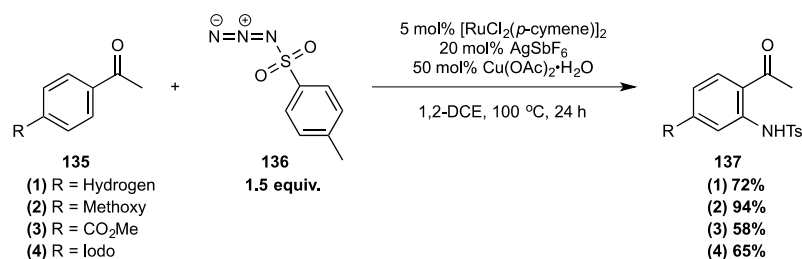
Scheme 1.42 – Ruthenium-catalysed *ortho* **amidation of acetophenone derivatives 135 with tosyl azide 136.**[72]

Electron-rich arylketones are well tolerated and preferred to electron-poor. Halogen-substituted arylketones were tolerated too, notably the iodine in **135(4)** was inert despite being a very labile bond. Aryl-aryl and aryl-alkyl ketones were also well tolerated in good yields. The tosyl azide **136** tolerated *para* substitution and preferred electron-poor substituents (not shown). The transformation doesn't compare to the Buchwald-Hartwig C-N bond forming

reaction in terms of the scope, however in excellent yields it is somewhat complimentary and alternative.

Many other transition metals have been successfully deployed in C-H functionalisations. Metals other than ruthenium include palladium, iron, rhodium and copper each with various degrees of success. Palladium-catalysed C-H functionalisation has been successfully deployed in rare *ortho* selective acylations of 2-phenylpyridine using various benzaldehydes (**138**). An example of this is shown in Scheme 1.43.[73]
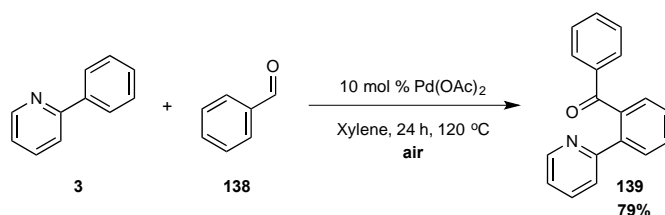
Scheme 1.43 – Regioselective palladium-catalysed directed *ortho* acylation of 3.

With a palladium loading of 10 mol. %, **3** undergoes a ligand-free directed C-H functionalisation with **138** yielding the desired product in a good yield of 79%. The authors do not note if they observed any di-functionalisation or whether exclusively mono-functionalisation is obtained however they do comment that GC-MS and NMR confirmed the product regioselectivity.[73]

While palladium is arguably the most effective and general cross-coupling method, it is very expensive and its use is unsustainable due to its rarity, particularly in 10 mol. % loading as in Scheme 1.43. Interest in using other metals for cross-coupling reactions, and indeed alternative C-C bond forming chemistry, is of interest from a cost, environmental, and sustainability point of view.

Iron is the most abundant metal on earth. It is environmentally benign and of low toxicity. Furthermore, it is inexpensive relative to other, rare, earth metals. In cost terms, $PdCl_2$ costs £4424 per mol while $FeCl_2$ costs just £228 per mol; 19 times cheaper than palladium.[74] Iron has been shown to be competent in C-H functionalisations, for example, consider Scheme 1.44.[75]
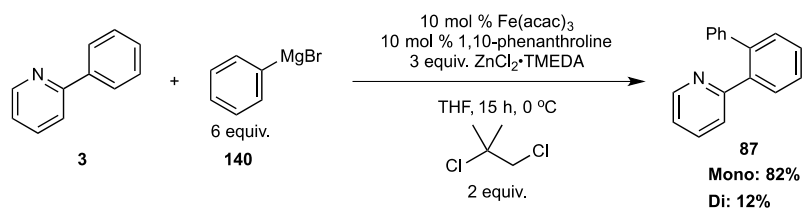
Scheme 1.44 – Iron-catalysed directed *ortho* arylation of 3.[75]

The full mechanism of this iron-catalysed transformation is not known but the authors show that these conditions can successfully arylate a variety of nitrogen-containing heterocycles such as pyridyl, pyrazole and pyrimidine species.[75] While iron is very attractive from a cost point of view, it is notoriously difficult to build any mechanistic understanding of since it can readily occupy a range of oxidation states and it is very sensitive to air and moisture under certain condition. Without a true mechanistic understanding its use becomes limited.

Directed *ortho* C-H functionalisations have been studied extensively. For ruthenium catalysis, much of this research has focussed on heteroarene substrates, such as **3** and examined particularly sp^2-sp^2 C-H coupling with aryl halides. There is a growing precedent of alternative functionalisations using secondary and tertiary alkyl-halides including alkyl chlorides, which are regarded as the most difficult electrophilic partners.

While authors have published increasingly detailed mechanistic studies and robust methodologies to yield *ortho* functionalised products, key understandings of the directing group ability and the balance of reactivity and selectivity are missing from the literature. For example, compare the diarylation preference of **89** in Scheme 1.29 with the monoarylation preference of **3** in Scheme 1.28 under very similar reaction conditions.

The mechanism of carboxylate-assisted ruthenium-catalysed *ortho* functionalisation shall be discussed in the next chapter.

1.3. Mechanism of C-H Activation

While there are several published mechanisms for ruthenium-catalysed C-H functionalisations, this subchapter will focus exclusively on carboxylate- and acetate-assisted ruthenium-catalysed arylation mechanisms because these are the most relevant to the findings presented in this report.

Initial research from Ackermann *et. al.* that set out to understand the mechanism first examined the nature of the active ruthenium catalyst in the presence of carboxylic acid additives,

specifically MesCOOH.[76] In a stoichiometric reaction, the research group isolated the biscarboxylate species according to Scheme 1.45.
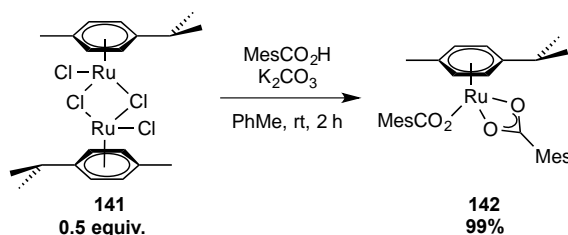
Scheme 1.45 – Synthesis of well-defined ruthenium biscarboxylate complex 142.[76]

Using this well-defined ruthenium complex **142**, the group showed that it was catalytically-competent in a series of heteroaryl *ortho* C-H functionalisation reactions with chlorobenzene derivatives. For example, consider the regioselective *ortho* arylation of a sterically-hindered 2-phenylpyridine **143** derivative in Scheme 1.46.
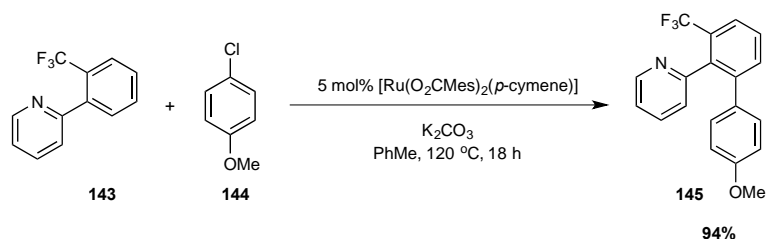
Scheme 1.46 – Regioselective *ortho* arylation using well-defined ruthenium biscarboxylate catalyst 142.[76]

Having demonstrated the competency of this well-defined catalyst across a series of heteroarenes that include pyridine, pyrazole, oxazoline and triazole, the authors then form a cyclometalated ruthenium-substrate complex from the biscarboxylate catalyst and identify this as a key intermediate in the catalytic cycle (**146**, Scheme 1.47). Furthermore, they showed that this well-defined complex was catalytically-competent through the stoichiometric addition of **144** as shown also in Scheme 1.47.
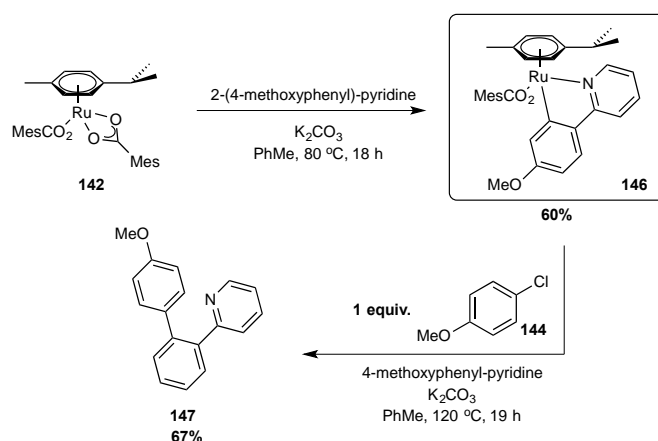
Scheme 1.47 – Synthesis of well-defined ruthenium-substrate metallocycle 146.[76]

The reader will indeed note that the authors inexplicably added an additional quantity of 4-methoxyphenylpyridine to the reaction to yield the isolated product shown and so therefore the competency of this intermediate cannot be fully concluded.

Jutand *et. al.* take a more in-depth examination of the catalytic process through a series of kinetic experiments using less bulky acetic acid in acetonitrile *in lieu* of MesCOOH in toluene. Their kinetic experiments show that there is an equilibrium process occurring as shown in Scheme 1.48.
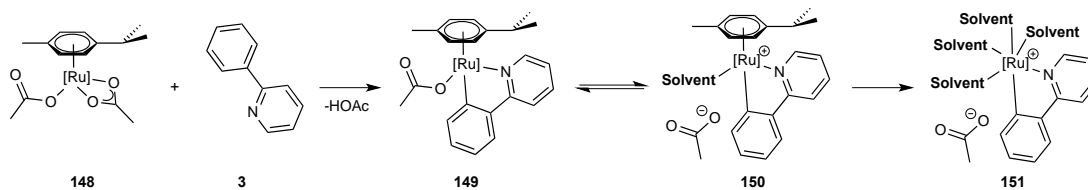
Scheme 1.48 – Equilibrium of the formation of cyclometalated ruthenium-2-phenylpyridine complex.[77]

From Scheme 1.48, they show that indeed ruthenium-bisacetate **148** forms cyclometalated complex **149** first but that over time an equilibrium exists wherein dissociation of acetate gives cationic complex **150**. Over prolonged times, solvent coordination leads to the irreversible removal of the *p*-cymene ligand in complex **151**.

The authors had difficulty obtaining a pure isolated sample of complex **149** to test for oxidative addition as Ackermann *et. al*. tested and so were unable to conclusively say if this species is catalytically competent. They isolated pure samples of complexes **150** and **151** and showed that complex **150** is catalytically competent but that complex **151** is not, as shown in Scheme 1.49.
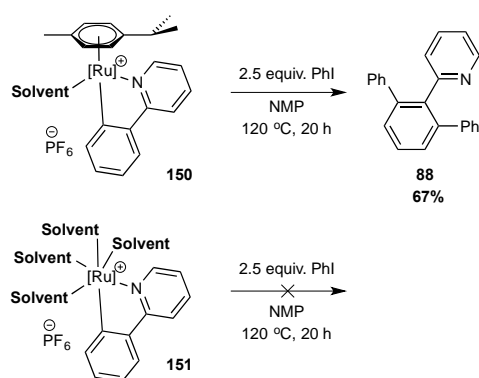
Scheme 1.49 – Oxidative addition of iodobenzene to cyclometalated complexes 150 and 151.[77]

Examining the formation of complex **149** more closely, Jutand *et. al*. find that the acetic acid coproduct increases the rate of formation of complex **149** in an autocatalytic process. With one equivalent of acetic acid added to the reaction, the rate of formation is significantly increased, requiring only 5 mins instead of 45 mins; added acetate salt also increases the rate of formation of complex **149**. Conversely, added base significantly decreases the rate of formation of complex **149** due to the neutralisation of the acetic acid coproduct. This confirms the autocatalytic process.

Based on this evidence, they propose an intermolecular S_E3 deprotonation mechanism since an intramolecular deprotonation should have no change in rate of formation with added acetate salt and this is shown at the centre of Scheme 1.50.[77]

Jutand *et. al.* find that when cyclometalation experiments were conducted at room temperature in deuterated acetonitrile with added deuterated water there was no incorporation of deuterium on 2-phenylpyridine. This indicated the cyclometalation step is irreversible. This contradicts Ackermann *et. al.* who completed a similar experiment with isotopically-labelled starting materials and showed a reversible C-H bond deprotonation metalation step based upon an observed D/H exchange.[76] Jutand *et. al.* use acetonitrile which is coordinating and polar, whereas Ackermann *et. al.* use non-polar toluene. With each author also using a different ligand set, this could explain the difference in findings of reversibility.

Based upon their findings from the kinetic experiments Jutand *et. al.* propose a catalytic cycle shown in Scheme 1.50.[77]
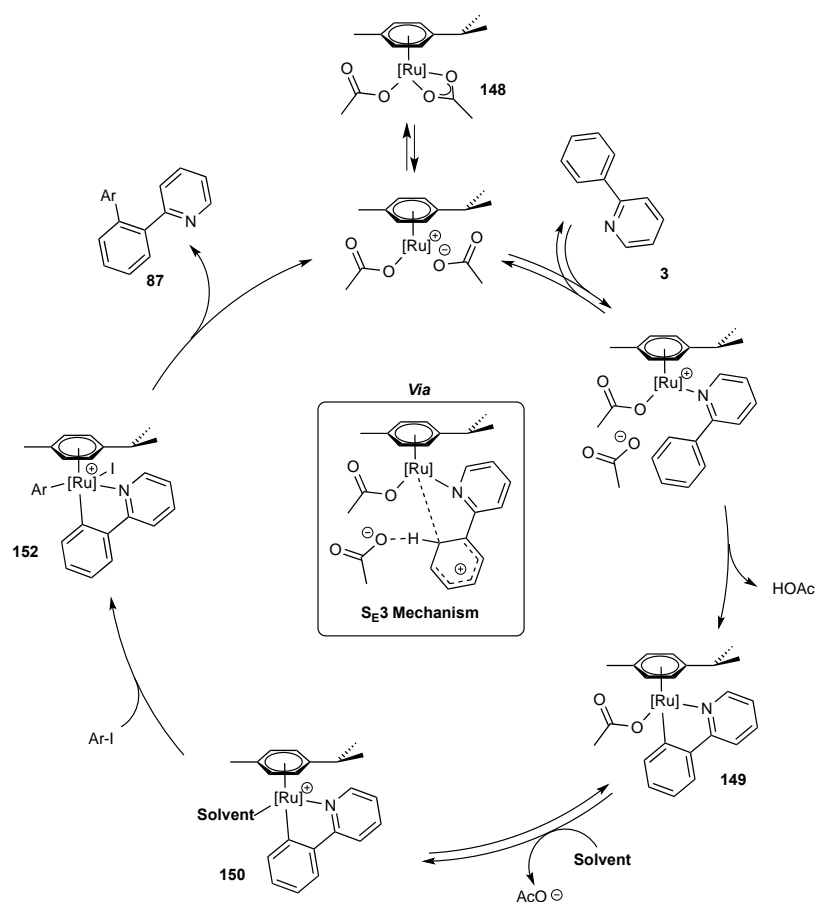
Scheme 1.50 – Carboxylate-assisted ruthenium-catalysed *ortho* C-H functionalisation of 3.[77]

Dissociation of acetate ligand from ruthenium-bisacetate **148** creates a cationic ruthenium centre than can reversibly coordinate **3** through lone-pair donation. An irreversible intramolecular deprotonation ensues via an S_E3 mechanism releasing acetic acid. The acetic acid functions in an autocatalytic process thus increasing the rate of formation of the cyclometalated ruthenium complex. Reversible dissociation of acetate ligand from the ruthenium-substrate complex creates cationic ruthenium centre **150** that oxidatively adds iodobenzene in the rate-limiting step. Irreversible reductive elimination yields **87** and regenerates the catalyst.

2. Aims

By focussing exclusively on a ruthenium-catalysed C-H activation strategy, and employing substrates capable only of directing group control of selectivity, this thesis will focus on building a qualitative and quantitative scale of directing group ability through a series of inter- and intramolecular competition reactions. This thesis will meet this object through several key steps:

- Identification of the scope of substrates suitable for competition reactions. An examination of the literature will be conducted to establish common substrates employed.
- Selection and testing of suitable reaction conditions for competition reactions.
- Identification and calibration of instrumentation for monitoring the competition reactions. Calibration is essential to ensure each reaction outcome can be compared directly through response factors unique to each substrate.
- Completing a series of competition reactions to develop a qualitative and quantitative scale of directing group ability. Relative rate data will be calculated using a least squares minimisation model of data obtained from competition reactions.
- Exploring the predictive ability of a quantitative scale of reactivity through intramolecular competition reactions. Using the qualitative scale as a predictive model, experimental intramolecular competition reactions will be used to test the predictability.

3. Results

3.1. Exploring Reaction Conditions

Nitrogen containing heterocycles are widely used throughout the literature for C-H activation chemistry because the lone pair on nitrogen readily facilitates functionalisation on the adjacent arene ring by coordinating to the metal centre. This directing group power is shown in Scheme 3.1 and is typically *ortho* directed with >99% selectivity.
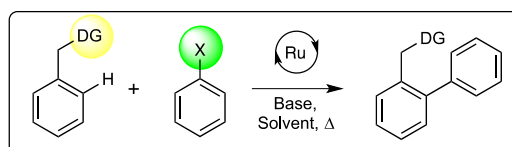
Scheme 3.1 - Directed arylation under ruthenium catalysis with aryl halide.

Arylation of nitrogen containing heterocycles with chlorobenzene was chosen as a model reaction due to its simplicity and the availability of the starting materials. Substrates such as 2-phenylpyridine are explored extensively in this type of chemistry and these nitrogen containing heterocycles, and aryl halides, are readily available from commercial sources.

In the literature there are very few systematic studies in which comparisons are made between different directing groups. There many examples of ruthenium-catalysed arylation, alkylation, alkenylation as well as oxidation.[56,59,78] Most arylation reactions seem to be pyridine[57] or oxazoline[58] or imine-directed,[64] while carbonyl-based groups appear to be widely used only for oxidation chemistry or arylation reactions with boronate esters.[79,80] Some selected examples of these are shown in Figure 3.1.

In these examples, an η^6-benzene ruthenium catalyst ligated with triphenylphosphine is used to arylate these substrates with bromobenzene as the aryl halide source in slight excess. 2-Phenylpyridine and *N*-(1-phenylethylidene)aniline arylate with high yields of 81 and 73% respectively, both showing promising preference for monoarylation. 2-Phenyloxazoline shows a poorly yielding reaction of 60% with a distinct preference for diarylation despite there only being a slight excess of bromobenzene. The oxidation of 2-*tert*butyl-acetophenone is interesting as a different class of functionalisation, the mechanism of which is not fully established; however, this type of oxidation chemistry will not be discussed further.
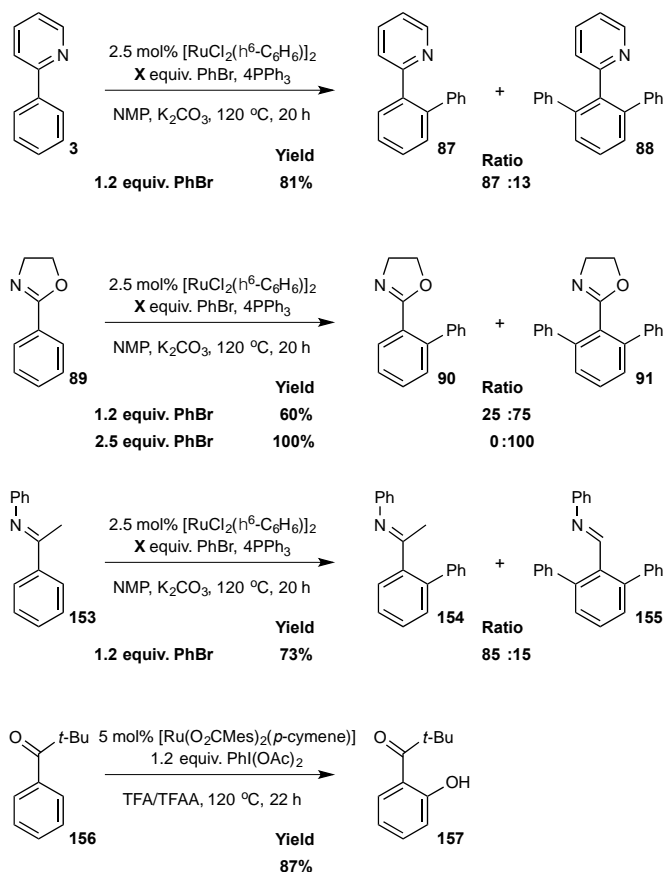
Figure 3.1 – Selected examples of arylation of 3, 89, and imine 153, and oxidation of ketone 156, under ruthenium catalysis.

Some substrates known to direct C-H activation under ruthenium catalysis, and some that have not yet been tested, are shown in Figure 3.2.
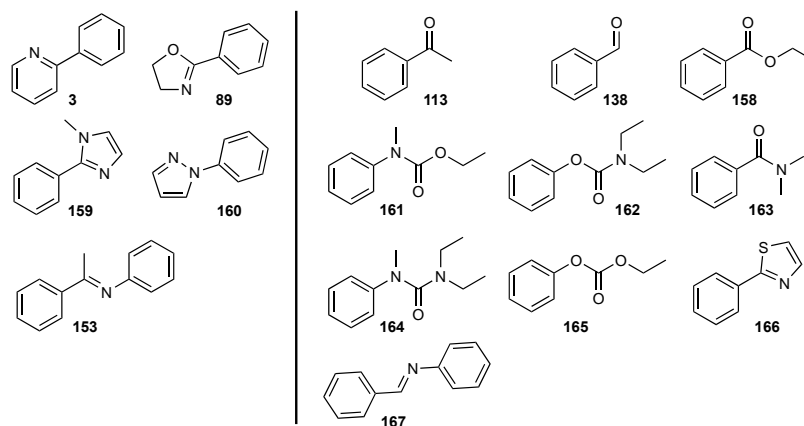
Figure 3.2 – List of substrates that may direct *ortho* arylation under the test reaction conditions.

During the initial phases of the research it was identified that –OH and –NH functional groups were problematic for GC analysis as the corresponding peaks were generally broad and could

not be accurately integrated with confidence. To overcome this, these groups were either avoided or protected by methylation. This is shown in the case of *N*-methyl-2-phenyl-imidazole **159** or in *N,N*-dimethyl-benzamide **163** in Scheme 3.2 and Figure 3.2 respectively.

On the left hand side of Figure 3.2, **3**, **89**, and 2-phenylpyrazole (**60**) were purchased from commercial sources. **159** and *N*-(1-phenylethylidene)aniline (**153**) were synthesised according to Scheme 3.2.
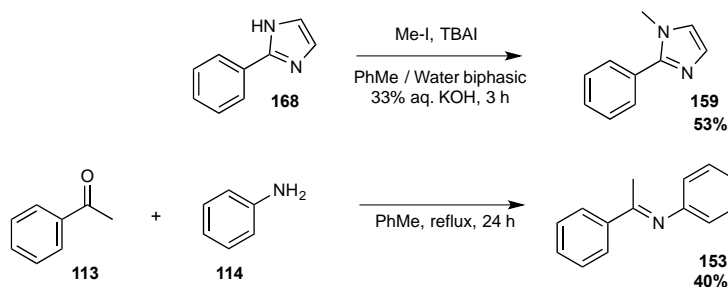
Scheme 3.2 – Preparation of 159 and 153 for use in competition experiments.

The synthesised products were purified before experimental reactions commenced and GC-FID calibrations were completed (*vide infra*). **158** crystallised spontaneously from the crude reaction mixture upon sitting forming yellow needles. **153** was purified by Kugelrohr distillation giving a yellow solid. Characterisation data were obtained for each purified product; for more information see the Experimental section.

For the purposes of GC calibration the monoarylated products from all substrates were prepared. Excluding **153**, all products were synthesised under ruthenium catalysis following Scheme 3.3 and purified using column chromatography according to the Experimental section. 0.5 equivalents of chlorobenzene (**169**) was used to inhibit diarylation in the product mixture.[76]
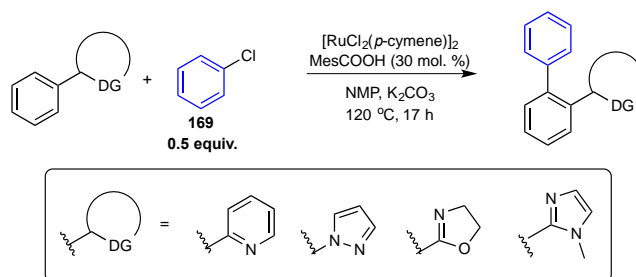
Scheme 3.3 – General procedure for the preparation of monoarylated products for calibration of GC-FID.

The monoarylated product of **153** was synthesised according to Scheme 3.4 (**172**). A palladium-catalysed Suzuki cross-coupling was used here because the ruthenium catalysed method was unable to generate the quantities needed for purification and GC calibration. As will be shown later, **153** is a weaker directing group under the ruthenium-catalysed reaction conditions explored.
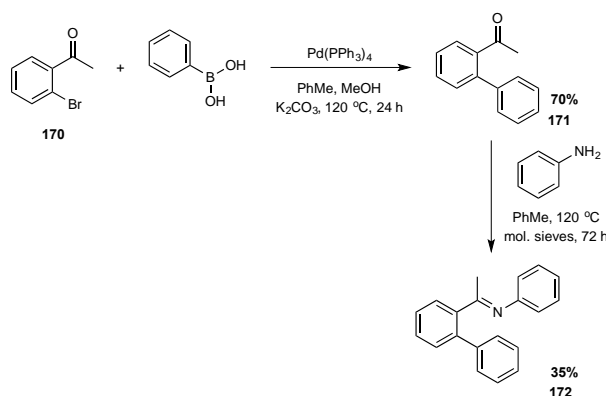
Scheme 3.4 - Synthesis of 172 for GC-FID calibration.

The substrate list in Figure 3.2 represents a range of species with varying expected degrees of arylation based on the current literature. For example, *ortho* arylation of pyridyl, oxazoline, and imine functionality is shown in Figure 3.1.

It was of interest to determine which substrates would arylate so that these could be followed in competition experiments. Well-defined [Ru(O$_2$CMes)$_2$(*p*-cymene)] **142** was used in the model reactions as the active catalytic species. A well-defined catalyst is used to eliminate any variable around the pre-formation of the catalyst in the reaction solution but it also ensures that the reactions receive the optimal ratio of metal to ligand. Because it is synthesised in advance, the purity can be tested to ensure the active catalyst is the species it should be using techniques including NMR spectroscopy and microanalysis. This is synthesised as shown in Scheme 3.5.
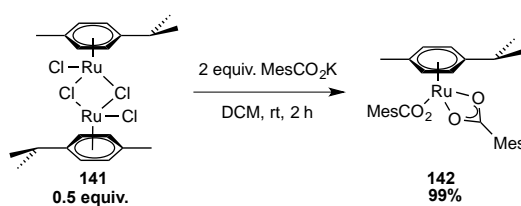
Scheme 3.5 - Synthesis of well-defined ruthenium biscarboxylate catalyst 142.

Reaction conditions were chosen based on conditions used successfully by Ackermann *et al.* in ruthenium-catalysed C-H activation chemistry.[76] The catalyst was used in 5 mol% loading with 0.2 mmol substrate and 0.05 mmol chlorobenzene. K_2CO_3 was used in 2 equiv. with respect to chlorobenzene. The reaction conditions chosen are shown in Scheme 3.6.
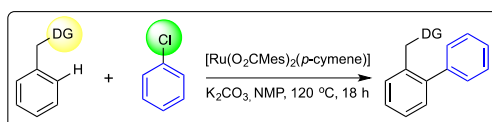
Scheme 3.6 - Reaction conditions for the ruthenium-catalysed *ortho* arylation of substrates.

The reaction conditions chosen were to avoid experimental issues identified during preliminary experiments. These were: using more polar *N*-methyl-2-pyrrolidone (NMP) over toluene due to random non-starting of some experiments, and using less than one equivalent of chlorobenzene to prevent diarylated substrate being produced. NMP, toluene and *m*-xylene are very commonly used in these ruthenium-catalysed C-H activation reactions.[56] Additionally, greener solvents such as diethylcarbonate and water have been published.[56,81,82] More rarely one can also find DCM, DMF and DCE being used too.[56]

Under these conditions only some heterocycles were successfully arylated. These are shown in Figure 3.2 on the left hand side. These five substrates were chosen from the list to be followed in competition experiments. These were 2-phenylpyridine **3**, 2-phenyloxazoline **89**, 2-phenylpyrazole **160**, *N*-methyl-2-phenyl-imidazole **159**, and *N*-(1-phenylethylidene)aniline **153**. Interestingly, these substrates all contain nitrogen as a directing group for the C-H activation and react via a 5-membered metallocycle as shown in Figure 3.3. With the exception of **153**, these substrates are all nitrogen-containing heterocycles.
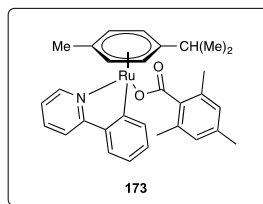
Figure 3.3 – Five-membered ruthenium-substrate metallocycle intermediate.

In Figure 3.2 the right hand side displays the substrates that did not present arylated product on the time scale examined as determined by GC-FID analysis. As GC-FID is a very sensitive technique, with an approximate lower limit of detection of 2% material, any small peaks in the GC trace would be easily identified and integrated. These unsuccessful substrates include carbonyl directing groups, which are generally weaker directing groups than nitrogen groups under these ruthenium-catalysed conditions,[83] and carbonate and carbamate functionality as well as esters and amides.

The unsuccessful list also contains substrates that would react via a 6-membered metallocycle. Six-membered transition states will have a different metallocycle strain than 5-membered transition states due to the increased ligand angle. It could rationally be assumed that these would proceed at a different energy cost. A larger 6-membered metallocycle would change the coordination chemistry at the metal centre and may compress or expand the angles between the other ligands. Surprisingly the aldimine **167** was unreactive under these reaction conditions and suggests that the ketimine family has an increased stability at the metallocycle stage of the reaction. In addition, it is surprising that 2-phenylthiazole (**166**) is also unreactive. This nitrogen containing heterocycle would progress via a 5-membered metallocycle in an *N*-directed C-H activation however arylated product was never identified under the reaction conditions tested. This is despite 2-phenyloxazoline **89** being reactive, a similar heterocyclic substrate. At present, and to the best of our knowledge, there is only one publication showing the arylation of **166** using a similar ruthenium-catalysed C-H activation approach as shown in Scheme 3.7.[59]
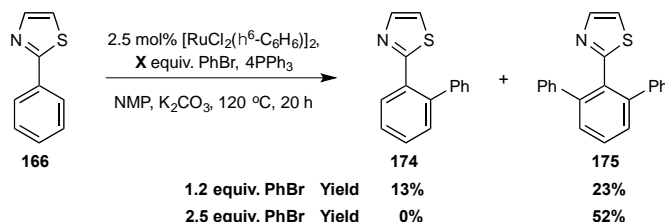
Scheme 3.7 – Ruthenium-catalysed C-H activation of 2-phenylthiazole.

Under a similar ruthenium-catalysed system employing a triphenylphosphine ligand and bromobenzene, a more labile electrophile than chlorobenzene, the authors find a weakly progressing reaction with a preference to diarylate. With 1.2 equivalents of bromobenzene only 36% yield is obtained as a mainly diarylated mixture of products, and with an excess of aryl bromide 52% yield is obtained exclusively as diarylated. While an increase in the number of equivalents of aryl halide increases the rate of the reaction, it also increases the diarylation and this difference in reactivity is not well understood in the literature. Recalling Figure 3.1, 2-phenyloxazoline also displays a preference to diarylate in a slow progressing reaction yielding 60% of a 25:75, mono:diarylated, product mixture.

The unsuccessful substrates may arylate over a longer time scale under the reaction conditions examined or under more forcing conditions however this has not been explored since catalyst decomposition might compete on a longer timescale, especially given the quite forcing conditions.

3.2. Calibrated Gas Chromatographic Analysis

The five substrates that were selected for competition experiments were reacted according to Scheme 3.6 with each substrate loaded in 0.1 mmol each (0.2 mmol total). These reactions were on such a small scale to increase throughput and to efficiently use material. Yields were not important in this study, only conversion data were used from GC chromatographs, therefore a smaller scale is sufficient.

GC-FID analysis was selected as the most appropriate technique to quantify the conversion of each reaction outcome. Due to the small scale, isolated yields would be very hard to accurately quantify with high reproducibility and would also be lengthy in time for each reaction. NMR is also unsuitable because the complex reaction mixture would have many overlapping signals in the aromatic region that would be difficult to assign to any one substrate or product. While GC-MS can also resolve the reaction components, it is difficult to achieve robust quantitative analyses and hence GC-FID was selected.

In order to ensure that the responses obtained from GC analysis are representative, tetradecane was used as an internal standard for each reaction. This ensures data reliability and was reinforced by completing a calibration of the GC-FID for each substrate and each monoarylated product. Tetradecane was chosen as an internal standard as it is unreactive towards any of the substrates, it is not volatile under reaction conditions, and it is resolved on the GC trace.

A known quantity of both substrate and tetradecane was mixed covering a range of substrate/tetradecane ratios. A nominal substrate to tetradecane ratio range of 0.05 to 5 was used because the concentration of the reactions explored would fall into this range. The monoaryl product of 2-phenylpyridine was synthesised and calibrated by a member of our group.[84]

Using *N*-methyl-2-phenyl-imidazole as an example, Figure 3.4 shows the calibration line of the substrate and the monoarylated *N*-methyl-2-phenyl-imidazole both of which display excellent analytically acceptable R^2 values > 0.999 and a linear relationship. This is important as it shows that the detector in the GC is not being saturated by the material and therefore calculating inaccurate quantitative information.
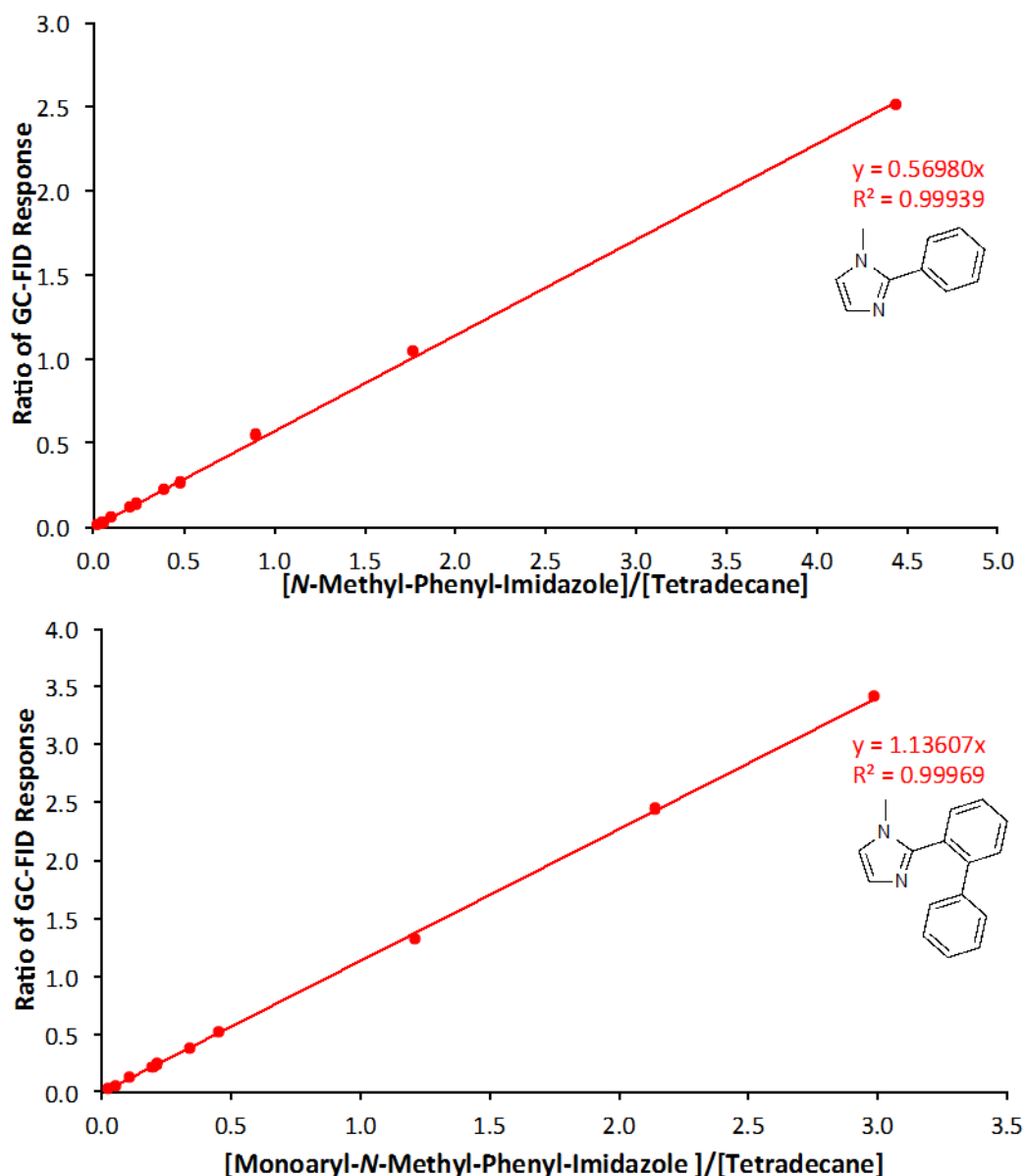
Figure 3.4 - Calibration lines for (a) *N*-methyl-2-phenyl-imidazole, and (b) monoaryl-*N*-methyl-2-phenyl-imidazole.

The slope of each line was used as the response factor for each substrate and each monoarylated product. With each competition experiment, the GC trace will show a response for each substrate and product that can then be divided by the response factor. This transforms the data into relative concentrations. This is a rigorous approach that allows for very accurate quantitative analysis of the data. This approach must be used because some response factors are hugely different as seen in Table 3.1.

Table 3.1 – Substrate and Monoaryl product response factors from GC-FID calibration.[84]

Entry	Substrate	Substrate Response Factor	Monoaryl Product Response Factor
1	2-Phenylpyridine **3**	0.70655	1.19858
2	2-Phenyloxazoline **89**	0.49460	0.60715
3	2-Phenylpyrazole **160**	0.53038	0.94125
4	*N*-(1-phenylethylidene)aniline **153**	0.88910	1.40340
5	*N*-methyl-2-phenyl-imidazole **159**	0.56980	1.13607

The importance of making GC-FID calibrations is evidenced when comparing the substrate response factors with the product response factors for both entries 4 and 5. In these entries, the product response is approximately double the substrate. If the instrument was not calibrated and the response factors not obtained then calculations would underestimate the substrate concentration and overestimate the product concentration.

3.3. Competition Experiments

The substrates in the left hand side of Figure 3.2 were explored in competition experiments. This was of interest to establish, qualitatively and quantitatively, which of these substrates reacts the quickest. This could then be used to build up a scale of relative reactivity.

From the literature, competition experiments have previously been used to demonstrate the preferential electronic properties of 2-substituted phenylpyridines.[76] This is shown in Scheme 3.8.
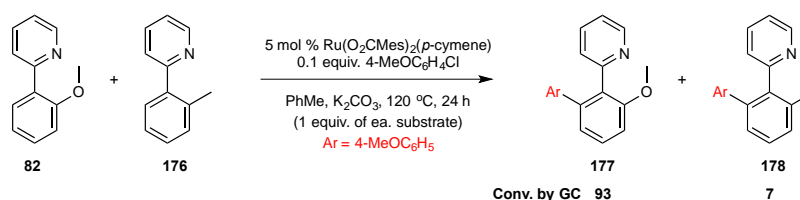
Scheme 3.8 - Competition experiment of 2-substitued phenylpyridines.[76]

This is the only example offered in this paper. The substitution of the 2-position on the phenyl ring is used to force monoarylation of each respective substrate. This is different from the system explored in this thesis wherein two different compounds react in competition.

Furthermore, the paper does not mention if the GC analysis is calibrated therefore accuracy cannot be concluded in conversion data. In addition, this example only compares two substrates here and does not easily allow a scale of reactivity to be created.

Another approach to competition-type reactions may be to build up profiles of the product concentrations against time. Similar work has been completed within this research group, for example consider Figure 3.5 in which a reaction profile has been established for the ruthenium-catalysed arylation of 2-phenylpyridine with 1 equivalent of PhCl.[84] The reaction profiles very effectively display qualitative rate information from the profile curves, however this type of reaction profiling would be very time consuming and limits higher throughput because the work would be very demanding for each profile and each substrate. In addition the reaction profiling suffers from reproducibility problems as evidenced for the arylation of 2-phenylpyridine in Figure 3.5.
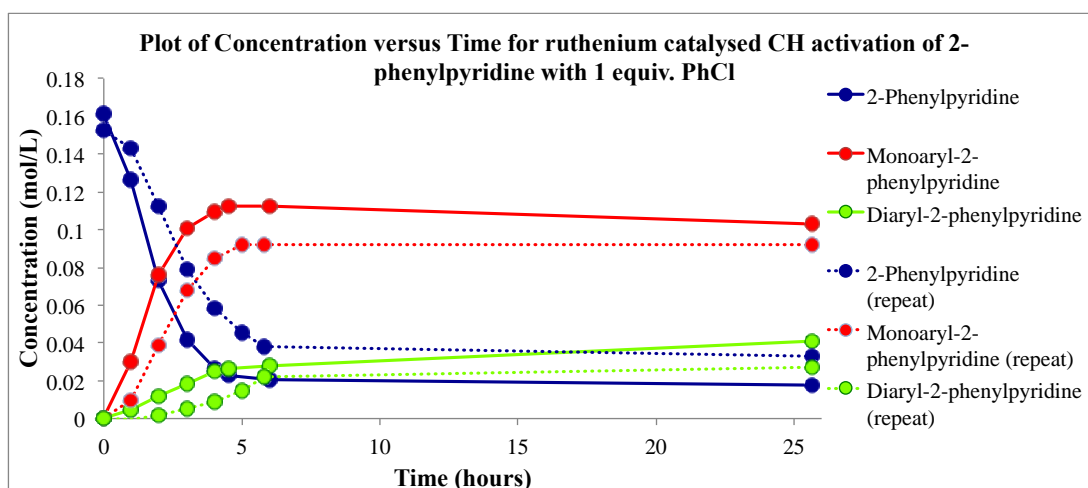
Figure 3.5 – A plot of concentration versus time showing the reaction profile of the arylation of 2-phenylpyridine with 1 equiv. PhCl.
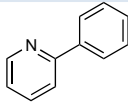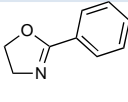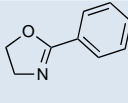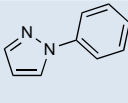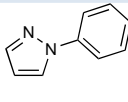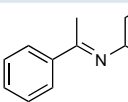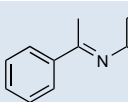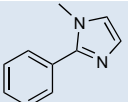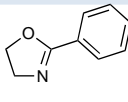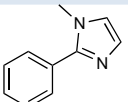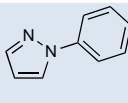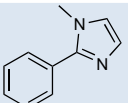
Herein, two substrates were combined in 0.1 mmol each (0.2 mmol total) according to Scheme 3.9. This method offers both a qualitative idea of directing group power and a qualitative scale from a single time point of 24 h.
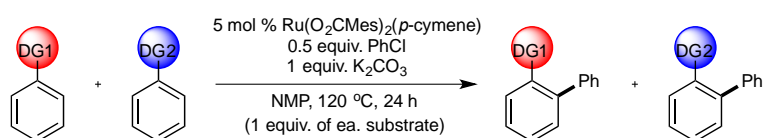
Scheme 3.9 - General experimental conditions of competition reactions.

45

Each substrate was compared to each other substrate in competition in at least duplicate. This was to ensure reproducibility and to gain average data. A sample of conversion data obtained from calibrated GC analyses is shown in Table 3.2.

Table 3.2 – Sample conversion data from competition experiments.

Entry	Substrate 1	Substrate 2	Repeat A		Repeat B	
			Conv. 1 (%)	Conv. 2 (%)	Conv. 1 (%)	Conv. 2 (%)
1	**3**	**89**	43	34	49	18
2	**89**	**160**	19	32	18	37
3	**160**	**153**	42	3.7	43	3.7
4	**153**	**159**	4.9	34	7.1	39
5	**89**	**159**	17	34	18	36
6	**160**	**159**	24	19	25	18

The data presented in Table 3.2 show an observable difference in competitive reactivity for each substrate based on calibrated conversion alone. From Table 3.2, **3** > **89** (entry 1) while **160** > **89** (entry 2). **160** > 159 > **89** (entries 5 and 6). **153** is the weakest across all substrates. This can be summarised according to Figure 3.6.
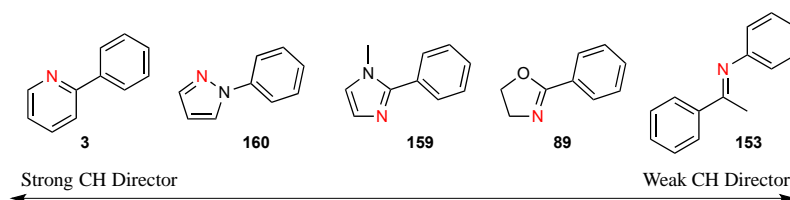
Figure 3.6 – Qualitative reactivity scale developed from calibrated conversion data.

The experimental data are very reproducible across two repeats; for example the conversion of Substrate 1 in entries 2, 3, 5, and 6 shows 1% difference. However **89** showed poor reproducibility, going from 34% conversion to 18% conversion in entry 1.

The reproducibility can be accounted for considering the poor GC-FID peak shape of **89** and monoarylated 2-phenyloxazoline (**90**), which can be seen as a broad peak at 14.7 min in Figure 3.7. This makes accurate integration difficult.
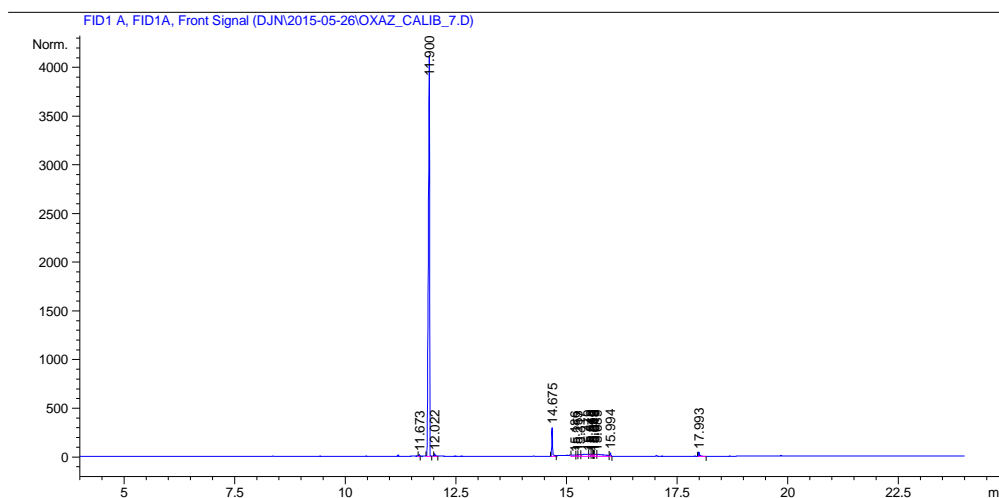
Figure 3.7 – GC-FID calibration of 89 showing poor peak quality.

The substrate is one of the weaker directing groups based on the qualitative reactivity scale in Figure 3.6. Additionally, **89** has a preference for diarylation under ruthenium-catalysed conditions as demonstrated earlier in Scheme 1.29. Therefore the use of this substrate in C-H activation is potentially very limited under these conditions.

From a single time point, competitive reactivity has been examined using conversion as determined by calibrated GC-FID. These data yielded valuable quantitative information and a qualitative scale of reactivity. The next chapter shall focus on turning this qualitative information into a predictable quantitative scale.

3.4. Linear regression

With a qualitative scale of reactivity successfully generated it was of interest to develop this into a quantitative scale. Since a qualitative scale can predict the favourable position of arylation, a quantitative scale will allow predictions about the proportions of each arylated product from reactions. A selectivity ratio of >90:10 is a valuable and synthetically useful ratio because it shows that the reaction is efficiently yielding desired product and that waste of products and starting materials is reduced. A reaction with a poor selectivity can have longer

and more complicated separation steps and it makes the reaction less valuable and usable in synthesis.

In 2010, Mayr used a series of competition experiments to determine the influence of differently substituted aryl bromides in palladium-catalysed Negishi cross-coupling reactions as a means to develop a greater understanding of the mechanism of the reaction.[85] The experimental conditions are detailed in Scheme 3.10.
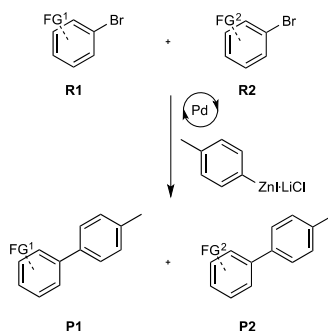
Scheme 3.10 – Palladium-catalysed Negishi competition experiments.

They achieved a greater understanding of palladium-catalysed Negishi cross-coupling by combining two differently substituted aryl bromides, **R1** and **R2**, with less than one equivalent of 4-tolylzinc iodide/lithium chloride thus creating the competition environment. The yield of the reaction is then obtained by the ratio [**P1**]/[**P2**] extracted from GC analysis.

In this Negishi competition experiment, a series of relative reactivities for **R1** and **R2** can be calculated from equation (1) in which κ is the competition constant, k is the rate constant, $[\mathbf{P}X]_t$ is the gas chromatographically determined concentration of product X at time t, and $[\mathbf{R}X]_t$ is the gas chromatographically determined concentration of substrate X at time t.

$$\kappa = \frac{k_1}{k_2} = \frac{\log(1+[\mathbf{P1}]_t/[\mathbf{R1}]_t)}{\log(1+[\mathbf{P2}]_t/[\mathbf{R2}]_t)} \qquad \textbf{Equation (1)}$$

Additionally it was shown through a series of time-control experiments that the competition constant κ is time-independent. With the complete dataset in hand, solving the series of overdetermined linear equations using least squares minimisation yields relative rate constants for each of the substrates.

In Mayr's data, bromobenzene is taken as the reference substrate ($k_{rel} = 1$) and all substituted bromobenzenes examined are quantified relative to this. In this data set, 2-phenylpyridine has been taken as the reference substrate ($k_{rel} = 1$) and all other substrates are quantified relative

to this. This makes it simpler to refer to the results of the experimental and adds value to their meaning. Part of Mayr's quantitative reactivity scale is shown in Figure 3.8.

Figure 3.8 – Mayr's quantitative reactivity scale for the oxidative addition of substituted arylbromides in palladium-catalysed Negishi cross couplings.

The methodology for Mayr's quantitiative scale is best demonstrated as a flow chart as shown in Figure 3.9.

Figure 3.9 – Flowchart showing the process to determine refined final rate constants for a given substrate set.

The experimental dataset is a series of experimentally obtained competition constants, κ_{exp}, for each competition reaction. These data are obtained from GC-FID analysis of each competition reaction. In this study the sum of least squares minimisation is calculated from linear regression using Microsoft Excel Solver.

For this study, each substrate was initially assigned an arbitrary rate constant of $k = 1$ and at this stage 2-phenylpyridine is fixed ($k_{rel} = 1$). This means that each substrate's rate constant determination will be relative to 2-phenylpyridine. From these values, calculated competition constants are obtained, κ_{calc}.

Next, the experimental competition constants κ_{exp} and the calculated competition constants κ_{calc} are compared and their differences minimised as the sum of least squares. Here we see that the arbitrary rate constant values that were assigned to each substrate are refined to obtain a value of least error in comparison to the experimental data. These refined calculated rate constants, k_1, k_2 etc., in-turn refine the calculated competition constants κ_{calc}. This cycle repeats until both κ_{exp} and κ_{calc} agree with a minimised error. This process determines the finalised rate constants for each substrate.

A graph of κ_{exp} versus κ_{calc} shows a linear relationship and hence a correlation with minimal error between both experimental and calculated data. This is shown in Figure 3.10.

Figure 3.10 – Plot of κ_{exp} versus κ_{calc} showing linear relationship.

From the data set, a series of relative rate constants has therefore been calculated and this is presented in Figure 3.11.

Figure 3.11 – Quantitative scale of reactivity developed from competition reactions.

From Figure 3.11 it can be seen that **3** is the strongest C-H activation director in the series. The second strongest directing group is **160** which is approximately 3-fold weaker than **3**. **160**, **159**, and **89** are similar to one another in relative reactivity terms. The weakest C-H activation director is **153** at approximately 30 fold weaker than **3**. Overall these data show a reactivity

range of 10^2. It is interesting to note that the data agree with the qualitative scale shown in Figure 3.6.

It is generally accepted that >90:10 site selectivity is synthetically useful because in this ratio the reaction is efficiently producing the desired product in high amounts therefore wastage of product and starting material is reduced. Additionally, high selectivity ratios may reduce the purification steps needed or simplify them. The reactivity differences observed in this study are useful, particularly for the weakest directing group, **153**. In the case of a substrate that contains two different functional groups, consider that shown in Figure 3.12, then a qualitative prediction of site regioselectivity and a quantitative prediction of the arylated product ratio is a valuable synthetic understanding.
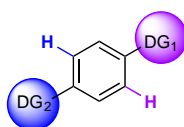
Figure 3.12 – Example of bifunctional intramolecular substrate to demonstrate site regioselectivity options.

The rate constants for the five substrates examined are able to provide such a quantitative prediction and this is shown in Table 3.3 wherein the relative proportions of each product from an arylation reaction are displayed.

Table 3.3 – Quantitative prediction of percentage site regioselectivity for a bifunctional substrate containing directing group 1 competing with directing group 2.

Substrate	Directing group 1 (pyridine)	(pyrazole)	(imidazole)	(oxazoline)	(imine)
(pyridine)		28%	19%	15%	3%
(pyrazole)	72%		37%	31%	7%
(imidazole)	81%	63%		43%	12%
(oxazoline)	85%	69%	57%		15%
(imine)	97%	93%	88%	85%	

Travelling down the columns of Table 3.3, the reader finds the predicted percentage of arylation at the site adjacent to directing group 1 when in the presence of directing group 2. With *N*-(1-phenylethylidene)aniline as directing group 2, 2-phenylpyridine, 2-phenylpyrazole, and *N*-methyl-2-phenyl-imidazole show synthetically useful site selectivity with predicted arylation next to the stronger directing group of 97%, 93%, and 88% respectively. Additionally, with *N*-(1-phenylethylidene)aniline as directing group 2, the data also predict a high percentage of arylation adjacent to 2-phenyloxazoline with 85% predicted arylation. These predictions were anticipated since *N*-(1-phenylethylidene)aniline is a very weak directing group relative to the others examined.

To the best of our knowledge, the quantitative scale presented in this thesis is the first scale based on a ruthenium-catalysed system and indeed the first for any catalyst system. Sanford *et. al.* have published similar insights into directing group ability in a palladium-catalysed C-H acetoxylation of various benzylheterocycles.[86] The author's *qualitative* directing group scale is presented in Figure 3.13 and it shows similarities when compared to the conclusions of this thesis' scale, which is shown in Figure 3.11.
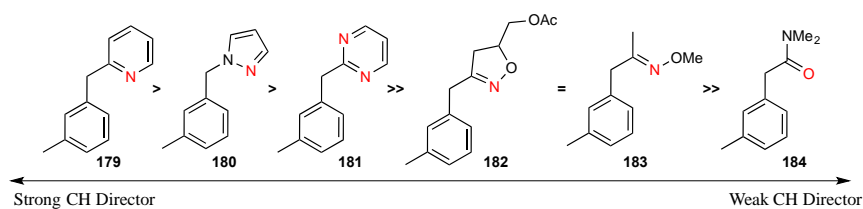
Figure 3.13 – Qualitative directing group scale for palladium-catalysed acetoxylation of benzylheteroarene substrates in AcOH/Ac₂O solvent.[86]

Generally, the authors find that more basic directing groups such as the pyridine (**179**) and pyrazole (**180**) groups are stronger C-H directors than less basic groups such as the oximes **182** and **183**. This is similar to this work's scale where the pyridine is also the strongest C-H director, and the imine is the weakest, with the pyrazole and oxazoline in the same order.

The work presented in this thesis opens an interesting avenue of intramolecular site selectivity and developing an experimental understanding of these site predictions will add strength to the research findings.

3.5. Intramolecular Systems

3.5.1. Developing Intramolecular Systems

With a route to a reproducible and predictive qualitative and quantitative reactivity scale thoroughly demonstrated, the next step of the research involves exploring intramolecular competition reactions. This subchapter will focus on the synthesis of three intramolecular species identified through the research that display varying directing group strengths (*vide infra*).

This is specifically relevant in the pharmaceutical and agrochemical research areas as any application of C-H activation chemistry in a synthetic design process will most likely encounter multiple areas of potential C-H direction from various functional groups present.

Therefore by exploring intramolecular competitive reactivity, the viability of this reactivity scale as a predictive tool for wider synthetic utility would be examined. Three interesting intramolecular competition substrates are shown in Figure 3.14; pyridine-oxazoline (**185**), imine-pyridine (**186**), and oxazoline-imine (**187**).
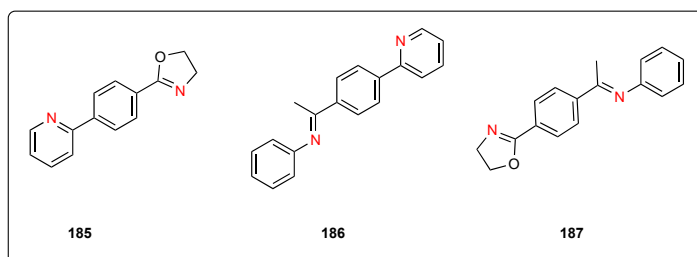
Figure 3.14 – Three intramolecular competition substrates.

Various synthetic strategies were used in an attempt develop these intramolecular substrates. **185** is synthesised according to Scheme 3.11.
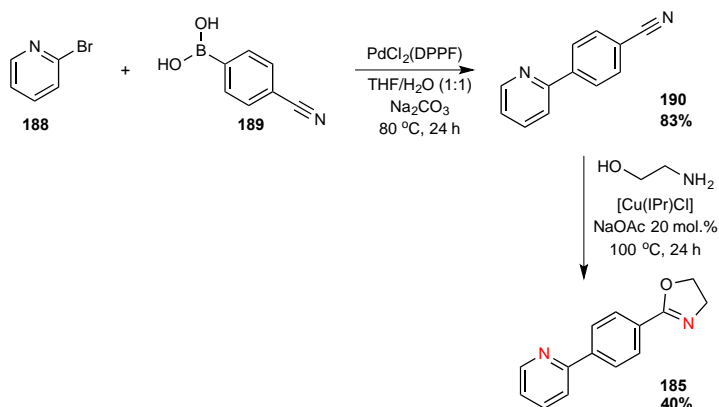
Scheme 3.11 – Synthesis of 185 for intramolecular competition experiments.

53

185 is first synthesised in palladium-catalysed Suzuki cross-coupling of 2-bromopyridine **188** and 4-cyano-phenylboronic acid **189**. This cyano-pyridine species **190** is crystallised from the crude reaction mixture in petroleum ether/diethyl ether and is high yielding. Next, a solvent-free copper-NHC catalysed oxazoline-forming reaction is completed with ethanolamine to form the saturated backbone of the oxazoline.[87] Despite going to 100% consumption of starting material as monitored by GC-FID, the reaction has issues related to the work up and so a low yield of 40% is obtained from this reaction as a pale pink solid. When the reaction is complete, as it cools from 100°C to room temperature the reaction forms an insoluble solid gummy material. It was observed that the gummy material enters dry methanol and is a method to overcome this synthetic challenge. Indeed the authors of the oxazoline-forming step find that the reaction can proceed in dry methanol instead of solvent-free.[87] Despite some synthetic hurdles, a route has been established for **185**, and full characterisation data have been collected.

Additionally, it was noted at this stage that the reaction product was never identified using GC-FID, however can successfully be identified by HPLC-MS. Later we will see that this is a key decision point in analysing the reaction outcomes for intramolecular species.

Similar to **185**, **186** synthesis begins with a palladium-catalysed Suzuki cross-coupling as shown in Scheme 3.12.
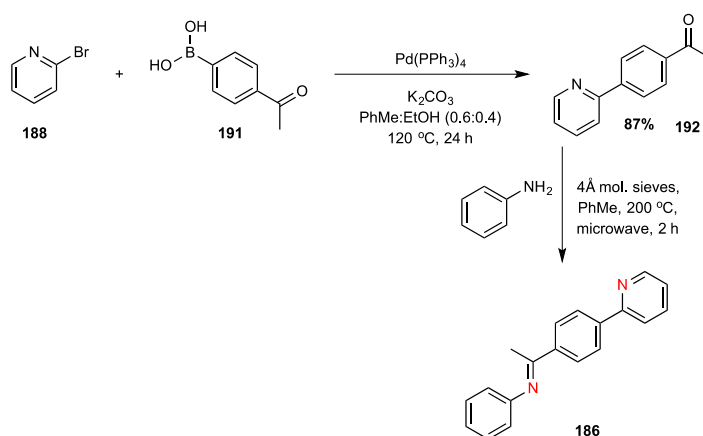
Scheme 3.12 – Synthesis of 186 for intramolecular competition experiments.

The Suzuki cross-coupling yields the desired acetyl-pyridine motif **192** in high conversion, and the yield is good upon workup at 87%. In order to remove remaining triphenylphosphine and triphenylphosphine oxide from the crude reaction mixture, the reaction is passed through a short pad of silica with diethylether. Further washing the silica pad with excess diethyl ether does not obtain a greater yield. The final stage in the synthesis is a condensation reaction with aniline in slight excess. This is completed in two hours under microwave irradiation with

molecular sieves used to drive the condensation towards imine formation. Work continued for much time, but with the fragility of many imine species considered, isolation remains the key challenge with risk of hydrolysis. To date isolation of pure material has not been achieved and full characterisation data are unavailable at this time. Again, similar challenges were encountered with **187**.

187 can be obtained from two routes, both of which were explored, as shown in Scheme 3.13.
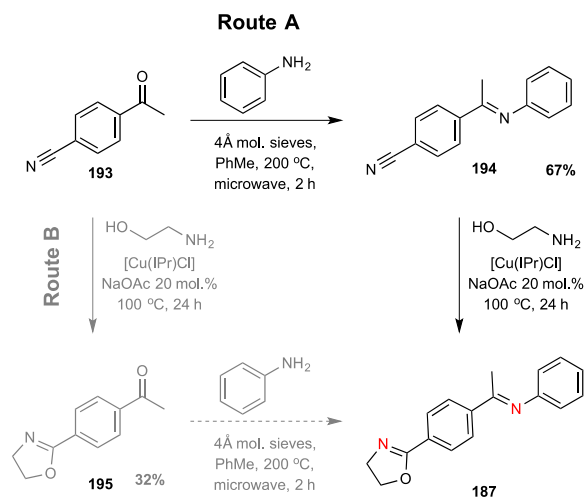
Scheme 3.13 – Routes A and B for the synthesis of 187 for intramolecular competition reaction.

In route A the condensation is completed and the imine product **194** is easily obtained in high yields from a recrystallisation. Next, the recrystallized product reacts with a copper-NHC and ethanolamine in the oxazoline-forming reaction and is completed with 100% conversion as monitored by crude NMR (data not provided). However, isolation of the desired product has thus far proved problematic. The imine functionality is sensitive to aqueous or acidic conditions, and contact with either can result in an equilibrium shift to the left therefore the product cannot be purified with silica due to its mild acidity. Indeed we did examine silica purification to find the ketone product at the end. Additionally, recrystallisation has failed to obtain the desired product.

In route B, the oxazoline-forming reaction yields the desired product **195** in a 32% isolated yield. It is recrystallized from diethyl ether and hexane as a yellow solid. As described earlier, the oxazoline-forming reaction goes with 100% conversion and the low yield is an isolation issue. The final stage of the synthesis is a condensation with aniline under microwave irradiation. No yields have been obtained from this step. While the reaction does progress into product as determined by crude NMR (data not provided), it was difficult to obtain a pure

product from the crude reaction mixture. To date, crystallisation from the reaction mixture has also failed to yield any product.

In developing intramolecular species, we were only able to develop a synthetic route to **185**, which will now be used further in intramolecular competition reactions. The key challenges for **186** and **187** remains purification of the imine product. In hindsight, a less fragile functional group may have been more viable.

3.5.2. Testing on an Intramolecular System

Based on the research findings presented earlier, it is anticipated that the directing group strengths will be replicated intramolecularly and this is demonstrated in Figure 3.15.
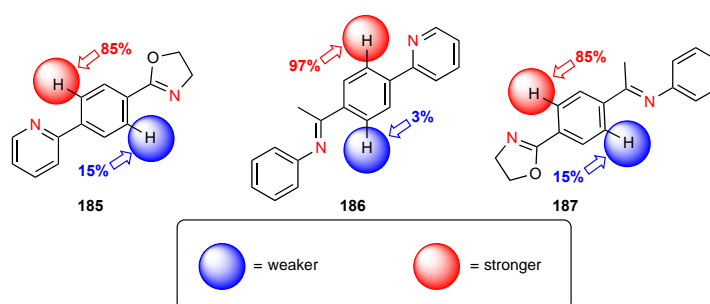
Figure 3.15 – Intramolecular competition substrates showing qualitative and quantitative prediction of regioselectivity.

For **185**, the pyridine is expected to be the stronger C-H activator compared to oxazoline. Based on the quantitative information obtained from this study displayed in Table 3.3, arylation is expected to occur in 85% adjacent to the stronger pyridine directing group while arylation will occur in 15% adjacent to the weaker oxazoline directing group. For **186**, again the pyridine should be the strongest activator and is expected to yield arylation in 97% adjacent to the pyridine group and 3% adjacent to the imine group. For **187**, the oxazoline should display 85% arylation compared with 15% arylation adjacent to the weaker imine directing group.

Sanford *et. al.* also examined one intramolecular-type competition reaction as shown in Scheme 3.14.
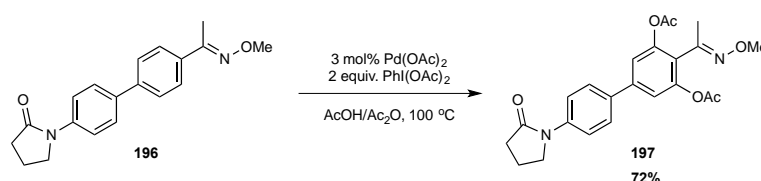
Scheme 3.14 – Palladium-catalysed intramolecular competition experiment.[86]

From the authors' experimental findings, they predicted the oxime functionality would be a stronger directing group than the amide. They showed that this was the case, with diacetoxylation adjacent to the oxime functionality exclusively with an isolated yield of 72%. The authors, however, fail to examine any other intramolecular substrate and they do not build any quantitative information from this.

At this stage it was anticipated that we would have three intramolecular species for testing, however having secured a reproducible route to **185** only, this was placed into competition reactions. This is the next step for the research and will demonstrate if the qualitative and quantitative scales produced are predictive in an intramolecular environment.

The reaction conditions are shown in Scheme 3.15 together with the possible regioisomeric products.
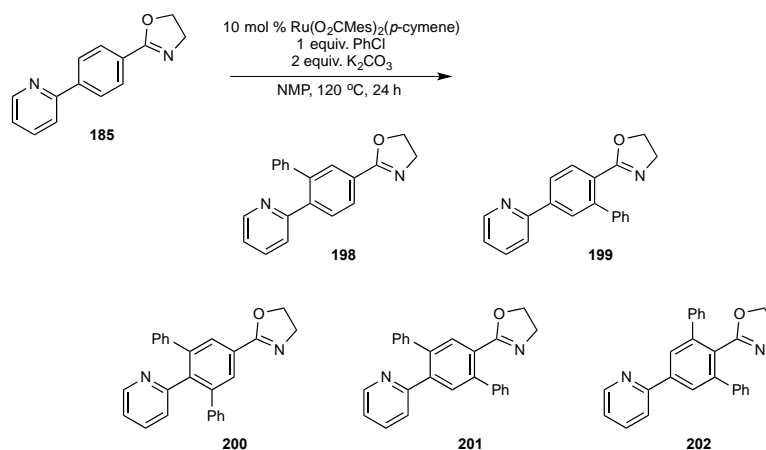
Scheme 3.15 – Intramolecular competition reaction conditions and resulting potential monoaryl and diaryl product mixture.

During the early reactions, it was identified that GC-FID analysis was not suitable for the starting material, and indeed this was confirmed here also for the analysis of the products. Instead, HPLC-MS fitted with a UV detector was used to allow for analysis.

This gave several advantages over GC-FID in this part of the research. The column chromatography allowed for the separation of reaction components, the Mass Spectrometer allowed for the mass identification of parent and child fragments for each reaction component, and the coupled UV detector could be used as an estimate of the concentration of each reaction mixture.

While a calibration of the instrumentation would be highly necessary to obtain accurate quantitative information from the intramolecular competition reactions, this material and the

products are too precious at this stage; a calibration cannot be completed. The Beer-Lambert law is shown in Equation 2.

$$A = \varepsilon\, b\, c \hspace{4cm} \textbf{Equation 2}$$

The Absorbance (A) equals the molar absorptivity (ε) multiplied by path length of unit cell (b) and concentration (c). To proceed, we are making the assumption that the molar absorptivities for the starting material and products shown in Scheme 3.15 are the same. This assumption has been made because structurally they are very similar. The path length of the analysis window in the instrument will not change during analysis, therefore we assume that that absorbance is proportional to the concentration, and will make approximations to the relative concentrations of the reaction outcome.

Following Scheme 3.15, unpublished work from the group using **185** in a series of test reactions with increasing equivalents of chlorobenzene revealed not only that the product is successfully arylated, but that the amount of arylation increases with increasing chlorobenzene.[88]

Table 3.4 – Percentages of 185 and products after reaction with increasing equivalents of chlorobenzene as approximated from uncalibrated HPLC-MS-UV peak area data.[88]

Entry	Equivalents PhCl	Unreacted 185 (%)	Monoaryl (%)	Diaryl (%)
1	0.5	53	43	4
2	1.0	11	56	33
3	2.5	1	27	72

With 0.5 equivalents of chlorobenzene, the reaction uses roughly half of the starting material to deliver 43% monoarylated product in the presence of 4% diarylated product. Increasing this to 1.0 equivalents, the major material is monoaryl product (56%), in the presence of diarylated product at 33% with 11% unreacted starting material. When the reaction is forced to completion with 2.5 equivalents of chlorobenzene, the major diarylated product is obtained in 72%, in the presence of 27% monoaryl and 1% unreacted starting material.

Recalling the arylation of 2-phenylpyridine and 2-phenyloxazoline in Scheme 1.28 and Scheme 1.29 respectively, albeit under slightly different arylating conditions, the results shown in Table 3.4 show an arylation preference between the two unique directing groups. With 1 equivalent of arylating reagent, 2-phenylpyridine showed a yield of 82% with 85:15, mono:diaryl. 2-phenyloxazoline had a stronger diaryl preference with 60% yield and ratio of 25:75. From Entry 2 in Table 3.4, conversion of 89% with a ratio 63:37.

With these encouraging results, we next set out to obtain isolable, and therefore characterisable, mono and diarylated products. This was of interest because the characterisation data can be used to determine the structural configuration of the product and would lead into quantitative analysis. Starting with mono arylated product, the reaction was prepared as shown in Scheme 3.16 using 1 equivalent of chlorobenzene to maximise monoaryl product yield.
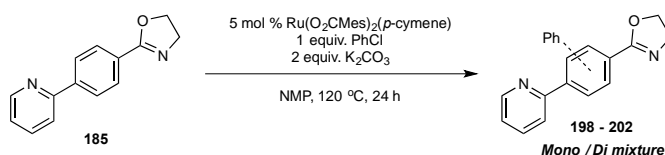
Scheme 3.16 – Synthesis of arylated 185 for the isolation of monoaryl product for characterisation.

As shown earlier in Scheme 3.15, the resulting product mixture contains many possible regioisomeric products which makes purifying this reaction challenging. To overcome this we employed Preparative HPLC equipped with a UV detector and collection by hand. The reaction was injected multiple times and the real-time UV trace allowed each identifiable UV-active product to be collected additively. The final product components were freeze-dried overnight. The UV-trace for one injection is shown in Figure 3.16.
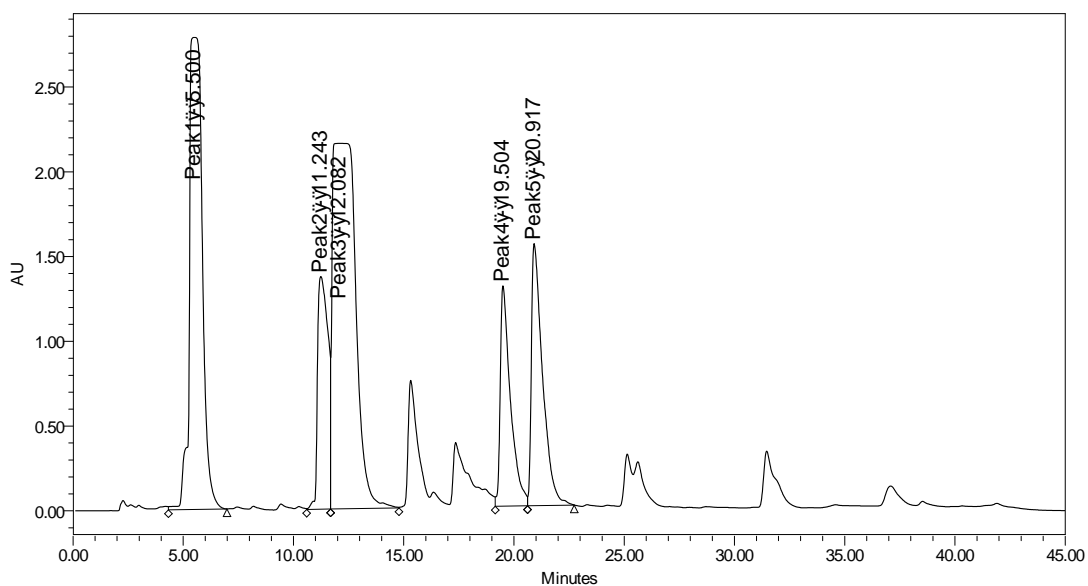
Figure 3.16 – HPLC UV trace of monoarylated product reaction mixture showing separated reaction products.

The order of elution corresponds to increasing steric bulk and there were 5 peaks of interest; 5.5min, 11.2 min, 12.1 min, 19.5 min, and 20.9 min. Each was collected separately. It was anticipated that the peak at 5.5 min would be starting material and this was confirmed by ^{1}H NMR analysis. Since the reaction conditions were selected to maximise monoaryl product, it was anticipated that the peak at 12.1 min would be monoarylated product due to the detector saturation - evident as a flat peak on the trace. The small peak at 11.2 min was suspected to be the monoaryl regioisomer however the quantity obtained was too weak for NMR analysis.

The peaks at 19.5 min and 20.9 min were suspected to be diarylated regioisomers. The collections for each peak were combined and freeze-dried each resulting in a white crystalline material (*vide infra*).

Dealing firstly with the peak at 12.1 min, an NMR was acquired and is shown in Figure 3.17.

Figure 3.17 – ¹H NMR spectrum of mono arylated 185 from peak 12.1 min. Solvent: CD₃CN, Field: 400MHz, Temperature: 300K.

From Figure 3.17, the signal of interest is that at 8.20 ppm which represents the singlet adjacent to the region of arylation. The two possible regioisomers are shown in Figure 3.18. There are two unique interactions that can be used to determine the regioisomers as shown in blue below.

Figure 3.18 – Demonstration of key HMBC interactions for the identification of regiosomer product of 185.

After arylation, the proton that has been coloured blue on the central aromatic ring in Figure 3.18 will show as a singlet with ¹H NMR spectroscopy. An interaction between this proton and quaternary pyridyl carbon (left) or quaternary oxazoline carbon (right) will determine the structure and be visible in [¹H, ¹³C] HMBC spectroscopy.

Based on the starting material, the quaternary oxazoline carbon appears at 163.1 ppm, while the quaternary pyridyl carbon appears at 155.7 ppm. The HMBC spectrum obtained for the product at 12.1 min is shown in Figure 3.19.

Figure 3.17 – ^{1}H NMR spectrum of mono arylated 185 from peak 12.1 min. Solvent: CD$_3$CN, Field: 400MHz, Temperature: 300K.

From Figure 3.17, the signal of interest is that at 8.20 ppm which represents the singlet adjacent to the region of arylation. The two possible regioisomers are shown in Figure 3.18. There are two unique interactions that can be used to determine the regioisomers as shown in blue below.

Figure 3.18 – Demonstration of key HMBC interactions for the identification of regiosomer product of 185.

After arylation, the proton that has been coloured blue on the central aromatic ring in Figure 3.18 will show as a singlet with ^{1}H NMR spectroscopy. An interaction between this proton and quaternary pyridyl carbon (left) or quaternary oxazoline carbon (right) will determine the structure and be visible in [^{1}H, ^{13}C] HMBC spectroscopy.

Based on the starting material, the quaternary oxazoline carbon appears at 163.1 ppm, while the quaternary pyridyl carbon appears at 155.7 ppm. The HMBC spectrum obtained for the product at 12.1 min is shown in Figure 3.19.

Figure 3.19 – [¹H, ¹³C] HMBC of monoarylated 185 showing correlation between singlet proton and oxazoline quaternary carbon. Solvent: CD₃CN, Field: 400MHz, Temperature: 300K.

The signal shown in a blue square in Figure 3.19 at 8.20 / 166.3 ppm, albeit weak, represents the singlet interaction at the oxazoline quaternary carbon site (^3J). As can also be seen in the spectrum, there is no correlation in the 155 ppm region. This confirms that the major product in the monoarylation of **185** is arylation adjacent to the pyridyl moiety: Figure 3.18 – **198**.

Diarylated product was synthesised similarly according to Scheme 3.17 below.
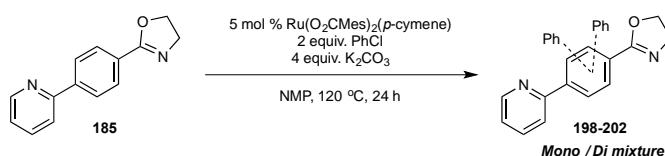
Scheme 3.17 – Synthesis of arylated 185 for the isolation of diaryl product.

Instead of using Preparative HPLC to isolate the product, manual chromatography was performed carefully over the course of a day. The collection was dried under high vacuum and NMR analysis was conducted revealing that diarylation had occurred at both positions adjacent to pyridine, the strongest directing group (see Figure 3.21 - **200**). This is indicated as a singlet in the ¹H NMR spectrum that accounts for two protons.
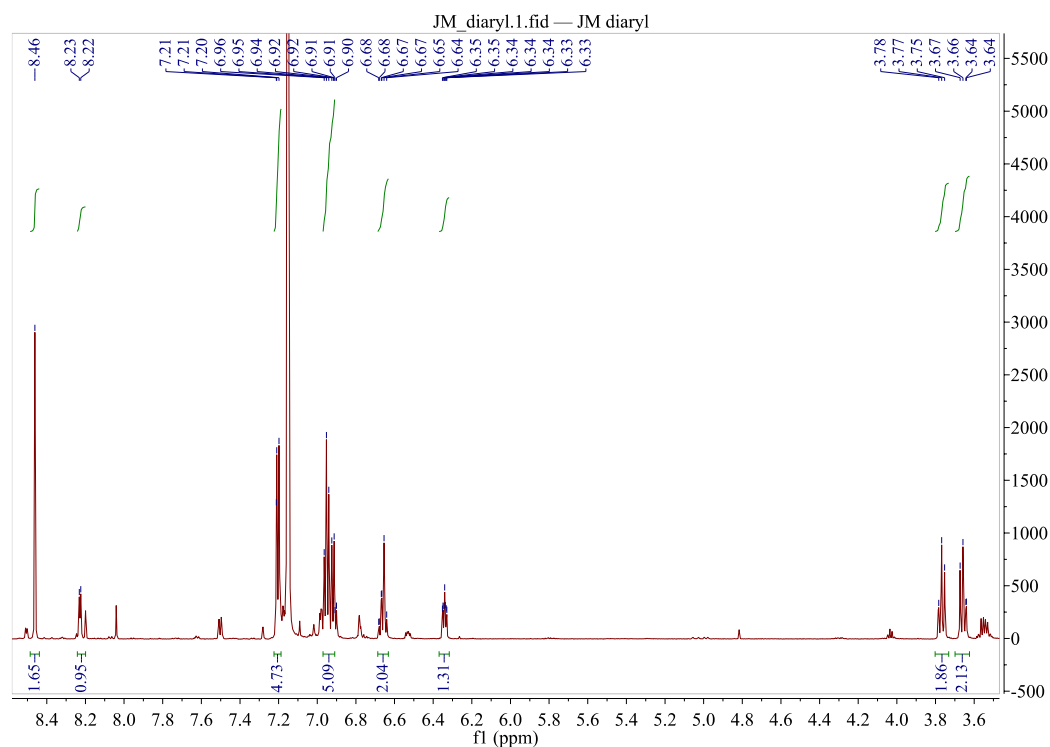
Figure 3.20 – ¹H NMR spectrum of diarylated 185 showing indicative singlet at δ 8.46. Solvent: C₆D₆, Field: 600MHz, Temperature: 310K.

There is baseline noise on the spectrum that could relate to the sterically favoured regioisomer; this would have two singlets and these could be those between δ 8.00 and 8.20 (not integrated) in Figure 3.20. However with reasonable consideration, the major isolated product shows diarylation occurring adjacent to the pyridine, and since separation of regioisomers with similar polarity is highly challenging, it should be considered that with these initial results, this is the major diarylation reaction outcome overall under these conditions.
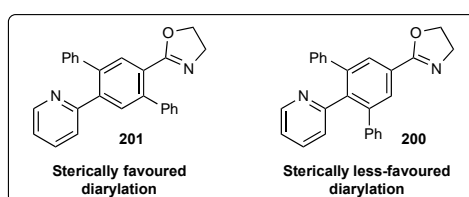
Figure 3.21 – Arylation product, sterically-favoured control versus sterically less-favoured control.

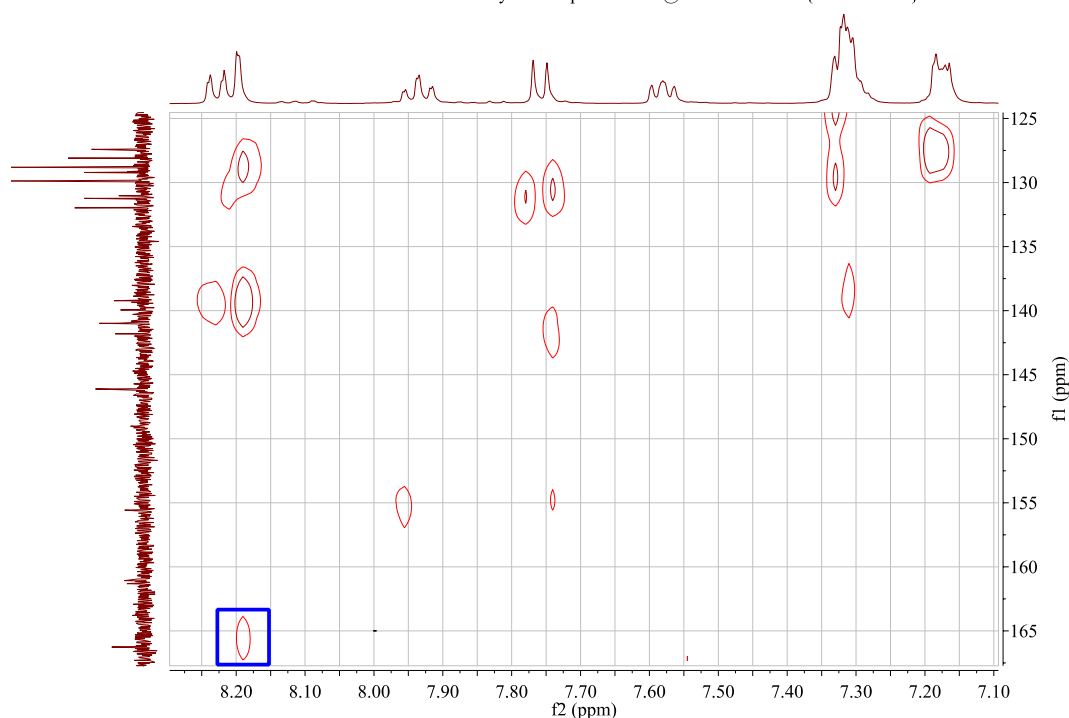Like monoarylation, the regioselectivity is identified through [¹H, ¹³C] HMBC as shown in Figure 3.22.
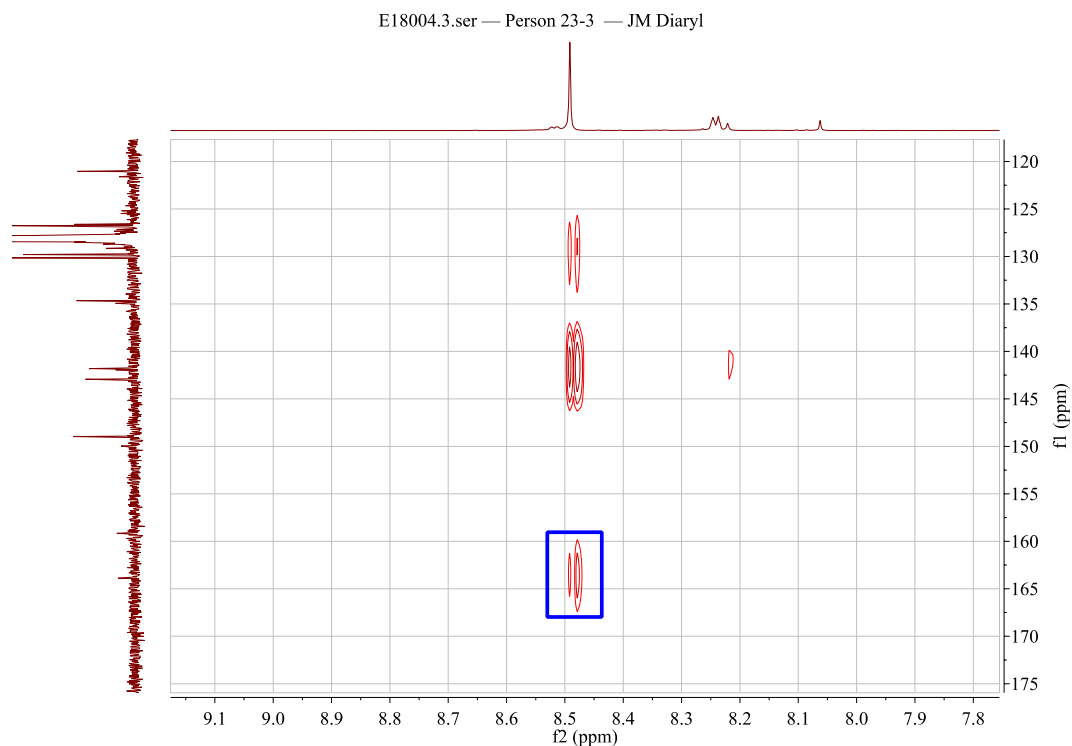
Figure 3.22 – [¹H, ¹³C] HMBC of diarylated 185 showing correlation between singlet proton and oxazoline quaternary carbon. Solvent: C₆D₆, Field: 600MHz, Temperature: 310K.

The quaternary oxazoline carbon is that at 163.9 ppm, and as is shown in Figure 3.22 the singlet proton shows a ^3J interaction, and no correlation to the pyridyl quaternary carbon at 159.2 ppm; thus indicating diarylation adjacent to the pyridine (**200**).

Now with a spectrographic view of both monoarylated and diarylated products, we returned to conduct NMR analyses on the peaks at 19.5 min and 20.9 min. Unfortunately both were very poor yielding isolations and resulted in weak ¹H NMR spectra. The spectrum for the peak at 19.5 min is shown in Figure 3.23.

Person 23-3
160916-1 HPLC pure F19min diaryl??
@proton CD3CN {C:\NMRdata} DJN 6
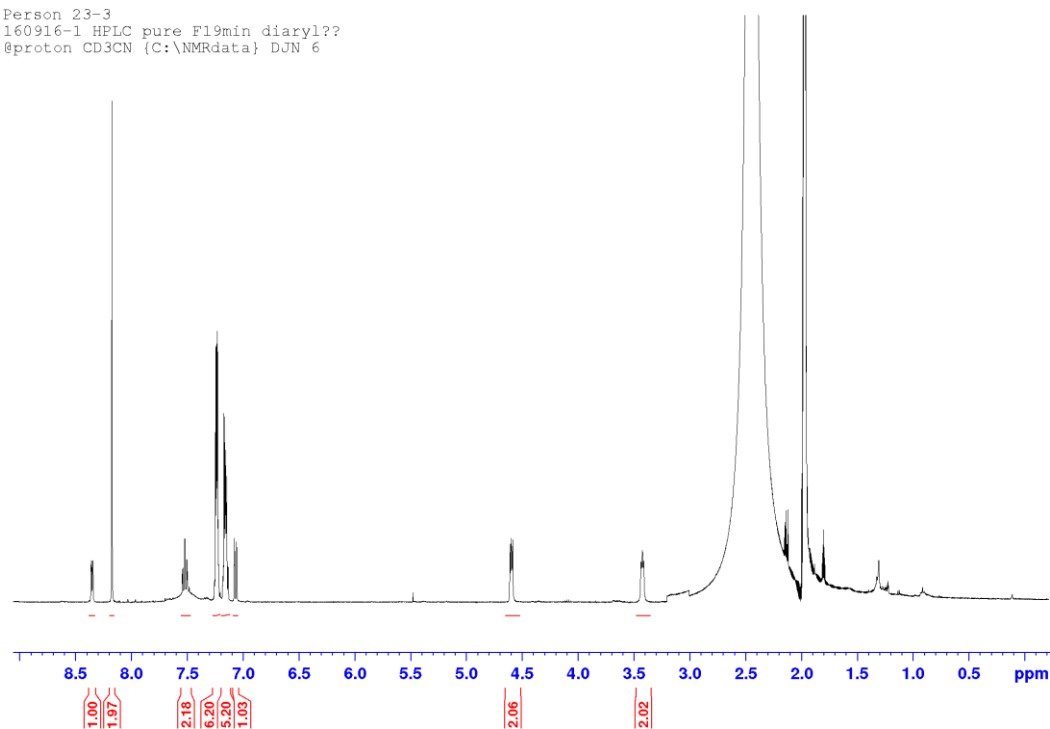
Figure 3.23 – ¹H NMR spectrum of suspected diarylated product at 19.5 min from preparative HPLC. Solvent: CD₃CN, Field: 400MHz, Temperature: 300K.

Despite being weak, the signals show what we would anticipate in diarylation next to a single functional group. The identifying oxazoline, pyridine, and phenyl signals are present in the spectrum but the key peak is that at ca. 8.2 ppm, which counts as 2 protons. Compare this spectrum to Figure 3.20, albeit in a different solvent, the two are very similar. So, this preliminary data set indicates diarylation most likely adjacent to pyridine such as shown in Figure 3.21 (sterically less-favoured **200**). To support this claim, more analysis is needed such as LCMS retention times comparing the manually isolated diarylated product to the 19.5 min isolate.

Similarly, the ¹H NMR spectrum of the peak at 20.9 min is shown in Figure 3.24.
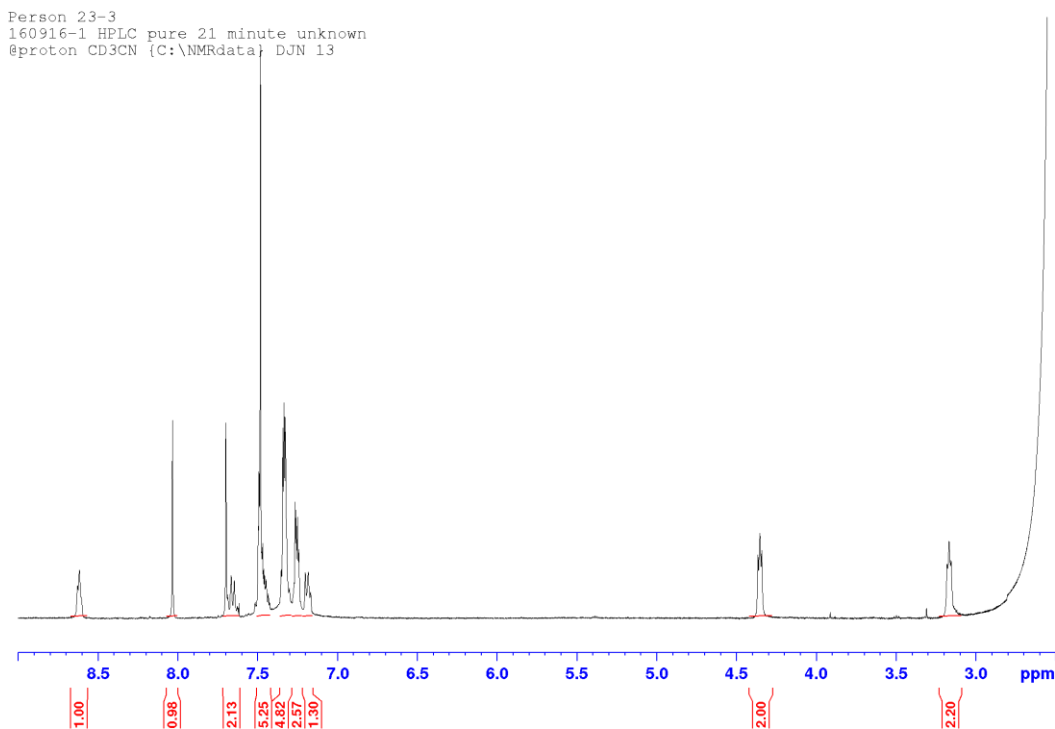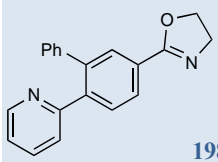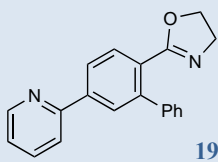
Figure 3.24 – ¹H NMR spectrum of suspected diarylated product at 20.9 min from preparative HPLC. Solvent: CD₃CN, Field: 400MHz, Temperature: 300K.

As with the peak at 19.5 min, the signals are weak and the integration is imperfect however the identifying oxazoline, pyridine and phenyl signals are present. In this spectrum, the key is two singlets at ca. 7.7 ppm and 8.0 ppm. These indicate diarylation adjacent to different functional groups. Recall the sterically-favoured diarylation fromFigure 3.21 (**201**).

It is worth noting that, when the reaction conditions employ 1 equivalent of chlorobenzene then the reaction yields diaryl product where diarylation has occurred adjacent to both functional groups (**201**). However, when the reaction conditions employ 2 equivalents of chlorobenzene then the major diaryl product has diarylation adjacent to the pyridine functional group (**202**). The detail of this is beyond the scope of this report but identifies an aspect of the chemistry that future research may need to explore.

To return these results to the qualitative model for monoarylation, we need to know the response for monoarylation adjacent to oxazoline. As discussed earlier, this was suspected to be the peak at 11.2 min in Figure 3.16 however the collection was too weak for NMR analysis. Since we have identified that the peak at 12.1 min is monoarylated product **198**, and since the peak at 11.2 is very close, we have made the assumption that this peak is monoarylated product adjacent to the oxazoline group (**199**). For discussion, the following results are thus obtained (Table 3.5).

Table 3.5 – Intramolecular directing group strength of 185.

-pyridine	-oxazoline	Conversion -pyridine (%)	Conversion -oxazoline (%)
198	**199**	50	14
	Ratio	78	22

In our qualitative model it is predicted that the pyridine is expected to be the stronger C-H activator compared to oxazoline. Based on the intermolecular quantitative information obtained from this study displayed in Table 3.3, that ratio is 85% adjacent to pyridine and 15% adjacent to oxazoline. From Table 3.5, the intramolecular ratio is 78:22% pyridine:oxazoline and is thus within an acceptable range of the quantitative model.

Confirmation of the true identity of the peak at 11.2 min is essential, and repeat experiments are necessary to strengthen the conclusion, however based on these assumptions the intermolecular quantitative model has been predictive in an intramolecular system for this experiment. This model does not allow for prediction of diarylation, or accommodate the complex paths that these reactions pass through after monoarylation – recall the different stereochemical diarylation outcomes observed when 1 equivalent chlorobenzene is used versus 2 equivalents in this system.

At this stage in the research, these preliminary findings indicate that the qualitative and quantitative model created holds true in this intramolecular setup. Further experimental work is essential to justifiably defend the model for intramolecular systems and research in this area is ongoing within the group.

4. Conclusions

Based upon well-developed mechanistic understandings of ruthenium biscarboxylate-catalysed directed *ortho* C-H arylations, and the prevalence of this catalyst system in the literature, this report explored competition reactions with [Ru(O$_2$CMes)$_2$(*p*-cymene)] **142** as a well-defined catalyst, and chlorobenzene in NMP solvent. The scale of competition reactions was 0.1 mmol of each substrate (0.2 mmol total). This was to enable high throughput and minimise the use of the precious metal catalyst.

In an examination of the literature, this report identified a selection of suitable substrates to use in the development of a qualitative and quantitative scale of reactivity. These substrates covered a broad range of functionalities: pyridine, pyrazole, oxazoline, imidazole, imine, aldehyde, amide, ester, carbamate, and carbonate. Under the experimental conditions used, this report found that only 2-phenylpyridine **3**, 2-phenylpyrazole **160**, 2-phenyloxazoline **89**, *N*-methyl-2-phenyl-imidazole **159**, and *N*-(1-phenylethylidene)aniline **153** were capable of *ortho* arylation. These substrates were therefore selected for intermolecular competition reactions. The limited substrate scope is a limitation of the chosen methodology.

GC-FID was selected as the analysis technique to generate quantitative data from the competition reactions. There were three reasons why this method was selected: GC-FID is very sensitive and was suitable for working on such a small scale; because the products from the competition reactions were aromatic, GC-FID would separate complex reaction mixtures into component parts for quantification; and the method allowed high throughput of multiple competition reactions. The instrumentation was calibrated for each substrate and arylated product to enable a direct comparison of each reaction outcome through correction for each substrate and product's unique response factor.

A series of intermolecular competition reactions were completed on each of the identified substrates. These were completed in at least duplicate to ensure consistent, reproducible, and average data were used for calculations. From a single time point, competitive reactivity was examined using conversion as determined by calibrated GC-FID. These data allowed the development of qualitative scale of directing group capability wherein 2-phenylpyridine > 2-phenylpyrazole > *N*-methyl-2-phenyl-imidazole > 2-phenyloxazoline > *N*-(1-phenylethylidene)aniline.

Using equation (**1**), and a linear regression with least squared minimisation strategy, a quantitative scale of directing group ability was established with rate data for each substrate. To the best of our knowledge, this quantitative scale is the first of its kind for any substrate and catalyst system. These data showed that 2-phenylpyridine (k_{rel} = 1.00) >> 2-

phenylpyrazole (0.385) > *N*-methyl-2-phenyl-imidazole (0.227) > 2-phenyloxazoline (0.170) >> *N*-(1-phenylethylidene)aniline (0.030). The scale shares a similar conclusion with a *qualitative* palladium-catalysed *ortho* acetoxylation scale of directing group ability.[86]

With a reproducible quantitative scale at hand, a predictive model was established for intramolecular competition experiments as shown in Figure 3.15 and Table 3.3. Synthetic routes were devised to create three substrates for intramolecular competition reactions (from Figure 3.14): pyridine-oxazoline **185**, imine-pyridine **186**, and oxazoline-imine **187**. With multiple attempts at all three, only **185** was successfully isolated in 40% yield and carried into intramolecular experiments.

Within the intramolecular space, HPLC was more suitable for analysis on the assumption that the molar absorptivity of each reaction product of **185** was similar due to their structural similarities. Through a combination of preparative HPLC, manual chromatography and [^{1}H, ^{13}C] HMBC, the reaction products were structurally characterised with the exception of the product wherein monoarylation occurred adjacent to 2-phenyloxazoline (Scheme 3.15 - **199**). While more robust characterisation is needed, the initial results has allowed preliminary conclusions.

With the assumption that the preparative HPLC peak at 11.2 min was **199**, it was shown that the quantitative intermolecular model holds true in an intramolecular system under the conditions explored; the intermolecular model predicts that arylation will occur 85:15%, pyridine:oxazoline. The intramolecular experiments found 78:22%.

Work in this area is still on going and it is expected that future results will add support to the assumptions made in this report.

5. Future Work

This author has identified several areas of future work to meet the aims of the report and to strengthen the findings.

Over the course of the development of the intramolecular quantitative systems, HPLC was used to quantify as well as isolate material. The importance of calibrating the GC-FID was demonstrated in Table 3.1, showing that variations may result in significant over- or underestimating of substrate and product concentrations. The impact of inaccurate quantification is therefore significant. A calibration of the HPLC is necessary in order to strengthen the intramolecular research, just as was completed for the GC-FID. In order to achieve this, additional effort must be applied to the generation and isolation of all reactant products of any new substrates that are explored and including **185**. Initially, this would focus on **185** and scaling up the synthesis of reaction products **198**-**202**.

While a calibration is a top priority for the research, the preliminary conclusions made for **185** warrant an extension to the substrate portfolio. Significant attempts were made to broaden the intramolecular scope (**186** and **187**), however, the stability of the ketimine products resulted in impossible isolation within the time constraints of this research. In hindsight, effort could have been spent on, for example, pyrazole-oxazoline **203** shown in Figure 5.1.
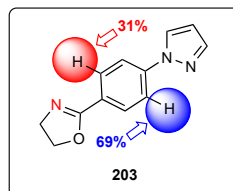
Figure 5.1 – Potential intramolecular test compound 203 for future research.

Compounds **185**, **186**, **and 187** were selected as they were predicted to achieve synthetically useful selectivity of 90:10. However, for the purpose of the research, if compound **203** were to achieve 69:31 then the model would be further strengthened for intramolecular systems. So while not synthetically useful it would be experimentally valuable. Importantly, any extension to the scope of this system must be completed in at least duplicate to obtain average quantitative data.

The quantitative inter- and intramolecular model introduced in this report does not hold up against the second arylation event, which may occur when the substrate concentration is not in excess of the electrophile. As discussed in the introductory chapters, the mechanistic understanding of the reaction is beginning to be exposed, but the model cannot be extended to diarylation until an understanding of how the second arylation event occurs is achieved.

Considering the first arylation event, after oxidative addition of the electrophile but before reductive elimination, does the monoarylated substrate reductively eliminate but remain coordinated to the metal centre, rotating and repeating the catalytic to generate diarylated product before finally uncoordinating? The answer to this type of question extends beyond this report, and the value of the qualitative and quantitative models presented is not under-valued without this understanding at this stage. But this question needs answered in order to further develop the model to the diarylation event.

In unpublished group research, well-defined [RuCl$_2$(PPh$_3$)(p-cymene)] catalyst was shown to have a similar reactivity profile to the catalyst used in this thesis. It employs a similar ligand set to conditions used by Inoue *et. al.* in examples that are shown in Figure 3.1. The different ligand set may allow for a broader substrate scope, which may be complimentary to that presented in this report. Additionally, it will be valuable to compare and contrast both catalysts for the purpose of the research area.

Additionally, an alternative [RuH$_2$(CO)(PPh$_3$)$_3$] catalyst has been shown to allow the directed *ortho* functionalisation of weaker directing groups such as ketones using phenylboronate esters.[80] In our initial studies, this catalyst allows the *ortho* functionalisation of a wider scope of substrates that would complement the quantitative reactivity scale presented. For example, we found that this catalyst showed almost exclusive (>95%) functionalisation adjacent to directing groups, including amide, ester, aldehyde, and ketone, compared to heterocyclic nitrogen-containing groups. As mentioned briefly in the introductory chapters, this catalyst operates through an unknown mechanism that is different to the catalyst used in this report. We developed an approximate qualitative scale of reactivity based on our investigations and this is shown in Figure 5.2.
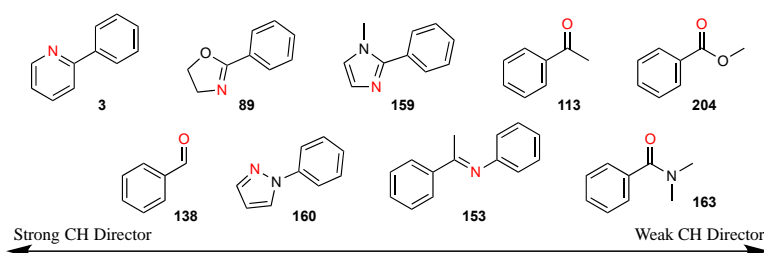
Figure 5.2 – Qualitative directing group power of [RuH$_2$(CO)(PPh$_3$)$_3$] from initial unpublished experiments.

From this initial qualitative scale, aldehyde is more competitive than the substrates examined within this report. Additionally, with this catalyst it was noted that our order of reactivity from this report is not reflected - oxazoline is more competitive than pyrazole.

71

These initial results do need further research effort, however the broader substrate scope and significant selectivity patterns observed would compliment this report's research outcomes.

6. Experimental

6.1. General Experimental

Unless otherwise stated, all reactions were carried out in flame dried glassware under a nitrogen atmosphere using careful Schlenk techniques to inhibit reaction decomposition under aerobic conditions.

Anhydrous solvents were obtained from an Innovative Technologies PureSolv Solvent Purification Apparatus (DCM, THF, toluene, hexane) or dried on activated 4 Å molecular sieves unless otherwise stated. Unless otherwise stated, all reagents were used as supplied without further purification.

NMR spectra were acquired on a Bruker AVIII 400 fitted with a Cryoprobe. The deuterated solvent was used as the lock and the internal reference. All NMR spectra were acquired at room temperature. Multiplicities are recorded as follows: d = doublet, dq = doublet of quartets, m = multiplet, s = singlet, sept = septet, t = triplet, tt = triplet of triplets.

GC-MS spectra were acquired on an Agilent Technologies 7890A GC System instrument fitted with a Restek Rxi-5Sil MS column (30 m, 0.25 mmID, 0.25 µm). Helium carrier gas flow 1 mL min^{-1}. The methods used were: "BASIC_PCI_GC320" as CI (methane) or "EI320" as EI. Both methods employ an inlet temperature 320 ºC and column temperature gradient: 40 ºC for 4 mins then 20 ºC min^{-1} to 320 ºC and hold for 10 mins. Total run time 28 mins.

GC-FID spectra were acquired on an Agilent Technologies 7890A GC System instrument fitted with a Restek Rxi-5Sil MS column (30 m, 0.32 mmID, 0.25 µm). Helium carrier gas flow 2 mL min^{-1} and FID flame of hydrogen (30 mL min^{-1})/compressed air (400 mL min^{-1}). The method used was "GC320" with an inlet temperature 320 ºC and column temperature gradient: 40 ºC for 5 mins then 20 ºC min^{-1} to 320 ºC and hold for 5 mins. Total run time 28 mins.

Column chromatography was performed manually on silica gel (Zeochem, Zeoprep 60 HYD, 40-63 µm). Thin layer chromatography was performed on pre-coated aluminium-backed silica gel plates (E.Merck, A.G.Darmstadt, Germany. Silica gel 60 F254, thickness 0.2 mm). Microwave reactions were completed using a Biotage Initiator instrument. Melting points were acquired on a Griffin EN61010-1. Preparative HPLC was carried out using 200–400 mesh silica gels on a Waters System.

6.2. Synthetic Procedures

[RuCl$_2$(*p*-cymene)]$_2$ 141 A 250 mL round bottom flask was charged with RuCl$_3$.3H$_2$O (3.6 g, 0.013 mol), α-phellandrene (18 mL, 0.11 mol) and 170 mL ethanol. The reaction was stirred at 80 °C for 4 h after which the reaction was placed in an ice bath for 1 h. Red crystals were collected by filtration and dried *in vacuo*. A second batch of crystals was formed by placing the filtrate in the freezer overnight. Yield 3.99 g, 94%, red crystals.

^{1}H NMR (CDCl$_3$, δ) 5.50 (d, 2H, Ar-*H*, ^3J = 6.0 Hz), 5.37 (d, 2H, Ar-*H*, ^3J = 6.0 Hz), 2.97 (sept, 1H, -C*H*(CH$_3$)$_2$, ^3J = 7.0 Hz), 2.18 (s, 3H, Ar-C*H$_3$*), 1.31 (d, 6H, -CH(C*H$_3$*)$_2$, *J* = 7.0 Hz).

Anal. Calculated for C$_{20}$H$_{28}$Cl$_4$Ru$_2$: C, 39.23; H, 4.61. Found: C, 39.19; H, 4.39.

[Ru(O$_2$CMes)$_2$(*p*-cymene)] 142 A 100 mL round bottom flask was charged with [RuCl$_2$(*p*-cymene)]$_2$ (520.4 mg, 0.85 mmol), MesCOOK (779.3 mg, 3.85 mmol, 4.5 equiv.) and 30 mL DCM. The reaction was stirred for 2 h at room temperature. Upon completion the reaction was filtered through Celite and the solvent removed *in vacuo*. The red oil was washed with n-hexane (50 mL total) resulting in precipitation of an orange solid that was dried *in vacuo*. Yield 0.94 g, 99%, orange powder.

^{1}H NMR (400 MHz, CDCl$_3$, δ) 6.68 (s, 4H, Mes-*H*), 5.98 (d, 2H, Ar-*H*), 5.78 (d, 2H, Ar-*H*), 2.96 (sept, 1H, -C*H*(CH$_3$)$_2$, ^3J = 7.0 Hz), 2.35 (s, 3H, C*H$_3$*), 2.19 (s, 6H, Mes-C*H$_3$*), 2.16 (s, 12H, Mes-C*H$_3$*), 1.43 (d, 6H, -CH(C*H$_3$*)$_2$, ^3J = 7 Hz).

Anal. Calculated for C$_{30}$H$_{36}$O$_4$Ru: C, 64.15; H, 6.46. Found: C, 63.85; H, 6.23.

Analytical data are consistent with the literature.[76]

***N*-(methyl)-2-phenylimidazole 159** A 500 mL round bottom flask was charged with 2-phenylimidazole (5.00 g, 35 mmol) and ^{n}Bu$_4$NI (0.92 g, 2.5 mmol). To this, toluene (150 mL) and 33% aq. KOH (190 mL) were added. The reaction was stirred with an overhead stirrer and iodomethane (2.4 mL, 38.5 mmol) was added before being stirred at room temperature for 3 hours. After this, distilled water (200 mL) and toluene (100 mL) were then added. The organic layer was collected in a separating funnel with cross washings, then washed with a saturated solution of Na$_2$S$_2$O$_3$, dried with MgSO$_4$ and reduced under vacuum to yield an orange oil. Crystals were obtained at room temperature from the oil. Yield 2.9 g, 53%, orange crystals.

¹H NMR (400 MHz, CDCl₃, δ) 7.60 – 7.57 (m, 2H, Ar-*H*), 7.43 – 7.33 (m, 3H, Ar-*H*), 7.08 (d, 1H, C-*H*, ^3J = 1.2 Hz), 6.91 (d, 1H, C-*H*, ^3J = 1.2 Hz), 3.67 (s, 3H, N-C*H₃*).

¹³C{¹H} NMR (100 MHz, CDCl₃, δ) 147.3, 130.2, 128.1, 128.0, 128.0, 127.9, 121.9, 33.9.

t$_R$ (GC) 12.6 min, *m/z* 159.1 [M+H]⁺, 187.1, 199.1.

Analytical data are consistent with the literature.[89]

N-(1-phenylethylidene)aniline 153 A 100 mL round bottom flask was charged with toluene (10 mL) and dried 3 Å molecular sieves followed by acetophenone (2 mL, 17.1 mmol) and aniline (3 mL, 32.9 mmol). The reaction was stirred for 17 hours at 120 ℃ before being filtered to remove the molecular sieves. Toluene was removed under reduced pressure and the product was purified by Kugelrohr distillation at 150 ℃ and 0.6 mbar. Yield 1.4 g, 40%, orange solid.

M.P. 38 – 41 ℃

¹H NMR (CDCl₃, δ) 8.05 – 8.02 (m, 2H, Ar-*H*), 7.52 – 7.48 (m, 3H, Ar-*H*), 7.40 (t, 2H, Ar-*H*, *J* = 7.6 Hz), 7.14 (tt, 1H, Ar-*H*, *J* = 7.5 Hz, 1.2 Hz), 6.87 – 6.85 (m, 2H, Ar-*H*), 2.28 (s, 3H, C-C*H₃*).

¹³C{¹H} NMR 165.0, 151.3, 139.1, 130.0, 128.5, 127.9, 126.7, 122.7, 118.9, 16.9.

t$_R$ (GC-MS, CI) 13.4 min, *m/z* 196.1 [M+H]⁺, 224.1, 236.1.

Analytical data are consistent with the literature.[90]

2'-phenyl-acetophenone 171 A flame dried 250 mL round bottom flask was charged with Pd(PPh₃)₄ (49 mg, 0.042 mmol), toluene (70 mL) and ethanol (46 mL) forming a yellow solution. To this, phenyl boronic acid (1.3 g, 10.5 mmol), K₂CO₃ (4 g, 28 mmol) and 2'bromoacetophenone (0.95 mL, 7 mmol) were added. The reaction was stirred at 120 ℃ for 17 hours after which the solvent was reduced under vacuum and the resulting black solution was filtered through celite. The product was collected by Kugelrohr distillation at 170 ℃ and 14 mbar pressure. Yield 0.96 g, 70%, clear colourless oil.

¹H NMR (CDCl₃, δ) 7.58 – 7.51 (m, 2H, Ar-*H*), 7.45 – 7.36 (m, 7H, Ar-*H*), 2.04 (s, 3H, CO-C*H₃*).

¹³C{¹H} NMR (CDCl₃, δ) 204.4, 140.4, 140.3, 140.1, 130.3, 129.8, 128.4, 128.2, 127.4 (2 carbons), 127.0, 30.0.

tᵣ (GC) 12.9 min, *m/z* 197.1 [M+H]⁺, 179.0.

Analytical data are consistent with the literature.[91]

N-(1-2'phenyl-phenylethylidene)aniline 154 In air, a 5 mL round bottom flask was charged with 2'phenyl-acetophenone (0.5 g, 2.5 mmol), aniline (360 µL, 3.75 mmol), toluene (2 mL) and dried 3 Å molecular sieves. The reaction was stirred at 120 °C for 3 days before being filtered to remove the molecular sieves. Toluene was removed under reduced pressure giving red/black oil. Purification by column chromatography (10 % diethyl ether in hexane) giving a yellow oil which was recrystallised from hexane at 5 °C. Yield 240 mg, 35%, yellow solid.

¹H NMR (400 MHz, CDCl₃, δ) (E:Z, 1:0.18). Major: 7.64 (d, 1H, Ar-*H*, ^3J = 7 Hz), 7.56 – 7.52 (m, 2H, Ar-*H*), 7.51 – 7.45 (m, 5H, Ar-*H*), , 7.38 – 7.33 (m, 3H, Ar-*H*), 7.09 (tt, 1H, Ar-*H*, ^3J = 7.4 Hz, ^4J = 1.2 Hz), 6.80 – 6.77 (m, 2H, Ar-*H*), 2.47, 1.70 (s, 3H, -C*H₃*).

¹³C{¹H} NMR (100 MHz, CDCl₃, δ) 170.9, 150.7, 141.3, 140.9, 139.4, 129.6, 128.6, 128.48, 128.47, 128.0, 127.7, 127.0, 126.9, 122.9, 118.7, 20.9.

tᵣ (GC-MS, CI) 15.9 min, *m/z* 272.1 [M+H]⁺, 256.0, 179.0.

Anal. Calculated for C₂₀H₁₇N: C, 88.52; H, 6.31; N, 5.16. Found: C, 88.27; H, 6.33; N, 5.17.

Analytical data are consistent with the literature.[92]

2-(2-phenyl)phenylpyrazole A flame dried 25 mL round bottom flask was charged with [RuCl₂(*p*-cymene)]₂ (46 mg, 0.075 mmol), MesCOOH (394 mg, 2.4 mmol) and K₂CO₃ (1.1 g, 8 mmol) and suspended in toluene (32 mL). 2-phenylpyrazole (1 mL, 8 mmol) and chlorobenzene (0.4 mL, 4 mmol) were added with stirring. The reaction was refluxed and stirred at 120 °C for 17 hours. When complete, the reaction was cooled to room temperature before the solvent was reduced under vacuum and diluted with methyl *tert*-butyl ether (25 mL). The resulting suspension was passed through celite giving a black oil. Purification achieved by column chromatography (10 % diethyl ether in hexane). Yield 206 mg, 23%, pale-yellow, clear oil.

¹H NMR (CDCl₃, δ) 7.66 – 7.44 (m, 2H, Ar-*H*), 7.51 – 7.49 (m, 3H, Ar-*H*), 7.32 – 7.30 (m, 3H, Ar-*H*), 7.16 – 7.13 (m, 2H, Ar-*H*), 7.10 (d, 1H, Ar-*H*, ³*J* = 2.4 Hz), 6.21 (t, 1H, Ar-*H*, ³*J* = 2.1 Hz).

¹³C{¹H} NMR 139.8, 138.1, 136.2, 130.8, 138.5, 128.1 (3C), 128.0 (2C), 127.9, 127.8, 126.9, 126.1, 105.9.

t_R (GC-MS, EI) 13.4 min, *m/z* 219.1 [M-H]⁻, 192.0, 165.0.

Analytical data are consistent with the literature.[93]

2'-phenyl-*N*-(methyl)-2-phenylimidazole 96 A flame dried 25 mL round bottom flask was charged with [RuCl₂(*p*-cymene)]₂ (38 mg, 0.0625 mmol), MesCOOH (164 mg, 1 mmol) and K₂CO₃ (525 mg, 3.8 mmol) and suspended in toluene (12 mL). *N*-methyl-2-phenyl-imidazole (396 mg, 2.5 mmol) and chlorobenzene (137 µL, 1.35 mmol) were added with stirring. The reaction was stoppered and stirred at 120 ºC for 17 hours. When complete, the reaction was cooled to room temperature before the addition of methyl tert-butyl ether (10 mL) and then passed through celite which was further washed with 2 x 10 mL methyl tert-butyl ether. Purification achieved by column chromatography (30 % acetone in hexane + 1% triethylamine). Yield 267 mg, 84%, clear yellow oil.

¹H NMR (400 MHz, CDCl₃, δ) 7.60 – 7.59 (m, 1H, Ar-*H*), 7.53 – 7.48 (m, 2H, Ar-*H*), 7.43 – 7.39 (m, 1H, Ar-*H*), 7.29 – 7.20 (m, 3H, Ar-*H*), 7.16 – 7.13 (m, 2H, Ar-*H*), 7.09 (d, 1H, C-*H*, ³*J* = 1.2 Hz), 6.68 (d, 1H, C-*H*, ³*J* = 1.2 Hz), 2.8 (s, 3H, N-C*H₃*).

¹³C{¹H} NMR (100 MHz, CDCl₃, δ) 147.2, 141.1, 140.1, 131.4, 129.2, 129.1, 128.9, 128.1, 127.89, 127.85, 127.0, 126.6, 120.1, 32.3.

t_R (GC-MS, CI) 14.8 min, *m/z* 235.1 [M+H]⁺, 263.1, 275.1.

Analytical data are consistent with the literature.[94]

2-(2-phenyl)phenyloxazoline 90 A flame dried 25 mL round bottom flask was charged with [RuCl₂(*p*-cymene)]₂ (77 mg, 0.125 mmol), MesCOOH (246 mg, 1.5 mmol) and K₂CO₃ (690 mg, 5 mmol) and suspended in *N*-methyl-2-pyrrolidone (10 mL). 2-phenyloxazoline (650 µL, 5 mmol) and chlorobenzene (150 µL, 1.2 mmol) were added with stirring. The reaction was stoppered and stirred at 120 ºC for 17 hours. When complete, the reaction was cooled to room

temperature before the addition of distilled water (50 mL), and the product was collected using ethyl acetate (100 mL total). The organic layers were collected in a separating funnel with cross washings, then dried with $MgSO_4$ and reduced under vacuum yielding a black oil. Purification achieved by column chromatography (40 % diethyl ether in hexane). Yield 190 mg, 71%, off-white, clear oil.

^{1}H NMR (400 MHz, CDCl$_3$, δ) 7.80 (d, 1H, Ar-*H*, *J* = 8.5 Hz), 7.54 − 7.50 (m, 1H, Ar-*H*), 7.43 − 7.35 (m, 7H, Ar-*H*), 4.13 (t, 2H, CH-*H*, ^3J = 9.8 Hz), 3.93 (t, 2H, CH-*H*, ^3J = 9.5 Hz).

^{13}C{^{1}H} NMR (100 MHz, CDCl$_3$, δ) 165.6, 141.4, 140.8, 130.0, 129.9, 129.6, 127.8, 127.5, 127.1, 126.7, 126.6, 67.3, 54.5.

t$_R$ (GC-MS, EI) 13.7 min, *m/z* 222.1 [M-H]$^-$, 178.0, 152.0.

Analytical data are consistent with the literature.[58]

2-(4-cyano)phenylpyridine 190 In air, a 50 mL round bottom flask was charged with PdCl$_2$(DPPF) (25 mg, 0.03 mmol), 4-cyanophenylboronic acid (661 mg, 4.5 mmol) and Na$_2$CO$_3$ (954 mg, 9 mmol) and suspended in premixed THF/H$_2$O (1:1) (30 mL). The reaction was stirred and heated to 40 °C at which point 2-bromopyridine (286 µL, 3 mmol) was added. The reaction was stoppered and stirred at 80 °C for 24 hours. When complete, the reaction was cooled to room temperature before the addition of distilled water (100 mL), and the product was collected using diethyl ether (3 x 50 mL). The organic layers were collected in a separating funnel with cross washings, then dried with MgSO$_4$ and reduced under vacuum yielding a yellow solid. Purification achieved by recrystallisation from diethyl ether and petroleum ether. Yield 450 mg, 83%, orange solid.

^{1}H NMR (400 MHz, CDCl$_3$, δ) 8.76 (dq, 1H, Ar-*H*, ^3J = 4.8 Hz, ^4J = 1 Hz), 8.16 − 8.13 (m, 2H, Ar-*H*), 7.86 − 7.77 (m, 4H, Ar-*H*), 7.36 − 7.33 (m, 1H, Ar-*H*).

^{13}C{^{1}H} NMR (100 MHz, CDCl$_3$ δ) 154.7, 149.6, 143.0, 136.6, 132.1, 126.9, 122.8, 120.5, 118.3, 112.0.

Analytical data are consistent with the literature.[95]

2-(4-acetyl)phenylpyridine 192 A flame dried 50 mL round bottom flask was charged with Pd(PPh$_3$)$_4$ (21 mg, 0.018 mmol), 4-acetylphenylboronic acid (738 mg, 4.5 mmol) and K$_2$CO$_3$

(1.21 g, 9 mmol) and suspended in premixed toluene/ethanol (0.6:0.4) (30 mL). The reaction was stirred and heated to 120 °C at which point 2-bromopyridine (286 μL, 3 mmol) was added. The reaction was stoppered and stirred at 120 °C for 24 hours. When complete, the reaction was cooled to room temperature before the addition of distilled water (100 mL), and the product was collected using diethyl ether (3 x 50 mL). The organic layers were collected in a separating funnel with cross washings, then dried with MgSO$_4$ and reduced under vacuum yielding an orange solid. Purification achieved by recrystallisation from diethyl ether and petroleum ether. Yield 517 mg, 87%, orange solid.

^{1}H NMR (400 MHz, CDCl$_3$, δ) 8.75 (d, 1H, Ar-*H*, ^3J = 4.9 Hz), 8.13 (d, 2H, Ar-*H*, ^3J = 8.6 Hz), 8.08 (d, 2H, Ar-*H*, ^3J = 8.5 Hz), 7.81 – 7.80 (m, 2H, Ar-*H*), 7.34 – 7.29 (m, 1H, Ar-*H*), 2.67 (s, 3H, C-C*H$_3$*).

^{13}C{^{1}H} NMR (100 MHz, CDCl$_3$ δ) 197.3, 149.4, 136.7, 136.5, 128.3, 126.5, 122.4, 120.5, 26.3.

Analytical data are consistent with the literature.[96]

***N*-(4-cyano-1-phenylethylidene)aniline 194** A flame dried 5 mL microwave vial was charged with 4-acetylbenzonitrile (508 mg, 3.5 mmol) and dried 4Å molecular sieves. Inert conditions were installed before aniline (352 μL, 3.85 mmol) and toluene (2 mL) were added. The reaction was stirred under microwave irradiation for 2 x 30 mins 150 °C then 60 mins at 200 °C. When complete, the reaction was cooled to room temperature before the addition of distilled water (150 mL), and the product was collected using diethyl ether (3 x 50 mL). The organic layers were collected in a separating funnel with cross washings, then dried with MgSO$_4$ and reduced under vacuum yielding an orange oil. Purification achieved by recrystallisation from DCM and pentane. Yield 514 mg, 67%, orange solid.

^{1}H NMR (400 MHz, CDCl$_3$, δ) 8.08 (d, 2H, Ar-*H*, ^3J = 8.6 Hz), 7.73 (d, 2H, Ar-H, ^3J = 8.7 Hz), 7.38 (t, 2H, Ar-*H*, ^3J = 7.8 Hz), 7.13 (t, 1H, Ar-*H*, ^3J = 7.4 Hz), 6.80 (d, 2H, Ar-*H*, ^3J = 8.2 Hz), 2.26 (s, 3H, C-C*H$_3$*).

^{13}C{^{1}H} NMR (100 MHz, CDCl$_3$ δ) 163.9, 150.9, 143.3, 132.2, 129.1, 127.8, 123.9, 119.1, 118.6, 113.8, 17.3.

2-(4-acetyl)phenyloxazoline 195 A flame dried 2 mL septum vial was charged with (IPr)Cu(Cl) (10mg, 0.02 mmol), 4-acetylbenzonitrile (145 mg, 1 mmol) and NaOAc (16 mg, 0.2 mmol). Inert conditions were installed before ethanolamine (241 µL, 4 mmol) was added. The reaction was stirred at 100 ºC for 24 hours. When complete, the reaction was cooled to room temperature before the sequential addition and transfer of DCM (5 mL) into a receptor vial. The crude DCM solution was passed through a short pad of silica with DCM. The solvent was reduced under vacuum yielding a yellow solid. Yield 60 mg, 32%, yellow solid.

^{1}H NMR (400 MHz, CDCl$_3$, δ) 8.06 (d, 2H, Ar-H, ^3J = 8.7 Hz), 8.01 (d, 2H, Ar-H, ^3J = 8.5 Hz), 4.49 (t, 2H, C-H_2, ^3J = 9.7 Hz), 4.12 (t, 2H, C-H_2, ^3J = 9.7 Hz), 2.66 (s, 3H, C-CH_3).

^{13}C{^{1}H} NMR (100 MHz, CDCl$_3$ δ) 197.0, 163.3, 138.5, 131.3, 127.9, 127.7, 67.3, 54.6, 26.3.

2-(4-(pyridin-2-yl)phenyl)-4,5-dihydrooxazole 185 A flame dried 2 mL septum vial was charged with (IPr)Cu(Cl) (135mg, 0.277 mmol), 2-(4-cyano)phenylpyridine (500 mg, 2.77 mmol) and NaOAc (114 mg, 1.39 mmol). Inert conditions were installed before ethanolamine (114 µL, 5.54 mmol) was added. The reaction was stirred at 100 ºC for 24 hours. When complete, the reaction was cooled to room temperature before the sequential aliquots of DCM (note: methanol may be preferred) and transfer into a separating funnel containing brine (200 mL). The product was collected using DCM (150 mL total). The organic layers were collected with cross washings, then dried with MgSO$_4$ and reduced under vacuum. The oil was taken into a small amount of toluene. Purification achieved by column chromatography (70 % ethylacetate in hexane). Yield 248 mg, 44%, pale pink solid.

^{1}H NMR (400 MHz, C$_6$D$_6$, δ) 8.53 (d, 1H, Ar-H, ^3J = 4.3 Hz), 8.33 (d, 2H, Ar-H, ^3J = 8.6 Hz), 8.13 (d, 2H, Ar-H, ^3J = 8.5 Hz), 7.23 (d, 1H, Ar-H, ^3J = 8.0 Hz), 7.06 (td, 1H, Ar-H, ^3J = 7.8 Hz, ^4J = 1.8 Hz), 6.63 (m, 1H, Ar-H), 3.73 (t, 2H, CH-H, ^3J = 9.0 Hz), 3.62 (t, 2H, CH-H, ^3J = 9.0 Hz).

^{13}C{^{1}H} NMR (100 MHz, C$_6$D$_6$ δ) 163.1, 155.7, 149.2, 141.3, 135.4, 128.4, 128.2, 126.3, 121.5, 119.5, 66.5, 54.6.

t$_R$ (HPLC-MS) 6.463 min, m/z 225.1 [M+H]$^+$, 182.1, 155.1

Anal. Calculated for C$_{14}$H$_{12}$N$_2$O: C, 74.98; H, 5.39; N, 12.49. Found: C, 74.28; H, 5.35; N, 12.34.

7. References

(1)   Miyaura, N.; Suzuki, A. *Chem. Rev.* **1995**, *95*, 2457.

(2)   Johansson Seechurn, C. C. C.; Kitching, M. O.; Colacot, T. J.; Snieckus, V. *Angew. Chem., Int. Ed.* **2012**, *51*, 5062.

(3)   Negishi, E.-i. *Angew. Chem., Int. Ed.* **2011**, *50*, 6738.

(4)   Suzuki, A. *Angew. Chem., Int. Ed.* **2011**, *50*, 6722.

(5)   Sigma   Aldrich.   http://www.sigmaaldrich.com/chemistry/chemistry-products.html?TablePage=16256939, (accessed May, 2016).

(6)   Suzuki, A. *J. Organomet. Chem.* **1999**, *576*, 147.

(7)   Rao, X.; Liu, C.; Qiu, J.; Jin, Z. *Org. Biomol. Chem.* **2012**, *10*, 7875.

(8)   Clayden, J. *Organolithiums: Selectivity for Synthesis*; Elsevier Science & Technology Books, 2002.

(9)   Walker, S. D.; Barder, T. E.; Martinelli, J. R.; Buchwald, S. L. *Angew. Chem., Int. Ed.* **2004**, *43*, 1871.

(10)   Marion, N.; Navarro, O.; Mei, J.; Stevens, E. D.; Scott, N. M.; Nolan, S. P. *J. Am. Chem. Soc.* **2006**, *128*, 4101.

(11)   Molander, G. A.; Biolatto, B. *J. Org. Chem.* **2003**, *68*, 4302.

(12)   Molander, G. A.; Canturk, B.; Kennedy, L. E. *J. Org. Chem.* **2009**, *74*, 973.

(13)   Chemla, F.; Ferreira, F.; Jackowski, O.; Micouin, L.; Perez-Luna, A. In *Metal-Catalyzed Cross-Coupling Reactions and More*; Wiley-VCH Verlag GmbH & Co. KGaA: 2014, p 279.

(14)   Nicolaou, K. C.; Bulger, P. G.; Sarlah, D. *Angew. Chem., Int. Ed.* **2005**, *44*, 4442.

(15)   Coleridge, B. M.; Bello, C. S.; Ellenberger, D. H.; Leitner, A. *Tetrahedron Lett.* **2010**, *51*, 357.

(16)   Dai, C.; Fu, G. C. *J. Am. Chem. Soc.* **2001**, *123*, 2719.

(17)   Zhou, J.; Fu, G. C. *J. Am. Chem. Soc.* **2003**, *125*, 12527.

(18)   Organ, M. G.; Avola, S.; Dubovyk, I.; Hadei, N.; Kantchev, E. A. B.; O'Brien, C. J.; Valente, C. *Chem.--Eur. J.* **2006**, *12*, 4749.

(19)   Milne, J. E.; Buchwald, S. L. *J. Am. Chem. Soc.* **2004**, *126*, 13028.

(20)   Sigma Aldrich. http://www.sigmaaldrich.com/, (accessed June, 2016).

(21)   Dieck, H. A.; Heck, R. F. *J. Am. Chem. Soc.* **1974**, *96*, 1133.

(22)   Wu, X.-F.; Anbarasan, P.; Neumann, H.; Beller, M. *Angew. Chem., Int. Ed.* **2010**, *49*, 9047.

(23)   Cabri, W.; Candiani, I. *Acc. Chem. Res.* **1995**, *28*, 2.

(24)   Kong, W.; Wang, Q.; Zhu, J. *J. Am. Chem. Soc.* **2015**, *137*, 16028.

(25)   Dounay, A. B.; Overman, L. E. *Chem. Rev.* **2003**, *103*, 2945.

(26)   Minatti, A.; Zheng, X.; Buchwald, S. L. *J. Org. Chem.* **2007**, *72*, 9253.

(27)   Brown, D. G.; Boström, J. *J. Med. Chem.* **2016**, *59*, 4443.

(28)   Schlummer, B.; Scholz, U. *Adv. Synth. Catal.* **2004**, *346*, 1599.

(29)   Hartwig, J. F. *Angew. Chem., Int. Ed.* **1998**, *37*, 2046.

(30)   Damon, D. B.; Dugger, R. W.; Scott, R. W.; Google Patents: 2004.

(31)   Hartwig, J. F. *Organotransition metal chemistry : from bonding to catalysis*; Sausalito, Calif. : University Science Books, 2010.

(32)   Paradine, S. M.; White, M. C. *J. Am. Chem. Soc.* **2012**, *134*, 2036.

(33)   Brown, H. C.; Cole, T. E. *Organometallics* **1983**, *2*, 1316.

(34)   Ishiyama, T.; Murata, M.; Miyaura, N. *J. Org. Chem.* **1995**, *60*, 7508.

(35)   Mkhalid, I. A. I.; Barnard, J. H.; Marder, T. B.; Murphy, J. M.; Hartwig, J. F. *Chem. Rev.* **2010**, *110*, 890.

(36)   Li, W.; Nelson, D. P.; Jensen, M. S.; Hoerrner, R. S.; Cai, D.; Larsen, R. D.; Reider, P. J. *J. Org. Chem.* **2002**, *67*, 5394.

(37)   Ishiyama, T.; Takagi, J.; Ishida, K.; Miyaura, N.; Anastasi, N. R.; Hartwig, J. F. *J. Am. Chem. Soc.* **2002**, *124*, 390.

(38)   Shimada, S.; Batsanov, A. S.; Howard, J. A. K.; Marder, T. B. *Angew. Chem., Int. Ed.* **2001**, *40*, 2168.

(39)   Calleja, J.; Pla, D.; Gorman, T. W.; Domingo, V.; Haffemayer, B.; Gaunt, M. J. *Nat Chem* **2015**, *7*, 1009.

(40)   Nakamura, M.; Matsuo, K.; Ito, S.; Nakamura, E. *J. Am. Chem. Soc.* **2004**, *126*, 3686.

(41)   Furukawa, T.; Tobisu, M.; Chatani, N. *Chem. Commun.* **2015**, *51*, 6508.

(42)   Natte, K.; Jagadeesh, R. V.; He, L.; Rabeah, J.; Chen, J.; Taeschler, C.; Ellinger, S.; Zaragoza, F.; Neumann, H.; Brückner, A.; Beller, M. *Angew. Chem., Int. Ed.* **2016**, *55*, 2782.

(43)   Wang, X.; Lane, B. S.; Sames, D. *J. Am. Chem. Soc.* **2005**, *127*, 4996.

(44)   Neufeldt, S. R.; Sanford, M. S. *Acc. Chem. Res.* **2012**, *45*, 936.

(45)   Wagner, A. M.; Sanford, M. S. *Org. Lett.* **2011**, *13*, 288.

(46)   Grimster, N. P.; Gauntlett, C.; Godfrey, C. R. A.; Gaunt, M. J. *Angew. Chem., Int. Ed.* **2005**, *44*, 3125.

(47)   Phipps, R. J.; Gaunt, M. J. *Science* **2009**, *323*, 1593.

(48)   Shen, P.-X.; Wang, X.-C.; Wang, P.; Zhu, R.-Y.; Yu, J.-Q. *J. Am. Chem. Soc.* **2015**, *137*, 11574.

(49)   Dong, Z.; Wang, J.; Dong, G. *J. Am. Chem. Soc.* **2015**, *137*, 5887.

(50)   Wan, L.; Dastbaravardeh, N.; Li, G.; Yu, J.-Q. *J. Am. Chem. Soc.* **2013**, *135*, 18056.

(51) Patra, T.; Bag, S.; Kancherla, R.; Mondal, A.; Dey, A.; Pimparkar, S.; Agasti, S.; Modak, A.; Maiti, D. *Angew. Chem., Int. Ed.* **2016**, *55*, 7751.

(52) Saidi, O.; Marafie, J.; Ledger, A. E. W.; Liu, P. M.; Mahon, M. F.; Kociok-Köhn, G.; Whittlesey, M. K.; Frost, C. G. *J. Am. Chem. Soc.* **2011**, *133*, 19298.

(53) Teskey, C. J.; Lui, A. Y. W.; Greaney, M. F. *Angew. Chem., Int. Ed.* **2015**, *54*, 11677.

(54) Hofmann, N.; Ackermann, L. *J. Am. Chem. Soc.* **2013**, *135*, 5877.

(55) Paterson, A. J.; St John-Campbell, S.; Mahon, M. F.; Press, N. J.; Frost, C. G. *Chem. Commun.* **2015**, *51*, 12807.

(56) Arockiam, P. B.; Bruneau, C.; Dixneuf, P. H. *Chem. Rev.* **2012**, *112*, 5879.

(57) Oi, S.; Fukita, S.; Hirata, N.; Watanuki, N.; Miyano, S.; Inoue, Y. *Org. Lett.* **2001**, *3*, 2579.

(58) Oi, S.; Aizawa, E.; Ogino, Y.; Inoue, Y. *J. Org. Chem.* **2005**, *70*, 3113.

(59) Oi, S.; Sasamoto, H.; Funayama, R.; Inoue, Y. *Chem. Lett.* **2008**, *37*, 994.

(60) Ackermann, L.; Vicente, R.; Althammer, A. *Org. Lett.* **2008**, *10*, 2299.

(61) Oi, S.; Funayama, R.; Hattori, T.; Inoue, Y. *Tetrahedron* **2008**, *64*, 6051.

(62) Merritt, E. A.; Olofsson, B. *Angew. Chem., Int. Ed.* **2009**, *48*, 9052.

(63) Ho, J. S.; Misal Castro, L. C.; Aihara, Y.; Tobisu, M.; Chatani, N. *Asian J. Org. Chem.* **2014**, *3*, 48.

(64) Oi, S.; Ogino, Y.; Fukita, S.; Inoue, Y. *Org. Lett.* **2002**, *4*, 1783.

(65) Chinnagolla, R. K.; Jeganmohan, M. *Org. Lett.* **2012**, *14*, 5246.

(66) Kakiuchi, F.; Kan, S.; Igi, K.; Chatani, N.; Murai, S. *J. Am. Chem. Soc.* **2003**, *125*, 1698.

(67) Murai, S.; Kakiuchi, F.; Sekine, S.; Tanaka, Y.; Kamatani, A.; Sonoda, M.; Chatani, N. *Nature* **1993**, *366*, 529.

(68) Ahmad, N.; Levison, J. J.; Robinson, S. D.; Uttley, M. F.; Wonchoba, E. R.; Parshall, G. W. In *Inorg. Synth.*; John Wiley & Sons, Inc.: 2007, p 45.

(69) Martinez, R.; Chevalier, R.; Darses, S.; Genet, J.-P. *Angew. Chem., Int. Ed.* **2006**, *45*, 8232.

(70) Ueno, S.; Chatani, N.; Kakiuchi, F. *J. Org. Chem.* **2007**, *72*, 3600.

(71) Ano, Y.; Tobisu, M.; Chatani, N. *Synlett* **2012**, *23*, 2763.

(72) Bhanuchandra, M.; Ramu Yadav, M.; Rit, R. K.; Rao Kuram, M.; Sahoo, A. K. *Chem. Commun. (Cambridge, U. K.)* **2013**, *49*, 5225.

(73) Jia, X.; Zhang, S.; Wang, W.; Luo, F.; Cheng, J. *Org. Lett.* **2009**, *11*, 3120.

(74) http://www.sigmaaldrich.com, (accessed March, 2016).

(75) Norinder, J.; Matsumoto, A.; Yoshikai, N.; Nakamura, E. *J. Am. Chem. Soc.* **2008**, *130*, 5858.

(76)   Ackermann, L.; Vicente, R. n.; Potukuchi, H. K.; Pirovano, V. *Org. Lett.* **2010**, *12*, 5032.

(77)   Ferrer Flegeau, E.; Bruneau, C.; Dixneuf, P. H.; Jutand, A. *J. Am. Chem. Soc.* **2011**, *133*, 10161.

(78)   Ackermann, L. *Chem. Rev.* **2011**, *111*, 1315.

(79)   Thirunavukkarasu, V. S.; Ackermann, L. *Org. Lett.* **2012**, *14*, 6206.

(80)   Kakiuchi, F.; Matsuura, Y.; Kan, S.; Chatani, N. *J. Am. Chem. Soc.* **2005**, *127*, 5936.

(81)   Arockiam, P.; Poirier, V.; Fischmeister, C.; Bruneau, C.; Dixneuf, P. H. *Green Chem.* **2009**, *11*, 1871.

(82)   Arockiam, P. B.; Fischmeister, C.; Bruneau, C.; Dixneuf, P. H. *Green Chem.* **2013**, *15*, 67.

(83)   De Sarkar, S.; Liu, W.; Kozhushkov, S. I.; Ackermann, L. *Adv. Synth. Catal.* **2014**, *356*, 1461.

(84)   Byron, D., The University of Strathclyde, 2015.

(85)   Dong, Z.-B.; Manolikakes, G.; Shi, L.; Knochel, P.; Mayr, H. *Chem.--Eur. J.* **2010**, *16*, 248.

(86)   Desai, L. V.; Stowers, K. J.; Sanford, M. S. *J. Am. Chem. Soc.* **2008**, *130*, 13285.

(87)   Trose, M.; Lazreg, F.; Lesieur, M.; Cazin, C. S. J. *J. Org. Chem.* **2015**, *80*, 9910.

(88)   Nelson, D. J. In *Arylation of 2-(4-(pyridin-2-yl)phenyl)-4,5-dihydrooxazole* 2016.

(89)   Bhanu Prasad, A. S.; Stevenson, T. M.; Citineni, J. R.; Nyzam, V.; Knochel, P. *Tetrahedron* **1997**, *53*, 7237.

(90)   Hansen, M. C.; Buchwald, S. L. *Org. Lett.* **2000**, *2*, 713.

(91)   Mousseau, J. J.; Vallée, F.; Lorion, M. M.; Charette, A. B. *J. Am. Chem. Soc.* **2010**, *132*, 14412.

(92)   Oi, S.; Ogino, Y.; Fukita, S.; Inoue, Y. *Org. Lett.* **2002**, *4*, 1783.

(93)   Boswell, M. G.; Yeung, F. G.; Wolf, C. *Synlett* **2012**, *2012*, 1240.

(94)   Miyamura, S.; Tsurugi, H.; Satoh, T.; Miura, M. *J. Organomet. Chem.* **2008**, *693*, 2438.

(95)   Zhang, E.; Tang, J.; Li, S.; Wu, P.; Moses, J. E.; Sharpless, K. B. *Chem.--Eur. J.* **2016**, *22*, 5692.

(96)   Colombe, J. R.; Bernhardt, S.; Stathakis, C.; Buchwald, S. L.; Knochel, P. *Org. Lett.* **2013**, *15*, 5754.